

DEPARTMENT OF PHYSICS AND ASTRONOMY
UNIVERSITY OF HEIDELBERG

MASTER THESIS
in PHYSICS

submitted by

CLARA MIRALLES VILA

born in Valencia, Spain

Heidelberg
2016

NATURALNESS AND THE HIERARCHY PROBLEM IN THE
TYPE I AND TYPE II SEE-SAW MODELS

MASTER THESIS

carried out by

Clara Miralles Vila

at the

Max Planck Institute for Nuclear Physics

Saupfercheckweg 1

69117 Heidelberg

submitted to the

Department of Physics and Astronomy,

University of Heidelberg

on November 2, 2016

SUPERVISOR: Dr. rer. nat. Werner Rodejohann

Abstract

In this thesis, the type I and type II see-saw models are considered separately as the mechanism to generate small neutrino masses and the radiative corrections to the Higgs mass induced by these models are studied. Especially, the influence of imposing naturalness is tested. As the naturalness criterion, it is assumed that quantum corrections should not be larger than the Higgs mass. Imposing this condition, limits on the new mass scale introduced in each model can be set, so that no hierarchy problem arises. For the type I, it is found that the mass of the right-handed neutrino could take values up to $\mathcal{O}(10^7 \text{ GeV})$ without generating large corrections. For the type II, the parameter space of the extended scalar potential is first restricted by imposing vacuum stability, unitarity of scattering processes and experimental constraints, before testing the influence of imposing naturalness. Only small values of the triplet vacuum expectation value, $\mathcal{O}(\text{eV})$, which give rise to sizeable Yukawa couplings, are considered. In this scenario, there exist a large parameter space satisfying the vacuum stability, unitarity and experimental constraints. Of this parameter space, all sets of parameters satisfy the naturalness condition for triplet masses below 1 TeV and a large subset satisfies naturalness for masses between 1 TeV and 3 TeV. If the triplet mass were located in this energy range, as preferred by naturalness, new particles corresponding to the triplet might be detectable at the Large Hadron Collider or future colliders and also lead to significant signals in lepton flavour violation experiments.

Zusammenfassung

In dieser Arbeit wird jeweils das See-Saw Modell des Typs I und des Typs II als der Mechanismus für die Erzeugung kleiner Neutrinomassen und die mit diesen Modellen verbundenen Quantenkorrekturen der Masse des Higgs-Bosons untersucht. Insbesondere wird der Einfluss eines Natürlichkeitskriterium getestet. Als solches Kriterium wird gefordert, dass die Quantenkorrekturen nicht größer als die Masse des Higgs-Bosons sein sollen. Unter diesem Kriterium werden Ausschlussgrenzen für die neue Massenskala jedes Modells gesetzt, sodass kein Hierarchieproblem entsteht. Für den Typ I wird gefunden, dass die Masse des rechtshändigen Neutrinos Werte bis zu $\mathcal{O}(10^7 \text{ GeV})$ annehmen kann, ohne dass das Hierarchieproblem auftritt. Für den Typ II wird der Parameterraum des erweiterten skalaren Potentials zunächst durch Kriterien der Vakuumstabilität, Unitarität der Streuprozesse und experimentellen Beobachtungen eingeschränkt, bevor der Einfluss des Natürlichkeitskriteriums getestet wird. Dabei werden nur kleine Werte des Triplet-Vakuumerwartungswertes, die zu merkbaren Yukawakopplungen führen, betrachtet. In diesem Szenario existiert ein großer Parameterraum, der die Kriterien der Vakuumstabilität, Unitarität und der experimentellen Beobachtungen erfüllen kann. Aus diesem Parameterraum erfüllt jeder Satz an Parametern das Natürlichkeitskriterium für Tripletmassen unter 1 TeV und ein großer Subraum erfüllt das Kriterium der Natürlichkeit für Massen zwischen 1 TeV und 3 TeV. Wenn die Tripletmasse in diesem Energiebereich läge, wie es von der Natürlichkeit bevorzugt ist, so wäre es möglich, die mit dem Triplet verbundenen neuen Teilchen am Großen Hadronen-Speicherring oder zukünftigen Teilchenbeschleunigern nachzuweisen oder signifikante Signale in Experimenten, die eine Verletzung der Lepton-Flavour Quantenzahl untersuchen, zu erhalten.

CONTENTS

1	INTRODUCTION	5
2	THE STANDARD MODEL AND BEYOND	9
2.1	The Standard Model of particle physics	9
2.1.1	Gauge sector	10
2.1.2	Fermion sector	11
2.1.3	The SM Higgs mechanism	12
2.2	Physics beyond the Standard Model	17
2.2.1	Neutrino masses and mixing	17
2.2.2	Absolute neutrino mass scale	19
2.2.3	Scalar masses and the hierarchy problem	21
3	TYPE I SEE-SAW MODEL	25
3.1	Neutrino masses	25
3.2	Radiative corrections and renormalisation	29
3.2.1	One-loop Higgs self-energy	31
3.2.2	Regularisation	34
3.2.3	Renormalisation	37
3.2.4	Higgs mass radiative correction	40
3.3	Results and discussion	44
4	TYPE II SEE-SAW MODEL	47
4.1	Neutrino masses	48
4.2	Scalar masses and mixing	49
4.3	Vacuum stability and unitarity conditions	51
4.4	Higgs mass radiative corrections	52
4.5	The renormalisation group equations	57
4.5.1	For $\mu < M_\Delta$	57
4.5.2	For $\mu > M_\Delta$	58
4.6	Lepton flavour violation processes	59
4.6.1	Summary of LFV-Bounds	62
4.7	Other constraints	64
4.7.1	Direct searches	64
4.7.2	Electroweak precision tests	65
4.8	Results and discussion	66
4.8.1	Allowed Parameter Space	66
4.8.2	Future prospects	70
5	CONCLUSIONS	73

A	APPENDIX	75
A.1	RGEs and matching conditions in the see-saw type II model	75
A.2	Parameter Scan Plots	78
A.2.1	IH - $m_{\nu_{\min}} = 0$, zero Majorana phases.	79
A.2.2	NH - $m_{\nu_{\min}} = 0.2$ eV, zero Majorana phases.	80
A.2.3	IH - $m_{\nu_{\min}} = 0.2$ eV, zero Majorana phases.	81
B	BIBLIOGRAPHY	83

1 INTRODUCTION

... it is unlikely that the macroscopic equations contain various free parameters that are carefully adjusted by Nature to give cancelling effects such that macroscopic systems have some special properties.

Gerard 't Hooft [1]

The Standard Model of particle physics (SM) is so far the best theory to explain the subatomic world and the forces governing it: the electromagnetic force, the weak force and the strong force. The current experimental results provided by the Large Hadron Collider (LHC) and other low energy precision measurements have validated this theory to a very high precision. Despite its major success, there is still a long list of open questions that the SM fails to answer. For example, the experimental observation of neutrino oscillations in solar [2], atmospheric [3], reactor [4] and accelerator beam [5] neutrino experiments have shown that active neutrinos have a non-zero mass, in contrast with the prediction of the SM, in which neutrinos are massless. This is one of the clearest evidences for physics beyond the SM and opens a window to explore new physics. Moreover, the fact that their masses are much smaller than those of the other SM fermions has risen the interest of many particle physicists and different models have been proposed to explain not only how neutrinos acquire mass but also why their masses are so small.

The nature and magnitude of the low energy effects associated to neutrino masses can be described through an effective low-energy field theory. The effect at low energies of the heavy fields present in a high-energy theory can be parametrized by an effective Lagrangian including corrections to the parameters of the SM Lagrangian and the addition of a tower of non-renormalisable higher-dimension operators, invariant under the SM gauge group, weighted by powers of the new energy scale [6]. This reads,

$$\mathcal{L}_{\text{eff}} = \mathcal{L}_{\text{SM}} + \delta\mathcal{L}^{d=5} + \delta\mathcal{L}^{d=6} + \dots \quad (1.1)$$

The only possible dimension 5 ($d = 5$) operator which respects the fundamental principles of Lorentz and gauge invariance is the famous Weinberg operator [7],

$$\delta\mathcal{L}^{d=5} = \frac{1}{2} C_{\alpha\beta}^{d=5} \left(\overline{L_{L\alpha}^C} \tilde{\Phi}^* \right) \left(\tilde{\Phi}^\dagger L_{L\beta} \right) + \text{h.c.}, \quad (1.2)$$

where L_L are the lepton weak doublets¹, Greek letters denote flavour indices and $\tilde{\Phi}$ is the conjugate Higgs doublet, which is related to the Higgs doublet $\Phi \equiv (\phi^+, \phi^0)$ by $\tilde{\Phi} = i\sigma_2\Phi^*$.

¹The charged conjugated spinor is denoted $\psi^c \equiv C\bar{\psi}^T$, where C is the Dirac charge conjugation matrix C , which satisfies $C^{-1}\gamma_\mu C = \gamma_\mu^T$ and $C^\dagger = C^{-1}$, $C^T = -C$.

The coefficients $\mathcal{C}_{\alpha\beta}^{d=5}$ are the elements of a coupling matrix of inverse mass dimensions, i.e.

$$\mathcal{C}_{\alpha\beta}^{d=5} = \frac{c_{\alpha\beta}^{d=5}}{M}, \quad (1.3)$$

with M being the new-physics mass scale and $c_{\alpha\beta}^{d=5}$ a dimensionless coupling determined by the high-energy theory. After spontaneous symmetry breaking (SSB), in which the Higgs doublet acquires a vacuum expectation value $\langle\phi^0\rangle = v/\sqrt{2}$, with $v \simeq 246$ GeV [8], this term results in a Majorana neutrino mass term,

$$\delta\mathcal{L}^{d=5} = \frac{1}{2}M_{\alpha\beta}^\nu \overline{\nu_{L\alpha}^C} \nu_{L\beta} + \text{h.c.}, \quad (1.4)$$

with

$$M_{\alpha\beta}^\nu = v^2 \cdot \frac{c_{\alpha\beta}^{d=5}}{M} \quad (1.5)$$

being the neutrino mass matrix. Note that this term violates lepton number, which is an accidental global symmetry of the SM. In order to reproduce the observed tiny neutrino masses, $m_\nu \lesssim \mathcal{O}(\text{eV})$, the coefficient in front of the Majorana term $\mathcal{C}_{\alpha\beta}^{d=5}$ have to be at least of the order $\mathcal{O}(10^{-14} \text{ GeV}^{-1})$. This can be accomplished having a very large new physics scale M , a very small (dimensionless) $c_{\alpha\beta}^{d=5}$ coefficient, or an intermediate solution between these two situations.

There are only three possible tree level processes that can lead to the effective Weinberg operator through the exchange of a new heavy field and which are invariant under the SM gauge group. These three possibilities give rise to the three types of see-saw models, which explain the tiny neutrino masses as a natural result from the exchange of: a heavy fermionic singlet N_R (type I), a heavy $SU(2)_L$ scalar triplet Δ (type II), or a heavy $SU(2)_L$ fermionic triplet Σ_R (type III). The three see-saw models are illustrated in Figure 1.1. In this thesis we will focus on the type I (Section 3) and type II (Section 4).

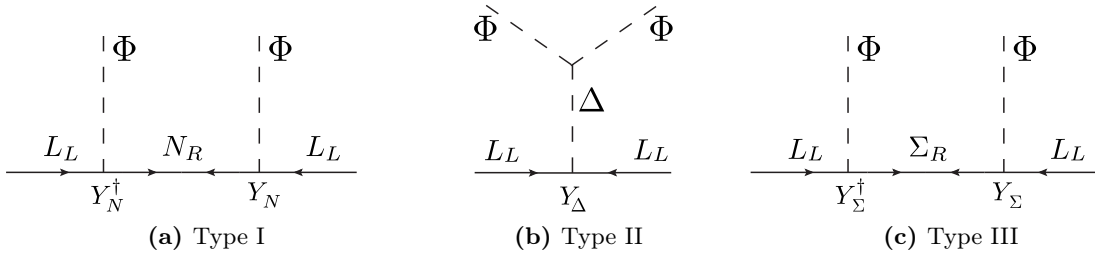


Figure 1.1: Feynman diagrams of the three different types of see-saw models that lead to the effective Weinberg operator through the tree level exchange of (a) a heavy fermionic singlet N_R , (b) a heavy $SU(2)_L$ scalar triplet Δ , or (c) a heavy $SU(2)_L$ fermionic triplet Σ_R .

Although embedding the SM into a high-energy theory, such as one of the different types of see-saw models, seems to be a reasonable continuation of the theoretical description of our universe, a conceptual issue appears when the new high-energy scale is too widely separated from the electroweak scale, which is known as the hierarchy problem. The hierarchy problem can arise when the SM is extended by new heavy particles. In this scenario, the Higgs mass parameter receive corrections from these new heavy particles due to quantum effects, which are quadratically proportional to new heavy particle masses [9]. Therefore, one would expect

the Higgs mass to be dragged towards the scale of the heavy particles. However, the discovery of the Higgs boson at the LHC with a mass of 125 GeV [10, 11], locates its mass at the electroweak scale. Thus, in the presence of a new high-energy scale much larger than the electroweak scale, a severe fine-tuning on the parameters of the theory is in principle needed in order to realize the physical Higgs mass.

Different attempts have been made to overcome the hierarchy problem addressing the root causes, for example by invoking new symmetries that protect scalar masses to suffer from large quantum corrections, such as supersymmetry [12, 13] and conformal symmetry (scale invariance) [14]; or by separating the scales not too widely, via e.g. extra-dimension theories [15, 16]. However, one should note that the presence of a new scale is necessary but not sufficient to generate the hierarchy problem. Indeed, from a pragmatic point of view one should take the model, calculate explicitly the new corrections to the scalar mass and express them in terms of measurable parameters. Only if those corrections are large compared to the measured values one can talk about a hierarchy problem. This argument can be turned around and use it to select possible extensions of the SM through a quantitative naturalness criterion. G. 't Hoff formulated this criterion as [1]

At any energy scale μ , a physical parameter or set of physical parameters $\alpha_i(\mu)$ is allowed to be very small only if the replacement $\alpha_i(\mu) = 0$ would increase the symmetry of the system.

According to this, small values for the fermions are accepted from a naturalness point of view thanks to the (broken) chiral symmetry of the SM Lagrangian. Indeed, although the electron mass, $m_e \sim \mathcal{O}(\text{MeV})$, is 10^{-5} orders of magnitude smaller than the electroweak scale, $\mathcal{O}(10^2 \text{ GeV})$, it is considered to be "naturally" small because $m_e \rightarrow 0$ induces an additional chiral symmetry, which allows to rotate the left- and right-handed fermion components leaving the theory unchanged. On the contrary, within the SM there is no symmetry that protects scalar masses. Thus, the smallness of the Higgs mass in the presence of an hypothetical large new physics scale is not acceptable from a naturalness perspective if a fine-tuning is needed to compensate for the quantum effects.

One can use the concept of naturalness as a guideline to set limits on the new large energy scales of the different extensions of the SM by requiring the radiative corrections to the Higgs mass parameter not to be too large. In the absence of large quantum corrections no hierarchy problem arises and the theory can still be considered to be "natural". This is the approach that we will take in this thesis. We will assume as the naturalness criterion that corrections to the Higgs mass introduced in the type I and the type II see-saw models should not be larger than the Higgs mass itself. We will then use this criterion to constrain the parameters and energy scales present in each of them².

The thesis is structured as follows. In Section 2, we will briefly review the SM of particle physics, focusing on the particle content and the characteristics of the different sectors and the Higgs mechanism for generating the gauge and fermion masses. We will also discuss further the two aspects of physics beyond the SM that will be addressed in this thesis: neutrino

²Note that in our discussion we will not rely on the Planck mass scale, since a quantum theory gravity is far from being established and its effects at low energies are yet unclear.

masses and the consequent neutrino mixing, and the hierarchy problem. In Section 3, we will study the type I see-saw model. We will present the theoretical framework and we will compute the new radiative corrections to the Higgs mass, putting an emphasis on the regularisation and renormalisation procedure. We will then discuss the implications of the results on the new mass scale from a naturalness point of view. In Section 4, we will consider the type II see-saw model. We will introduce the theoretical framework and the different constraints on the parameters of the model obtained by imposing the stability of the scalar vacuum and the unitarity of different tree-level scattering processes. We will then compute the radiative corrections to the Higgs mass parameter within this model. We will present the different experimental constraints coming from searches for lepton flavour violation (LFV) signals, direct searches at the LHC and electroweak precision data. Applying these constraints together with the vacuum stability, unitarity and perturbativity conditions up to the Planck scale, we will obtain the allowed parameter space and will analyse the implications on the observation of LFV processes in current and future experiments. Finally, we will summarize our conclusions in Section 5.

2 THE STANDARD MODEL AND BEYOND

2.1 THE STANDARD MODEL OF PARTICLE PHYSICS

The Standard Model of particle physics (SM) is a gauge theory based on the symmetry group $SU(3)_C \times SU(2)_L \times U(1)_Y$ that describes strong, weak and electromagnetic interactions through the exchange of spin one gauge fields: eight massless gluons, three massive vector bosons, W^\pm and Z , and one massless photon. The fermionic matter content is given by the known quarks and leptons, which appear in a three-fold family structure, and their corresponding antiparticles.

As we will see, the (unbroken) gauge invariance of the theory forbids explicit mass terms for both the gauge and the fermion sector. However, this is in contradiction with the experimentally observed non-zero masses of the W^\pm and Z bosons and the SM fermions. The solution to this problem is achieved by introducing a $SU(2)_L$ -doublet scalar with a non-zero vacuum expectation value (vev), which triggers the spontaneous symmetry breaking (SSB) of the electroweak group to the electromagnetic subgroup:

$$SU(3)_C \times SU(2)_L \times U(1)_Y \xrightarrow{SSB} SU(3)_C \times U(1)_Q. \quad (2.1)$$

This is the so-called Higgs mechanism, which generates masses for the weak gauge bosons and the SM fermions and lead to the appearance of a new physical scalar particle, the Higgs particle.

The SM particle content is summarized in Figure 2.1. In the following, we will describe the gauge, fermion and the scalar sectors of the SM and the Higgs mechanism to generate masses for the gauge and fermion fields. This section is based on Ref. [17], which gives a clear and pedagogical introduction to the electroweak symmetry breaking in the SM.

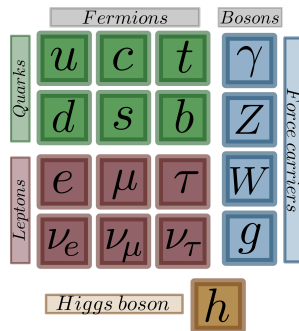


Figure 2.1: SM particle content.

2.1.1 Gauge sector

The dynamics of the gauge boson sector are encoded in the Lagrangian in terms of the field strength tensors

$$\mathcal{L}_{gauge} = -\frac{1}{4}G_{\mu\nu}^a G^{a\mu\nu} - \frac{1}{4}W_{\mu\nu}^a W^{a\mu\nu} - \frac{1}{4}B_{\mu\nu}B^{\mu\nu}, \quad (2.2)$$

where $G_{\mu\nu}^a$, $W_{\mu\nu}^a$ and $B_{\mu\nu}$ are the field strength tensors for the $SU(3)_C$, $SU(2)_L$ and $U(1)_Y$ interactions, respectively.

For the $U(1)_Y$ hypercharge interaction, the field strength tensor has the same form as in electromagnetism,

$$B_{\mu\nu} = \partial_\mu B_\nu - \partial_\nu B_\mu. \quad (2.3)$$

For the $SU(2)_L$ weak interaction, the field tensor can be written as

$$W_{\mu\nu}^a = \partial_\mu W_\nu^a - \partial_\nu W_\mu^a + g\epsilon^{abc}W_\nu^b W_\mu^c, \quad (2.4)$$

where g is the weak interaction coupling and ϵ^{abc} is the Levi-Civita tensor, with a, b, c running from 1 to 3.

For the $SU(3)_C$ strong interaction, the field tensor takes the form

$$G_{\mu\nu}^a = \partial_\mu G_\nu^a - \partial_\nu G_\mu^a + g_s f^{abc}G_\nu^b G_\mu^c, \quad (2.5)$$

where g_s is the strong interaction coupling and f^{abc} are the antisymmetric structure constants of $SU(3)$, defined in terms of the group generators t^a as

$$[t^a, t^b] = i f^{abc} t^c, \quad (2.6)$$

with a, b, c running from 1 to 8. Eq. (2.5) is in fact the general form for the field strength tensor of a non-abelian group. The last term, which involves the structure constants of the group, gives rise to self-interactions between the gauge fields. This is a characteristic feature of non-abelian theories.

The infinitesimal gauge transformations of the gauge boson fields are given by

$$U(1)_Y : B_\mu \rightarrow B_\mu + \frac{1}{g'} \partial_\mu \lambda_Y(x) \quad (2.7)$$

$$SU(2)_L : W_\mu^a \rightarrow W_\mu^a + \frac{1}{g} \partial_\mu \lambda_L^a(x) + \epsilon^{abc} W_\mu^b \lambda_L^c(x) \quad (2.8)$$

$$SU(3)_C : G_\mu^a \rightarrow G_\mu^a + \frac{1}{g_s} \partial_\mu \lambda_C^a(x) + f^{abc} G_\mu^b \lambda_C^c(x) \quad (2.9)$$

where g' , g and g_s are the coupling strengths of the hypercharge, weak and strong interactions, respectively.

A mass term for a gauge boson takes the form

$$\mathcal{L}_{m_B} = \frac{1}{2} m_B^2 B_\mu B^\mu. \quad (2.10)$$

Since this term is not gauge invariant, it cannot be inserted by hand into the Lagrangian. Therefore, (unbroken) gauge invariance implies that gauge bosons are all massless.

2.1.2 Fermion sector

The chiral fermionic matter content is given by the known quarks and leptons, which are organized in three generations. The three generations have identical gauge interactions and differ only by their mass and flavour quantum number. The content of one generation, together with their hypercharge Y , the third component of their $SU(2)_L$ isospin I_3 and their $SU(3)_C$ (color) transformation properties is given in Table 2.1. Note that the left-handed fields transform as doublets under $SU(2)_L$, while their right-handed partners transform as $SU(2)_L$ singlets. In our convention their charge is give by $Q = T^3 + Y$.

The infinitesimal gauge transformations of the SM fermion fields are given by

$$U(1)_Y : \psi \rightarrow e^{i\lambda_Y(x)Y} \psi, \quad (2.11)$$

$$SU(2)_L : \psi \rightarrow e^{i\lambda_L^a(x)T^a} \psi, \quad (2.12)$$

$$SU(3)_C : \psi \rightarrow e^{i\lambda_C^a(x)t^a} \psi, \quad (2.13)$$

where Y is the hypercharge operator, and T^a and t^a are the $SU(2)$ and $SU(3)$ generators, respectively. T^a is just $\sigma^a/2$ when acting on a doublet representation of $SU(2)$, with σ^a being the Pauli matrices¹. Note that the $SU(2)_L$ and $SU(3)_C$ transformations only apply for the $SU(2)_L$ -doublets and the $SU(3)_C$ -triplets, respectively, while those which are singlets under these transformations remain unchanged.

The left- and right-handed chiral fermion fields are obtained from an unpolarized Dirac spinor using the projection operators:

$$P_R = \frac{1}{2}(1 + \gamma^5), \quad P_L = \frac{1}{2}(1 - \gamma^5), \quad (2.14)$$

such that

$$\psi_R \equiv P_R \psi, \quad \psi_L \equiv P_L \psi. \quad (2.15)$$

The projection operators satisfy $P_R^2 = P_R$, $P_L^2 = P_L$ and $P_L + P_R = \mathbb{1}$.

The Dirac Lagrangian for a generic fermion ψ with mass m is given by

$$\mathcal{L} = \bar{\psi} i \partial_\mu \gamma^\mu \psi - m \bar{\psi} \psi. \quad (2.16)$$

This can be rewritten in terms of the chiral states by inserting a factor of $\mathbb{1} = (P_L^2 + P_R^2)$ before ψ and using the anticommutator relation $\{\gamma^\mu, \gamma^5\} = 0$ of the gamma matrices, which leads to

$$\mathcal{L} = \bar{\psi}_L i \partial_\mu \gamma^\mu \psi_L + \bar{\psi}_R i \partial_\mu \gamma^\mu \psi_R - m \bar{\psi}_R \psi_L - m \bar{\psi}_L \psi_R. \quad (2.17)$$

The kinetic term separates neatly into two terms, one involving only ψ_L and another only ψ_R . To make this term gauge invariant we promote the derivative ∂_μ to a covariant derivative \mathcal{D}_μ . The covariant derivative is defined according to the field on which it acts, since the fields

¹The Pauli matrices are given by: $\sigma_1 = \begin{pmatrix} 0 & 1 \\ 1 & 0 \end{pmatrix}$; $\sigma_2 = \begin{pmatrix} 0 & -i \\ i & 0 \end{pmatrix}$; $\sigma_3 = \begin{pmatrix} 1 & 0 \\ 0 & -1 \end{pmatrix}$.

Particle content	Quarks			Leptons	
	$Q_L \equiv \begin{pmatrix} u_L \\ d_L \end{pmatrix}$	u_R	d_R	$L_L \equiv \begin{pmatrix} \nu_L \\ e_L \end{pmatrix}$	e_R
Hypercharge (Y)	1/6	2/3	-1/3	-1/2	-1
Isospin (I_3)	$\begin{pmatrix} 1/2 \\ -1/2 \end{pmatrix}$	0	0	$\begin{pmatrix} 1/2 \\ -1/2 \end{pmatrix}$	0
Colour	triplet	triplet	triplet	singlet	singlet

Table 2.1: Chiral fermion content of a single generation of the SM with their respective hypercharges Y , the third component of their isospin I_3 and their $SU(3)_C$ (color) transformation properties. In our convention their charge is given by $Q = I_3 + Y$.

have different gauge transformation properties depending on whether they are charged or not under each gauge transformation. It is given by:

$$\mathcal{D}_\mu Q_L = \left(\partial_\mu - i\frac{g'}{6}B_\mu - igW_\mu^a \frac{\sigma^a}{2} - ig_s G_\mu^{at^a} \right) Q_L, \quad (2.18)$$

$$\mathcal{D}_\mu u_R = \left(\partial_\mu - i\frac{2}{3}g'B_\mu - ig_s G_\mu^{at^a} \right) u_R, \quad (2.19)$$

$$\mathcal{D}_\mu d_R = \left(\partial_\mu + i\frac{1}{3}g'B_\mu - ig_s G_\mu^{at^a} \right) d_R, \quad (2.20)$$

$$\mathcal{D}_\mu L_L = \left(\partial_\mu + i\frac{1}{2}g'B_\mu - igW_\mu^a \frac{\sigma^a}{2} \right) L_L, \quad (2.21)$$

$$\mathcal{D}_\mu e_R = \left(\partial_\mu + ig'B_\mu \right) e_R. \quad (2.22)$$

Note that the covariant derivative gives rise to the interaction terms between gauge bosons and fermions. The different coefficients of the hypercharge gauge interaction are given by the values of the hypercharge Y (see Table 2.1).

In contrast with the kinetic term, the mass terms involve fermions of both chiralities. Since the right- and left-handed fermions of the SM transform differently under $SU(2)_L \times U(1)_Y$, such mass terms are not gauge invariant and thus cannot be inserted by hand into the Lagrangian without explicitly breaking the symmetry. Therefore, (unbroken) gauge invariance implies that all the SM fermions are massless.

2.1.3 The SM Higgs mechanism

In order to give masses to the gauge bosons and the SM fermions, we need to add a $SU(2)_L$ -doublet of complex scalar fields:

$$\Phi = \begin{pmatrix} \phi^+ \\ \phi^0 \end{pmatrix} = \frac{1}{\sqrt{2}} \begin{pmatrix} \phi_1 + i\phi_2 \\ \phi_3 + i\phi_4 \end{pmatrix}, \quad (2.23)$$

with hypercharge $Y = 1/2$, called Higgs doublet. Here $\phi_1, \phi_2, \phi_3, \phi_4$ are properly normalized real scalar fields. Under an infinitesimal gauge transformation, Φ transforms as

$$U(1)_Y : \Phi \rightarrow e^{i\lambda_Y(x)\cdot\frac{1}{2}}\Phi, \quad (2.24)$$

$$SU(2)_L : \Phi \rightarrow e^{i\lambda_L^a(x)\frac{\sigma^a}{2}}\Phi. \quad (2.25)$$

Since Φ is not color-charged, it remains invariant under $SU(3)_C$.

The Lagrangian for the Higgs doublet is given by

$$\mathcal{L}_\Phi = (\mathcal{D}_\mu\Phi)^\dagger(\mathcal{D}^\mu\Phi) - V(\Phi) + \mathcal{L}_{\text{Yukawa}}. \quad (2.26)$$

The first term contains the kinetic and gauge interaction terms via the covariant derivative, which reads

$$\mathcal{D}_\mu = \partial_\mu - i\frac{g'}{2}B_\mu - igW_\mu^a\frac{\sigma^a}{2}. \quad (2.27)$$

The second term is the scalar potential,

$$V(\Phi) = -\mu^2\Phi^\dagger\Phi + \lambda(\Phi^\dagger\Phi)^2, \quad (2.28)$$

with $\lambda > 0$ and $-\mu^2 < 0$. Finally, the third term contains the Yukawa couplings of the scalar field to pair of fermions,

$$\mathcal{L}_{\text{Yukawa}} = -\bar{Q}_LY_d\Phi d_R - \bar{Q}_LY_u\tilde{\Phi}u_R - \bar{L}_LY_e\Phi e_R + \text{h.c.}, \quad (2.29)$$

where Y_d, Y_u, Y_e are dimensionless 3×3 complex matrices, called Yukawa coupling matrices, and $\tilde{\Phi}$ is the conjugate Higgs doublet, given by

$$\tilde{\Phi} \equiv i\sigma_2\Phi^* = (\phi^{0*} \quad -\phi^-)^T, \quad (2.30)$$

with hypercharge $Y = -1/2$.

The signs of the two parameters in the Higgs potential are crucial. The requirement of λ to be positive ensures that the potential is bounded from below and therefore there exist a stable vacuum state. The mass parameter μ^2 could be taken to be positive or negative. If $-\mu^2 > 0$, the potential energy function has a trivial minimum at zero. On the other hand, for $-\mu^2 < 0$ the potential energy function develops a Mexican hat shape, with an infinite set of equivalent minimum energy states away from zero. Once a particular vacuum is chosen, the vacuum state is not invariant under $SU(2)_L \times U(1)_Y$ anymore: we say that the gauge symmetry is spontaneously broken in the vacuum.

To find the vacuum expectation value we first minimize the potential in Eq. (2.28). The minimum of the potential corresponds to those field configurations satisfying

$$\Phi^\dagger\Phi = \frac{\mu^2}{2\lambda}. \quad (2.31)$$

Since the electric charge is a conserved quantity, only the neutral scalar field can acquire a vev: $\langle\phi^0\rangle \equiv v/\sqrt{2}$. We can choose the ground state such that the vevs for the four real scalar fields are:

$$\langle\phi_3\rangle \equiv v = \sqrt{\frac{\mu^2}{\lambda}}, \quad \langle\phi_1\rangle = \langle\phi_2\rangle = \langle\phi_4\rangle = 0, \quad (2.32)$$

and define a new real scalar field h with zero vacuum value, $\langle h \rangle = 0$, according to

$$\phi_3 = h + v. \quad (2.33)$$

Then, the doublet scalar field becomes

$$\Phi = \frac{1}{\sqrt{2}} \begin{pmatrix} \phi_1 + i\phi_2 \\ v + h + i\phi_4 \end{pmatrix}. \quad (2.34)$$

The Higgs doublet can also be parametrized in the form

$$\Phi = \frac{1}{\sqrt{2}} \exp\left(\frac{i\xi^a \sigma^a}{v}\right) \begin{pmatrix} 0 \\ v + h \end{pmatrix}, \quad (2.35)$$

which is equivalent to Eq. (2.34) up to linear order in the fields with the identification $\xi^1 = \phi_2$, $\xi^2 = \phi_1$ and $\xi^3 = -\phi_4$.

The local $SU(2)_L$ symmetry of the Lagrangian allows us to gauge away the fields ξ^a , or equivalently ϕ^1, ϕ^2, ϕ^4 , and arrive to

$$\Phi = \frac{1}{\sqrt{2}} \begin{pmatrix} 0 \\ v + h \end{pmatrix}, \quad (2.36)$$

which is called unitary gauge. We will use unitary gauge in the rest of this section. The fields ξ^a , which have been completely removed from the Lagrangian by means of gauge invariance, are called Goldstone bosons. They are no physical degrees of freedom, but their degrees of freedom are associated to those corresponding to the longitudinal modes of the gauge bosons W^\pm and Z once these acquire mass.

After SSB, mass terms for the gauge bosons and the SM fermions are generated, as well as a mass term for the physical Higgs field.

Gauge boson masses

The mass of the gauge bosons is obtained from the gauge-kinetic term after SSB,

$$\begin{aligned} \mathcal{L}_{\text{kin}} &= (\mathcal{D}_\mu \Phi)^\dagger (\mathcal{D}^\mu \Phi) \\ &= \frac{1}{2} (\partial_\mu h) (\partial^\mu h) + \frac{1}{4} g^2 (v + h)^2 W_\mu^+ W^{-\mu} + \frac{1}{8} (g^2 + g'^2) (v + h)^2 Z_\mu Z^\mu \end{aligned}$$

where we have defined the charged W and the neutral Z bosons as

$$W_\mu^+ = \frac{W_\mu^1 - iW_\mu^2}{\sqrt{2}}, \quad W_\mu^- = \frac{W_\mu^1 + iW_\mu^2}{\sqrt{2}} \quad (2.37)$$

and

$$Z_\mu = \frac{1}{\sqrt{g^2 + g'^2}} (gW_\mu^3 - g'B_\mu). \quad (2.38)$$

Expanding the $(v + h)^2$ -term we obtain the mass terms for W^\pm and Z and their interaction terms with the Higgs. Their masses are given by

$$M_W^2 = \frac{g^2 v^2}{4}, \quad M_Z^2 = \frac{(g^2 + g'^2) v^2}{4}. \quad (2.39)$$

Fermion masses

The mass of the quarks and leptons are obtained from the Yukawa term after SSB,

$$\begin{aligned}\mathcal{L}_{\text{Yukawa}} &= -y_{ij}^u \bar{Q}_{Li} \tilde{\Phi} u_{Rj} - y_{ij}^d \bar{Q}_{Li} \Phi d_{Rj} - y_{ij}^e \bar{L}_{Li} \Phi e_{Rj} + \text{h.c.} \\ &= -y_{ij}^u \bar{u}_{Li} \frac{(v+h)}{\sqrt{2}} u_{Rj} - y_{ij}^d \bar{d}_{Li} \frac{(v+h)}{\sqrt{2}} d_{Rj} - y_{ij}^e \bar{e}_{Li} \frac{(v+h)}{\sqrt{2}} e_{Rj} + \text{h.c.},\end{aligned}\quad (2.40)$$

where y_{ij}^u , y_{ij}^d , y_{ij}^e are the entries of the Yukawa matrices Y_u , Y_d and Y_e , respectively. From this expression we obtain the fermion mass matrices in generation space

$$\mathcal{M}_{ij}^u = \frac{v}{\sqrt{2}} y_{ij}^u, \quad \mathcal{M}_{ij}^d = \frac{v}{\sqrt{2}} y_{ij}^d, \quad \mathcal{M}_{ij}^e = \frac{v}{\sqrt{2}} y_{ij}^e, \quad (2.41)$$

each containing 9 complex entries.

To find the quark mass eigenstates we just need to diagonalize \mathcal{M}_{ij}^u and \mathcal{M}_{ij}^d , which can be done by an appropriate unitary transformation,

$$\begin{pmatrix} u_1 \\ u_2 \\ u_3 \end{pmatrix}_{L,R} = U_{L,R} \begin{pmatrix} u \\ c \\ t \end{pmatrix}_{L,R}, \quad \begin{pmatrix} d_1 \\ d_2 \\ d_3 \end{pmatrix}_{L,R} = D_{L,R} \begin{pmatrix} d \\ s \\ b \end{pmatrix}_{L,R}, \quad (2.42)$$

where u_i and d_i ($i = 1, 2, 3$) are the flavour-eigenstates and u, c, t and d, s, b are the mass eigenstates. These transformations are chosen such that,

$$U_L \mathcal{M}^u U_R^\dagger = \begin{pmatrix} m_u & 0 & 0 \\ 0 & m_c & 0 \\ 0 & 0 & m_t \end{pmatrix}, \quad D_L \mathcal{M}^d D_R^\dagger = \begin{pmatrix} m_d & 0 & 0 \\ 0 & m_s & 0 \\ 0 & 0 & m_b \end{pmatrix}. \quad (2.43)$$

Diagonalizing the mass matrices \mathcal{M}^u and \mathcal{M}^d in this way simultaneously diagonalizes the Yukawa matrices, which gives the relation between the quark Yukawa couplings and their masses:

$$m_q = y_q \frac{v}{\sqrt{2}}, \quad (2.44)$$

where y_q is the appropriate eigenvalues of the Yukawa matrix Y_u of Y_d .

Notice that the up-type quarks and down-type quarks are diagonalized by different matrices. This will show up in the charged-current weak interaction, which contains combinations of u_{Lj} and d_{Lj} of the same flavour-family:

$$\bar{u}_{L1} \gamma^\mu d_{L1}, \quad \bar{u}_{L2} \gamma^\mu d_{L2}, \quad \bar{u}_{L3} \gamma^\mu d_{L3}. \quad (2.45)$$

The sum of these terms can be written in matrix form as

$$(\bar{u}_1, \bar{u}_2, \bar{u}_3)_L \gamma^\mu \begin{pmatrix} d_1 \\ d_2 \\ d_3 \end{pmatrix}_L = (\bar{u}, \bar{c}, \bar{t})_L U_L^\dagger \gamma^\mu D_L \begin{pmatrix} d \\ s \\ b \end{pmatrix}_L \quad (2.46)$$

After writing it into mass eigenstates, transitions within different mass generations appear, which are described by the Cabibbo-Kobayashi-Maskawa (CKM) matrix:

$$V_{CKM} \equiv U_L^\dagger D_L. \quad (2.47)$$

On the other hand, the neutral current interactions, which are mediated by the photon and the Z boson, couple pairs of u_{Lj} and d_{Lj} of the same flavour family separately. The sum can be written, e.g. for the up-type quark, as

$$(\bar{u}_1, \bar{u}_2, \bar{u}_3)_L \gamma^\mu \begin{pmatrix} u_1 \\ u_2 \\ u_3 \end{pmatrix}_L = (\bar{u}, \bar{c}, \bar{t})_L U_L^\dagger \gamma^\mu U_L \begin{pmatrix} u \\ c \\ t \end{pmatrix}_L \quad (2.48)$$

Since $U_L^\dagger U_L = \mathbb{1}$, the neutral currents are automatically flavour diagonal. This is a manifestation of the GIM mechanism [18], which forbids flavour changing neutral currents (FCNCs) at tree level in the SM. Since the content of this thesis is not connected to the electroweak quark currents, the CKM matrix and the GIM mechanism will not be discussed further.

For the lepton masses, we can diagonalize \mathcal{M}^e similarly to the quark case, defining

$$\begin{pmatrix} e_1 \\ e_2 \\ e_3 \end{pmatrix}_{L,R} = E_{L,R} \begin{pmatrix} e \\ \mu \\ \tau \end{pmatrix}_{L,R}, \quad (2.49)$$

such that

$$E_L \mathcal{M}^e E_R^\dagger = \begin{pmatrix} m_e & 0 & 0 \\ 0 & m_\mu & 0 \\ 0 & 0 & m_\tau \end{pmatrix}. \quad (2.50)$$

Within the SM, neutrinos are massless. Therefore, there is no neutrino mass matrix which needs to be diagonalized. By redefining the neutrino fields as $\tilde{\nu}_{Li} \equiv E_L^\dagger \nu_{Li}$, the effect of the rotation of the electron-type leptons is reabsorbed and no mixing within mass generations appear in the charged current interactions in the lepton sector, unlike for the quark sector. However, it is known that neutrinos, although being very light, are in fact massive. Regardless of how their masses are produced, this fact induces a mixing matrix analogous to the CKM, called the Pontecorvo-Maki-Nakagawa-Sakata (PMNS) matrix, which allows for mixing within the different generations. We will discuss further on neutrino mixing in the next subsection.

Higgs mass

Finally, the Higgs mechanism also gives mass to the Higgs boson. Going back to the Higgs potential,

$$\begin{aligned} V(\Phi) &= -\mu^2 \Phi^\dagger \Phi + \lambda (\Phi^\dagger \Phi)^2 \\ &= -\lambda v^2 h^2 - \lambda v h^3 - \frac{\lambda}{4} h^4 + \text{const.}, \end{aligned} \quad (2.51)$$

where the relation $\mu^2 = \lambda v^2$, which is obtained after minimizing the potential, was used (see Eq. (2.31)). The first term gives the mass for the real scalar Higgs field:

$$m_h^2 = 2\lambda v^2. \quad (2.52)$$

Experimentally, the values at tree-level are given by $m_h^2 = 125 \text{ GeV}$ and $v \simeq 246 \text{ GeV}$ [8]. The second and third terms in Eq. (2.51) are the self-interaction terms of the Higgs boson.

2.2 PHYSICS BEYOND THE STANDARD MODEL

In this section we will focus on the physics beyond the SM which will be addressed in this thesis: the non-zero mass of neutrinos and the electroweak hierarchy problem.

2.2.1 Neutrino masses and mixing

The nature of neutrinos is yet unknown: they could be Dirac particles, just like all the other fermions, or Majorana particles, if they were their own antiparticle. Note that only neutrinos can have a Majorana nature, since they are the only fundamental neutral fermion. If neutrinos are Dirac fields, a Dirac mass term can be written for them in analogy to the up-type quark mass term. If neutrinos are Majorana, also a Majorana mass term can be introduced, in addition to the Dirac one. We will study the form of the two possible terms in the following.

Dirac masses

Independently of the nature of the neutrinos, we can introduce three right-handed neutrino fields ν_{Ri} ($i = 1, 2, 3$) and write Dirac neutrino masses in a similar way than the up-type quark masses:

$$\mathcal{L}_{\text{Yukawa}} \supset -\bar{L}_L Y_\nu \tilde{\Phi} e_R + \text{h.c.} \quad (2.53)$$

Including also the charged lepton mass term we obtain the Yukawa term of the whole lepton sector, which in component notation is given by:

$$\begin{aligned} \mathcal{L}_{\text{Yukawa}}^{\text{lep}} &= -y_{ij}^u \bar{Q}_{Li} \tilde{\Phi} u_{Rj} - y_{ij}^e \bar{L}_{Li} \Phi e_{Rj} + \text{h.c.} \\ &= -y_{ij}^\nu \bar{\nu}_{Li} \frac{(v+h)}{\sqrt{2}} \nu_{Rj} - y_{ij}^e \bar{e}_{Li} \frac{(v+h)}{\sqrt{2}} e_{Rj} + \text{h.c.}, \end{aligned} \quad (2.54)$$

where y_{ij}^ν and y_{ij}^e are the entries of the Yukawa matrix Y_ν and Y_e . The lepton mass matrices in generation space are

$$\mathcal{M}_{ij}^\nu = \frac{v}{\sqrt{2}} y_{ij}^\nu, \quad \mathcal{M}_{ij}^e = \frac{v}{\sqrt{2}} y_{ij}^e, \quad (2.55)$$

each containing 9 complex entries.

Analogously to the quark sector, the Dirac masses for the charged lepton and neutrinos the mass eigenstates e_1, e_2, e_3 and the neutrino eigenstates ν_1, ν_2, ν_3 are obtained by diagonalizing the mass matrices:

$$V_L \mathcal{M}^\nu V_R^{-1} = \begin{pmatrix} m_1 & 0 & 0 \\ 0 & m_2 & 0 \\ 0 & 0 & m_3 \end{pmatrix} \quad E_L \mathcal{M}^e E_R^{-1} = \begin{pmatrix} m_e & 0 & 0 \\ 0 & m_\mu & 0 \\ 0 & 0 & m_\tau \end{pmatrix}, \quad (2.56)$$

with the transformations

$$\begin{pmatrix} \nu_1 \\ \nu_2 \\ \nu_3 \end{pmatrix}_{L,R} = V_{L,R} \begin{pmatrix} \nu_e \\ \nu_\mu \\ \nu_\tau \end{pmatrix}_{L,R} \quad \begin{pmatrix} e_1 \\ e_2 \\ e_3 \end{pmatrix}_{L,R} = E_{L,R} \begin{pmatrix} e \\ \mu \\ \tau \end{pmatrix}_{L,R}. \quad (2.57)$$

Parameter	Hierarchy	best-fit	1σ range	3σ range
$\delta m^2/10^{-5} \text{ eV}^2$	NH or IH	7.37	7.21 – 7.54	6.93 – 7.97
$\Delta m^2/10^{-3} \text{ eV}^2$	NH	2.50	2.46 – 2.54	2.37 – 2.63
$\Delta m^2/10^{-3} \text{ eV}^2$	IH	2.46	2.42 – 2.51	2.33 – 2.60
$\sin^2 \theta_{12}/10^{-1}$	NH or IH	2.97	2.81 – 3.14	2.50 – 3.54
$\sin^2 \theta_{13}/10^{-2}$	NH	2.14	2.05 – 2.25	1.85 – 2.46
$\sin^2 \theta_{13}/10^{-2}$	IH	2.18	2.06 – 2.27	1.86 – 2.48
$\sin^2 \theta_{23}/10^{-1}$	NH	4.37	4.17 – 4.70	3.79 – 6.16
$\sin^2 \theta_{23}/10^{-1}$	IH	5.69	4.28 – 4.91 \oplus 5.18 – 5.97	3.83 – 6.37
δ/π	NH	1.35	1.13 – 1.64	0 – 2
δ/π	IH	1.32	1.07 – 1.67	0 – 2

Table 2.2: Best fit values 1σ and 3σ allowed ranges of the 3-neutrino oscillation parameters. The squared-mass differences are defined as $\delta m^2 = m_2^2 - m_1^2$ and $\Delta m^2 = m_3^2 - (m_1^2 + m_2^2)/2$, with $+\Delta m^2$ for normal hierarchy (NH) and $-\Delta m^2$ for inverted hierarchy (IH). The CP violation phase is taken in the (cyclic) interval $\delta/\pi \in [0, 2]$ [19].

Alternatively, it is also possible to choose the basis in which the charged lepton flavour eigenstates are diagonal, i.e. are also the mass eigenstates, and absorb into the neutrino rotation matrix the rotation matrix of the charged leptons. Then, the flavour eigenstates of the neutrinos ν_1, ν_2, ν_3 are related to their mass eigenstates by

$$\begin{pmatrix} \nu_e \\ \nu_\mu \\ \nu_\tau \end{pmatrix}_L = U_{\text{PMNS}} \begin{pmatrix} \nu_1 \\ \nu_2 \\ \nu_3 \end{pmatrix}_L, \quad (2.58)$$

where U_{PMNS} is the Pontecorvo-Maki-Nakagawa-Sakata matrix, which is the lepton analogue of the CKM matrix. It is related with the rotation matrices of Eq. (2.57) through

$$U_{\text{PMNS}} = E_L V_L^\dagger. \quad (2.59)$$

The elements in the PMNS matrix are typically denoted by indices, e.g. U_{e1} corresponds to the (1,1) element, which makes easy to remember the form of Eq. (2.58). It is parametrized in terms of the three mixing angles $\theta_{12}, \theta_{23}, \theta_{13}$, and one Dirac phase δ , and two Majorana CP -phases α_1, α_2 . It is usually written in terms of three rotations and a phase matrix:

$$U_{\text{PMNS}} = \begin{pmatrix} 1 & 0 & 0 \\ 0 & c_{23} & s_{23} \\ 0 & -s_{23} & c_{23} \end{pmatrix} \begin{pmatrix} c_{13} & 0 & s_{13}e^{-i\delta} \\ 0 & 1 & 0 \\ -s_{13}e^{i\delta} & 0 & c_{13} \end{pmatrix} \begin{pmatrix} c_{12} & s_{12} & 0 \\ -s_{12} & c_{12} & 0 \\ 0 & 0 & 1 \end{pmatrix} \text{diag}(1, e^{i\alpha_1}, e^{i\alpha_2}), \quad (2.60)$$

where we have used the standard notation $c_{ij} \equiv \cos \theta_{ij}$ and $s_{ij} \equiv \sin \theta_{ij}$. The three mixing angles are often called atmospheric (θ_{23}), reactor (θ_{13}) and solar (θ_{12}) angle, according to the type of experiments in which they are better measured. The Dirac phase δ leads to CP violation for values $\delta \neq \{0, \pi\}$. The Majorana phases (α_1, α_2) are only present if neutrinos are Majorana particles.

The recent global analysis of three-neutrino oscillation data is reported in Table 2.2.

Note that the Yukawa couplings needed to generate the neutrino masses are extremely small: for a neutrino mass $m_\nu \sim 0.1$ eV, the corresponding neutrino Yukawa coupling would be

$$y_\nu = \frac{\sqrt{2}}{v} m_\nu \simeq 6 \times 10^{-13}. \quad (2.61)$$

The smallness of the Yukawa couplings have lead many physicist to wonder about the possibility of a hidden mechanism that could account for the small values of neutrino masses.

Majorana mass

If neutrinos are Majorana, a Majorana mass term is also allowed in the Lagrangian. This term was already discussed in the introduction, Section 1, so we will just briefly review it here. The dimension five Weinberg operator,

$$\mathcal{L}_{\text{Majorana}} = \frac{1}{2} \frac{c_{\alpha\beta}^{d=5}}{M} \left(\overline{L_{L\alpha}^C} \tilde{\Phi}^* \right) \left(\tilde{\Phi}^\dagger L_{L\beta} \right) + \text{h.c.}, \quad (2.62)$$

leads, after SSM $\langle \phi^0 \rangle = v/2$, to a Majorana mass term for the neutrino:

$$\mathcal{L}_{\text{Majorana}} \supset \frac{1}{2} M_{\alpha\beta}^\nu \overline{\nu_{L\alpha}^C} \nu_{L\beta} + \text{h.c.}, \quad (2.63)$$

with the neutrino mass matrix defined as

$$M_{\alpha\beta}^\nu = v^2 \cdot \frac{c_{\alpha\beta}^{d=5}}{M} \quad (2.64)$$

Here M indicates the scale beyond which a more complete theory must reveal itself, and $c_{\alpha\beta}^{d=5}$ a dimensionless coefficient determined by the high-energy theory. Neutrino masses of $m_\nu \sim 0.1$ eV require $c_{\alpha\beta}^{d=5}/M \sim \mathcal{O}(10^{-14} \text{ GeV}^{-1})$. For $c_{\alpha\beta}^{d=5} \sim \mathcal{O}(1)$, the new energy scale would have to be of order $\mathcal{O}(10^{14} \text{ GeV})$. Nevertheless, the required energy scale can be lowered if the coefficients $c_{\alpha\beta}^{d=5}$ take smaller values.

2.2.2 Absolute neutrino mass scale

To date, the absolute scale of the active neutrino masses is unknown, and only upper limits have been set. These can be obtained from Kurie plot experiments, neutrinoless double beta decay and from cosmological considerations, which we will discuss here briefly.

Tritium β -decay

A limit on the mass of the electron neutrino can be determined by measuring the spectrum of electrons near the endpoint in ${}^3\text{H}$ β -decays with high precision. The current best limit is given by the Mainz experiment [20]

$$m_{\nu_e}^{(\text{eff})} \equiv \left(\sum_i |U_{ei}|^2 m_{\nu_i}^2 \right)^{1/2} < 2.3 \text{ eV}. \quad (2.65)$$

The KATRIN experiment [21] is expected to improve this limit by one order of magnitude down to 0.2 eV or discover the actual mass, if it is larger than 0.35 eV.

In addition to the direct mass measurement from beta spectroscopy, there are two further observables which are sensitive to the absolute mass scale, namely, the effective Majorana mass in neutrinoless double beta decay, $\langle m_{ee} \rangle$, and the sum of relativistic neutrino species Σ_ν .

Neutrinoless double beta decay

Neutrinoless double beta decay ($0\nu\beta\beta$) is an exotic process in which two neutrons in an isotope (A, Z) decay simultaneously into two protons and two electrons without the emission of neutrinos:

$$0\nu\beta\beta : (A, Z) \rightarrow (A, Z + 2) + 2e^- . \quad (2.66)$$

This process can only take place under the condition that neutrinos are massive and are their own antiparticles, i.e. they are Majorana neutrinos. In addition to confirming the Majorana nature of the neutrinos, the observation of neutrinoless double beta decay would also give information on the absolute neutrino mass scale, Majorana phases in the PMNS matrix and potentially the neutrino mass hierarchy [22]².

The decay rate is proportional to the square of the effective Majorana neutrino mass, which is defined as

$$\langle m_{ee} \rangle = \left| \sum_{i=1}^3 U_{ei}^2 \cdot m_i \right|. \quad (2.67)$$

The current searches involving ^{76}Ge (GERDA [23]) and ^{136}Xe (KamLAND-Zen [24] and EXO-200 [25]) provide upper limits on $\langle m_{ee} \rangle \sim 0.2\text{--}0.4$ eV. The recently published improved search from KamLAND-Zen [26] lowers this upper limits to the range 61 – 165 eV, which provides the strongest constraint on the lightest neutrino mass $m_{\text{lightest}} < (180 - 480)$ meV. However, these bounds are limited by the nuclear matrix element calculations and might be a bit to stringent.

Note that since the Majorana CP-phases are unknown, strong cancellations in the sum over all neutrino states can occur for the effective Majorana mass m_{ee} , Eq. (2.67). This cancellations cannot happen for $m_{\nu_e}^{(\text{eff})}$, Eq. (2.65), since in its expression the squared mixing matrix elements $|U_{ei}|^2$ are involved and therefore the sum contains only non-negative elements. Hence, the neutrino mass $m_{\nu_e}^{(\text{eff})}$ obtained from experiments fixes the absolute neutrino mass scale ($m_1 \approx m_2 \approx m_3$), given the small values of Δm^2 [21].

Cosmology

Finally, the sum of relativistic neutrino species is defined as

$$\Sigma_\nu = \sum_{i=1}^3 m_i, \quad (2.68)$$

and can be constrained by cosmological observables. The current limits from cosmology are rather model dependent and vary strongly with the data combination adopted. For example,

²Neutrinoless double beta decay can be mediated not only by massive light neutrinos (standard interpretation) but also by other exotic particles present in different extensions of the SM. For example, the scalar triplet introduced in the type II see-saw model could also contribute to the process. However, the branching ratio for the triplet scalar exchange is very suppressed with respect to the neutrino exchange [22].

using baryon acoustic oscillations (BAO) and temperature fluctuations in the spectrum of the cosmic microwave background (CMB) data, an upper limit for the sum of the neutrino masses of 0.23 eV (95% CL; *Planck*+WP+highL+BAO) is found [27]. However, this constrain can be weakened adopting a different data combination. We refer to [27] and citations therein for further details on the different possible cosmological constrains.

2.2.3 Scalar masses and the hierarchy problem

Because the SM is as a quantum field theory, radiative effects modify the correlation functions, i.e. the particle propagators and the different interaction processes. These quantum effects can be expressed via loop diagrams. During the calculation of these loop contributions, one often encounters unphysical divergences. In order to make the physical results finite, the theory needs to be renormalised. In particular, the infinities appearing in the self-energy loops, which are the loop graphs contributing to the two-point functions, are removed by the mass and field strength renormalisation of the scalar field, which introduces a finite set of the so-called counterterms. These counterterms cancel the different divergent parts and are scheme-dependent, i.e. they are defined differently in different renormalisation schemes. Figure 2.2 shows schematically some examples of loop corrections contributing to the scalar propagator coming from scalar (left), fermion (middle) and vector boson (right) particles that couple to the scalar field.

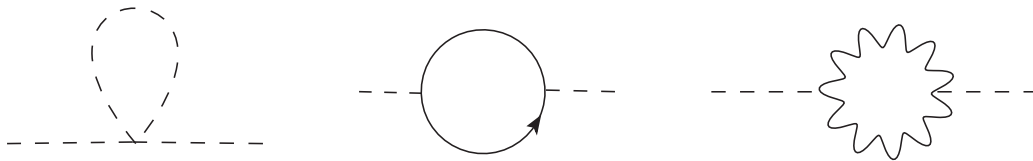


Figure 2.2: Three basic examples of loop diagrams that contribute through radiative corrections to a generic scalar propagator. From left to right: scalar (dashed line), fermionic (solid line) and vector (wavy line) loop.

In the on-shell renormalisation scheme, the pole of the propagator is set at the renormalised mass with residue one. Then, by construction, the on-shell renormalised mass is set to be identical to the physical mass, which is an experimentally measurable quantity, and does not receive any correction. Therefore, this scheme gives a clear and physical interpretation on the renormalised mass parameter. Nevertheless, in many calculations it is more efficient to use the minimal subtraction (MS) scheme, in which the counterterms are simply defined such that they remove only the divergent terms. Even more common is the modified minimal subtraction scheme ($\overline{\text{MS}}$), which is just a slight variation of the MS-scheme. The $\overline{\text{MS}}$ mass for the Higgs boson differs from the experimentally measured pole mass. The difference between the $\overline{\text{MS}}$ mass and the pole mass has the form [9]:

$$m_{\text{pole}}^2 - m_{\overline{\text{MS}}}^2(\mu^2) = a \cdot M^2 + b \cdot M^2 \ln \left(\frac{M^2}{\mu^2} \right), \quad (2.69)$$

where M is the mass of the particle inside the loop (cf. Fig. 2.2), a and b are some constants which include the coupling between the scalar and the particle inside the loop, and μ is an auxiliary renormalisation scale. Although the difference is finite, as M becomes larger the

difference also grows very large, which implies that the difference is sensitive to particles much heavier than the mass of the scalar. This behaviour is rather anti-intuitive. Indeed, in the presence of two well separated scales one expects the physics at the low energy (large length) scale not to depend much on the higher energy (small length) scale, so that one can describe physical phenomena at the low energy (macroscopic) scale while ignoring the substructure and degrees of freedom at the higher energy (microscopic) scale. However, the sensitivity of the scalar mass to the high-energy scale denotes exactly the opposite, which, although not being mathematically wrong, clashes with our physical intuition.

Let us assume that the SM is not a complete theory, but an effective theory of some other theory which is realized at a much larger energy scale. We know that a new theory has to come in at least at the Planck scale $M_{\text{Pl}} \sim 10^{19}$ GeV, which is the energy at which quantum gravity effects need to be included in our physical description of the world. However, it is also reasonable to expect new physics between the electroweak scale, ~ 100 GeV, and the Planck scale, which could account for at least some of the open questions which are unsolved in the SM, such as neutrino masses, dark matter, etc. As we will prove in Section 3,

$$m_{\text{pole}}^2 = m_R^2 + \Sigma_R(m_{\text{pole}}^2), \quad (2.70)$$

where m_R is the renormalised mass parameter and $\Sigma_R(m_{\text{pole}}^2)$ is the renormalised self-energy, which gives the finite loop-contributions to the renormalised mass, evaluated at external momentum $p^2 = m_{\text{pole}}^2$. The above equation is the definition of the pole mass and is valid for any subtraction scheme. Therefore, considering the $\overline{\text{MS}}$ scheme it holds that

$$m_{\text{pole}}^2 = m_{\overline{\text{MS}}}^2 + \Sigma_{\overline{\text{MS}}}(m_{\text{pole}}^2). \quad (2.71)$$

From Eq. (2.69) we know that $\Sigma_{\overline{\text{MS}}}$ is proportional to M^2 , which represents the new physics scale corresponding to the mass scale of the new particle (or particles) appearing in the high-energy theory. Then, the renormalised mass parameter $m_{\overline{\text{MS}}}^2$ has to be also of the order M^2 but must be given with a precision of $\mathcal{O}(m_{\text{pole}}^2/M^2)$ in order to reproduce the experimentally measurable pole mass m_{pole}^2 .

If the new energy scale were at the Planck scale $M \sim M_{\text{Pl}} \sim 10^{19}$ GeV, in order to achieve a value of the Higgs mass at the electroweak scale, $\mathcal{O}(10^2$ GeV) we would have to fine-tune the $m_{\overline{\text{MS}}}^2$ parameter with a precision of $\mathcal{O}(10^{-34})$. Of course, the new-physics scale could be at a lower energy than the Planck scale, which would mitigate this fine-tuning. However, the UV-sensitivity of the scalar masses to any new physics that couples to them would make us expect the Higgs mass to be not at the electroweak scale, but at the high-energy scale M , so that the fine-tuning in Eq. (2.71) would not be present. The unexpected smallness of the Higgs mass compared to the Planck scale or any other scale where the UV completion for the SM might live is called the hierarchy problem.

Different explanations to solve the hierarchy problem have been proposed. We review briefly some of them here.

Supersymmetry

In supersymmetric models [12, 13] a new symmetry that relates bosons and fermions is introduced, such that the corrections to the scalar masses due to fermionic loops are compensated

order by order in perturbation theory by bosonic loops and vice versa. Supersymmetry predicts the existence of a mass-degenerated supersymmetric partner for every SM particle with opposite spin-statistics. If supersymmetry is present in nature it must be somehow broken, since no supersymmetric particles with equal mass to the SM particles are observed. In this case, the cancellation between the fermion and scalar loops is not exact, but depends on the mass difference between the fermions and their scalar partners. The non-observation of these particles at the LHC is pushing the mass limits higher and higher, disfavouring supersymmetry as the answer to the hierarchy problem .

Extra dimensions

N. Arkani-Hamed, S. Dimopoulos and G. Dvali proposed in 1998 [15] a new framework for solving the hierarchy problem based on the existence of new large extra dimensions. They assume there is only one fundamental scale in nature, which is the weak scale, and explain the enormity of the Planck scale as a consequence of the large size of the new dimensions. In particular, the Planck scale, M_{Pl} , would be the effective four-dimensional scale of a fundamental $(4 + d)$ -dimensional Planck scale, M . In the simplest cases, they are related by $M_{\text{Pl}}^2 = M^{n+2} V_n$, where V_n is the volume of the n -dimensional compact space. The gravitational force would propagate in these extra dimensions, while the SM fields would remain at our three spatial dimensions. Other higher-dimensional mechanisms have been also proposed, such as warped extra dimensions [16]. In this scenario, the weak scale is generated from the Planck scale through an exponential "warp" factor that multiplies the metric. However, none of the expected signals from extra-dimension models have been seen at the LHC.

Conformal Symmetry

The hierarchy problem arises in the presence of the explicit mass term in the scalar potential. Conformal theories [14] rely on the idea that this term can be avoided, such that the theory is initially conformally (scale) invariant. The spontaneous symmetry breaking, which is needed to generate masses of the vector bosons, fermions and the scalar itself, is induced by radiative corrections via the Coleman-Weinberg mechanism [28]. The implementation of this mechanism in the context of the SM fails for a variety of different reasons. In particular, the Coleman-Weinberg effective potential is unbounded from below when the top quark is heavier than the Z boson. A solution to this is to extend the scalar sector in the SM by new degrees of freedom. The new particles required by the conformal symmetry must lie close to the electroweak scale, since the Coleman-Weinberg mechanism predicts that there can be only one symmetry breaking scale. Therefore, the new scalar particles would be in principle accessible at the LHC.

Multiverse

A quite different explanation to the hierarchy problem comes from the anthropic principle and the notion of multiverse. The anthropic principle states that the fine-tuning of our universe is the result of a selection bias. There may exist other patches of the universe, or other universes, with different values of the Higgs vev. It is then natural for us to live in the only one whose value supports life, and therefore, observe this necessary fine-tuning. Following this line of reasoning, we are led to the philosophical question of whether our "fine-tuned" universe could be just the result of a selection from a statistical population of universes that allows for life. At this point, there are however no testable predictions of the anthropic principle. For further

reading on the idea of multiverse and the anthropic principle see e.g. Ref. [29, 30].

Relaxation

A new class of solutions to the electroweak hierarchy problem was recently proposed by P. W. Graham, D. E. Kaplan, and S. Rajendran [31]. In these type of models, it is assumed that a dynamical evolution of the Higgs mass in the early universe drives it to a much smaller value than the cut-off of the theory. The central prediction of this class of models is the existence of an axion-like dark-matter particle, which could be probed by direct detection in the new low-energy experiments focused on light bosons, which are now emerging in the experimental particle physics field.

Although all these extensions of the SM that aim to solve the hierarchy problem are well motivated, none of the signatures predicted by any of them has been seen at the LHC or any other experiment up to now. In our work we will take a different approach based on the assertion that extensions of the SM do not necessarily lead to the hierarchy problem if the radiative corrections to the Higgs mass are not too large and thus, the parameters must not be extremely fine-tuned. In this sense, we will consider an extension of the SM to be natural if the correction to the Higgs mass squared in the $\overline{\text{MS}}$ -scheme is, at most, of the same order of the physical Higgs mass squared itself, which defines our naturalness condition³. In particular, we will consider the type I and type II see-saw models as extensions of the SM, and will try to set limits on parameters of the models and the masses of the new particles involved basing the analysis on this naturalness condition.

³This condition can be weakened or straightened, by allowing larger or only smaller corrections. However, we find that imposing all radiative corrections of the Higgs mass squared to be of the same order of the Higgs mass squared itself is a good balance between being too strict and too permissive.

3 TYPE I SEE-SAW MODEL

In the type I see-saw model, three right-handed neutrinos (one per family) N_R are introduced. They are fermionic singlets, which transforms as $(\mathbf{1}, \mathbf{1}, 0)$ under the SM $SU(3)_C \times SU(2)_L \times U(1)_Y$ gauge group. The minimal leptonic Lagrangian is given by

$$\mathcal{L}_{\text{leptons}} = \mathcal{L}_{\text{kinetic}} + \mathcal{L}_Y + \mathcal{L}_{\text{Majorana}}. \quad (3.1)$$

$\mathcal{L}_{\text{kinetic}}$ refers to the kinetic term for the leptons, which contains the kinetic energy and the gauge interaction terms of the left-handed lepton doublets $L_L = (\nu_L, e_L)^T$, the right-handed charged leptons e_R and the right-handed neutrinos N_R . It is given by

$$\mathcal{L}_{\text{kinetic}} = i\bar{L}_L \not{D} L_L + i\bar{e}_R \not{D} e_R + i\bar{N}_R \not{D} N_R, \quad (3.2)$$

where $\not{D} = \gamma^\mu D_\mu$ contains the covariant derivative, given in Eqs. (2.21, 2.22). Note that the right-handed neutrinos N_R do not have gauge interactions, since they are singlets under the SM gauge symmetries.

\mathcal{L}_Y is the Yukawa interaction term of the lepton sector with the SM Higgs doublet Φ ,

$$\mathcal{L}_Y = -\bar{L}_L \Phi Y_e e_R - \bar{L}_L \tilde{\Phi} Y_N^\dagger N_R + \text{h.c.} \quad (3.3)$$

where Y_e and Y_N are 3×3 arbitrary complex matrices and $\tilde{\Phi}$ is the conjugate Higgs doublet, given in Eq. (2.30).

Finally, $\mathcal{L}_{\text{Majorana}}$ is the Majorana mass term of the gauge-singlet right-handed neutrinos

$$\mathcal{L}_{\text{Majorana}} = -\frac{1}{2} \overline{N_R^c} M_R N_R + \text{h.c.}, \quad (3.4)$$

which introduces a new energy scale M_R . The matrix M_R is a 3×3 symmetric matrix.

3.1 NEUTRINO MASSES

In the type I see-saw model, there are two mass sources for the neutral lepton sector, which lead to massive neutrinos. On the one hand, a Dirac mass term is generated from the Yukawa interaction term through the Higgs mechanism after SSB, as explained in Section 2.1.3. On the other hand, a Majorana mass term is introduced in the Lagrangian for the right-handed neutrinos N_R , Eq. (3.4), which preserves the SM gauge symmetries.

In this section we will work in the unitary gauge for the scalar Higgs-field, writing the Higgs doublet as

$$\Phi = \frac{1}{\sqrt{2}} \begin{pmatrix} 0 \\ v + h \end{pmatrix}. \quad (3.5)$$

After SSB and using the unitary gauge, the Yukawa interaction term between the right- and left-handed neutrinos is given by

$$\begin{aligned}
\mathcal{L}_Y &\supset -\bar{L}_L \tilde{\Phi} Y_N^\dagger N_R + \text{h.c.} \\
&= -\frac{1}{\sqrt{2}} \bar{\nu}_L (h + v) Y_N^\dagger N_R + \text{h.c.} \\
&= -\frac{1}{\sqrt{2}} \left[h \bar{\nu}_L Y_N^\dagger N_R + v \bar{\nu}_L Y_N^\dagger N_R \right] + \text{h.c.}, \tag{3.6}
\end{aligned}$$

The first term corresponds to the interaction vertex between the left- and right-handed neutrinos and the Higgs and the second is the Dirac mass term for the neutrino sector:

$$\mathcal{L}_{\text{Dirac}} = -\bar{\nu}_L M_D N_R + \text{h.c.}, \tag{3.7}$$

where we have defined the Dirac mass matrix as

$$M_D \equiv \frac{v}{\sqrt{2}} Y_N^\dagger, \tag{3.8}$$

which is in general a complex 3×3 matrix.

Writing together both the Dirac and Majorana mass term, Eqs. (3.7, 3.4), we obtain

$$\begin{aligned}
\mathcal{L}_{\text{mass}} &\equiv \mathcal{L}_{\text{Dirac}} + \mathcal{L}_{\text{Majorana}} \\
&= -\bar{\nu}_L M_D N_R - \frac{1}{2} \overline{N_R^C} M_R N_R + \text{h.c.} \\
&= -\frac{1}{2} \left(\bar{\nu}_L \overline{N_R^C} \right) \begin{pmatrix} 0 & M_D \\ M_D^T & M_R \end{pmatrix} \begin{pmatrix} (\nu_L)^C \\ N_R \end{pmatrix} + \text{h.c.} \\
&= -\frac{1}{2} \overline{\Psi^C} \mathbf{M} \Psi + \text{h.c.} \tag{3.9}
\end{aligned}$$

In the last two lines we have rewritten the equation in terms of a Majorana basis of right-handed fields:

$$\Psi = \begin{pmatrix} (\nu_L)^C \\ N_R \end{pmatrix} \tag{3.10}$$

using the identity $\bar{\nu}_L M_D N_R = \overline{N_R^C} M_D^T (\nu_L)^C$, and we have defined the mass matrix

$$\mathbf{M} = \begin{pmatrix} 0 & M_D \\ M_D^T & M_R \end{pmatrix}. \tag{3.11}$$

The mass matrix \mathbf{M} is not diagonal. Therefore, the flavour fields ν_L and N_R are mixed and do not correspond to the mass eigenstates.

The type I see-saw relies on the assumption that the mass scale of the Majorana mass term M_R is much larger than the mass scale of the Dirac mass term M_D . Denoting m_R and m_D the mass scales of M_R and M_D , respectively, the see-saw condition can be written as

$$m_R \gg m_D. \tag{3.12}$$

Our aim is to decouple the heavy neutrino fields from the light neutrino fields and derive the effective mass matrices for each of them. We can do this by performing a unitary transformation of the neutrino fields by means of a unitary matrix U ,

$$\begin{pmatrix} (\nu_L)^C \\ N_R \end{pmatrix} = U \begin{pmatrix} \chi_{\text{light}} \\ \chi_{\text{heavy}} \end{pmatrix}_R, \quad (3.13)$$

which transforms the 6×6 matrix \mathbf{M} (recall that ν_L and N_R are three components vectors each, with one component for every family) into a block diagonal matrix of the form

$$U^T \mathbf{M} U = \begin{pmatrix} M_{\text{light}} & 0 \\ 0 & M_{\text{heavy}} \end{pmatrix}, \quad (3.14)$$

with symmetric 3×3 matrices M_{light} and M_{heavy} . Note that these sub-matrices are not diagonalized a priori and lead to lepton mixing within the light states and the heavy states separately. The lepton mixing of the light neutrinos is encoded in the PMNS matrix, as described in Section 2.2.1.

The unitary matrix U can be written as [32]:

$$U = \begin{pmatrix} \sqrt{\mathbb{1} - \rho\rho^\dagger} & \rho \\ -\rho^\dagger & \sqrt{\mathbb{1} - \rho^\dagger\rho} \end{pmatrix}, \quad (3.15)$$

where ρ is a 3×3 matrix which must be fixed as a function of M_D and M_R . The square roots in Eq. (3.15) should be understood as a power series,

$$\sqrt{\mathbb{1} - \rho\rho^\dagger} = \mathbb{1} - \frac{1}{2}\rho\rho^\dagger - \frac{1}{8}\rho\rho^\dagger\rho\rho^\dagger - \dots \quad (3.16)$$

The matrix U is unitary by construction. It can be understood as a generalization for matrices of the usual 2×2 orthogonal matrix

$$\begin{pmatrix} \sqrt{1 - \sin^2 \theta} & \sin \theta \\ -\sin \theta & \sqrt{1 - \sin^2 \theta} \end{pmatrix}.$$

The condition of the vanishing of the off-diagonal matrices in Eq. (3.14) is given by

$$\sqrt{\mathbb{1} - \rho^T \rho^*} M_D^T \sqrt{\mathbb{1} - \rho\rho^\dagger} - \rho^T M_D \rho^\dagger - \sqrt{\mathbb{1} - \rho^T \rho^*} M_R \rho^\dagger = 0 \quad (3.17)$$

This equation may be solved assuming that ρ is a power series in $1/m_R$ [32]. Using the notation ρ_i for the terms proportional to $(m_R)^{-i}$, the solution reads [32]

$$\rho = \rho_1 + \rho_3 + \dots \quad (3.18)$$

$$\sqrt{\mathbb{1} - \rho\rho^\dagger} = \mathbb{1} - \frac{1}{2} B_1 B_1^\dagger - \frac{1}{2} \left(\rho_1 \rho_3^\dagger + \rho_3 \rho_1^\dagger + \frac{1}{4} \rho_1 \rho_1^\dagger \rho_1 \rho_1^\dagger \right) - \dots \quad (3.19)$$

with

$$M_R \rho_1^\dagger = M_D^T \quad (3.20)$$

$$M_R \rho_3^\dagger = -M_R^{-1*} M_D^\dagger M_D M_R^{-1} M_D^T - \frac{1}{2} M_D^T M_D^* M_R^{-1*} M_R^{-1} M_D^T. \quad (3.21)$$

Therefore, the matrix ρ can be written as

$$\rho = M_D^*(M_R^\dagger)^{-1} + \mathcal{O}\left(\frac{m_D^3}{m_R^3}\right). \quad (3.22)$$

The effective mass matrices for the light and heavy neutrinos are given by [32]

$$M_{\text{light}} = -M_D M_R^{-1} M_D^T + \mathcal{O}\left(\frac{m_D^3}{m_R^2}\right) \quad (3.23)$$

$$M_{\text{heavy}} = M_R + \mathcal{O}\left(\frac{m_D^2}{m_R}\right). \quad (3.24)$$

Usually, considering only the lowest order of these matrices might be sufficient. However, in some instances it might be necessary to include further terms, e.g. if the scales m_R and m_D are not separated enough. Let us illustrate it with two extreme cases [33]:

- (i) **High scale see-saw:** assuming $m_R \sim \mathcal{O}(10^{15} \text{ GeV})$ and a Dirac mass scale at the electroweak scale $m_D \sim \mathcal{O}(10^2 \text{ GeV})$, one obtains naturally $M_\nu \sim \mathcal{O}(10^{-2} \text{ eV})$ from the relation $M_{\text{light}} \simeq -M_D M_R^{-1} M_D^T$. In this conventional case, $\rho \sim \mathcal{O}(m_D/m_R) \sim \mathcal{O}(10^{-13})$ and thus, higher order effects are small enough to be neglected.
- (ii) **Low scale see-saw:** if $m_R \sim \mathcal{O}(1 \text{ TeV})$ one would naively expect a relatively small Dirac mass $m_D \sim \mathcal{O}(10^{-3} \text{ GeV})$ in order to generate neutrino masses not larger than $\mathcal{O}(\text{eV})$. However, it is possible to have Dirac masses at the electroweak $m_D \sim \mathcal{O}(10^2 \text{ GeV})$ and heavy neutrinos at the TeV scale, and still realize small neutrino masses if one imposes specific structure cancellations on the matrices M_D and M_R [34, 35]. In this scenario, the fraction $\rho \sim \mathcal{O}(m_D/m_R) \sim \mathcal{O}(0.1)$ can become significant and the higher order terms may lead to some observable effects [32, 33].

In the following, we will not consider any specific structure for the mass matrix M_D and M_R , since this is outside the scope of this work. We will further assume that higher order terms are negligible and the first order approximation is accurate enough for our purpose.

The fields χ_{light} and χ_{heavy} , are related to the original fields ν_L and N_R through the inverse of Eq. (3.13), which gives

$$\chi_{\text{light}} = (\nu_L)^C - \rho N_R \quad (3.25)$$

$$\chi_{\text{heavy}} = N_R + \rho^\dagger (\nu_L)^C. \quad (3.26)$$

Here we have neglected terms of order $\rho^\dagger \rho \sim \mathcal{O}(m_D^2/m_R^2)$. These fields are not yet Majorana particles, since they only have right chiralities and thus, $\chi_i^C \neq \chi_i$ ($i = \{\text{light, heavy}\}$). However, it is possible to define two Majorana fields from them as

$$n_i = \chi_i + \chi_i^C, \quad (3.27)$$

with $i = \{\text{light, heavy}\}$, which fulfil the Majorana condition $n_i = n_i^C$. Explicitly

$$n_{\text{light}} = \chi_{\text{light}} + \chi_{\text{light}}^C = (\nu_L + (\nu_L)^C) - (\rho N_R + \rho^*(N_R)^C), \quad (3.28)$$

$$n_{\text{heavy}} = \chi_{\text{heavy}} + \chi_{\text{heavy}}^C = (N_R + (N_R)^C) + (\rho^T \nu_L + \rho^\dagger (\nu_L)^C). \quad (3.29)$$

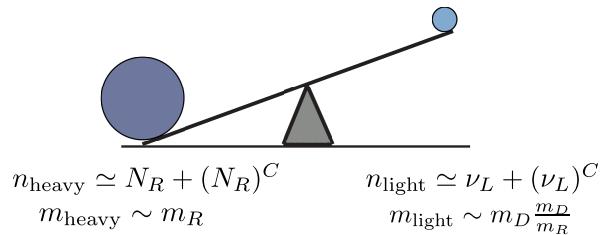


Figure 3.1: Graphical illustration of the see-saw mechanism. The two Majorana states, n_{light} and n_{heavy} , correspond roughly to the active ν_L and the sterile N_R neutrinos, respectively. The mass of the heavy state n_{heavy} corresponds approximately to the heavy scale m_R . The mass scale of the light state n_{light} is proportional to the Dirac mass m_D , expected to be of the order of magnitude of the other leptons and quarks, but it is suppressed by the heavy mass scale m_R through the ratio m_D/m_R .

From the above definition of the Majorana mass eigenstates we observe that the Majorana field n_{light} is mainly a state formed by the SM active neutrinos ν_L , with a small contribution from the sterile neutrinos N_R , which is suppressed by $\rho \sim m_D/m_R$. Its mass scale $m_{\text{light}} \sim m_D \cdot m_D/m_R$ (see Eq. (3.23)) is proportional to the Dirac mass, which is expected to be of the order of magnitude of the other leptons and quarks, but suppressed by the factor m_D/m_R . The second Majorana state n_{heavy} is a state mainly formed by the sterile neutrinos N_R , with a small contribution of the SM active neutrinos ν_L , which is suppressed by the ratio m_D/m_R . Its mass scale $m_{\text{heavy}} \sim m_R$ (see Eq. (3.24)) corresponds to the new heavy mass scale and is therefore expected to be larger than the electroweak scale.

This suppression effect of the new heavy scale m_R on the Dirac scale m_D could explain the measured smallness of the active neutrino masses and is the origin for the name "see-saw" for this mechanism, as illustrated in Fig. 3.1.

3.2 RADIATIVE CORRECTIONS AND RENORMALISATION

Using the Lagrangian of the type I see-saw model, Eq. (3.1), one can perform calculations at tree level and obtain finite answers, which then can be compared to experimental results. However, in higher order perturbation theory divergences appear, which must be removed in a consistent way. If the theory is renormalisable, the divergences can be systematically absorbed by a redefinition of the fields and couplings of the bare theory through the insertion of a finite number of counterterms. The strategy is to split the bare Lagrangian into two parts: a renormalised piece and a counter term Lagrangian that compensates for the infinities order by order in perturbation theory, leading to finite final results.

In this section, we will illustrate the renormalisation procedure studying the one-loop correction to the Higgs mass introduced by the new heavy right-handed neutrinos, Fig. 3.2. For simplicity, we only consider one family of fermions. The relevant parts of the Lagrangian for the analysis are only those terms which contain a power of two Higgs fields, which are the Higgs kinetic and mass term,

$$\mathcal{L}_h = \frac{1}{2} \partial_\mu h \partial^\mu h - \frac{1}{2} m_h^2 h^2. \quad (3.30)$$

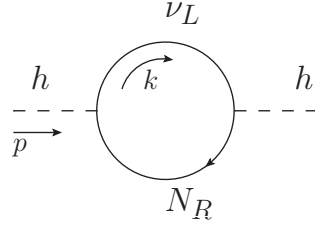


Figure 3.2: Feynman diagram of the loop-contribution to the Higgs self-energy from the neutrino-loop including the new right-handed neutrino N_R ; p is the momentum of the Higgs h whereas k is the loop-momentum.

We will consider the renormalisation of the time-ordered connected two-point correlation function, also called Green's function:

$$G(x, y) = \langle \Omega | T \{ h(x) h(y) \} | \Omega \rangle \equiv \langle h(x) h(y) \rangle. \quad (3.31)$$

It is usually helpful to study $\langle h(x) h(y) \rangle$ in momentum space. The Green's function in momentum-space is defined by the Fourier transform

$$\langle h(x) h(y) \rangle = \int \frac{d^4 p}{(2\pi)^4} e^{-ip(x-y)} iG(p^2). \quad (3.32)$$

At tree level, $G(p^2)$ just corresponds to the momentum-space scalar propagator:

$$iG_0(p^2) \equiv \frac{i}{p^2 - m^2}. \quad (3.33)$$

However, at higher loop order it gets corrections due to radiative graphs. It can be shown that the entire Green's function can be written only in terms of one-particle irreducible (1PI) diagrams, which are diagrams that cannot be subdivided into two disconnected diagrams by cutting a single internal propagator [9].

Let us denote the sum of all 1PI insertions into the scalar propagator by $-i\Sigma(p^2)$, where $\Sigma(p^2)$ is called the particle self-energy,

$$-i\Sigma(p^2) = \text{---} \textcircled{\text{1PI}} \text{---} = \text{---} \text{---} \text{---} + \text{---} \text{---} \text{---} + \text{---} \text{---} \text{---} + \dots \quad (3.34)$$

Then the full two-point function is given by the geometric series

$$\begin{aligned} iG(p^2) &= \text{---} \textcircled{\text{---}} \text{---} = \text{---} \text{---} \text{---} + \text{---} \textcircled{\text{1PI}} \text{---} + \text{---} \textcircled{\text{1PI}} \text{---} \textcircled{\text{1PI}} \text{---} + \dots \\ &= \frac{i}{p^2 - m^2} + \frac{i}{p^2 - m^2} (-i\Sigma(p^2)) \frac{i}{p^2 - m^2} + \dots \\ &= \frac{i}{p^2 - m^2 - \Sigma(p^2)}. \end{aligned} \quad (3.35)$$

The pole of the full propagator corresponds to the physical (pole) mass of the particle. With our sign convention for the 1PI self-energy, a positive contribution to $\Sigma(p^2)$ corresponds

to a positive shift of the scalar particle mass in the full propagator:

$$m_{\text{pole}}^2 = m^2 + \Sigma(m_{\text{pole}}^2). \quad (3.36)$$

As we will see in the next section, the naive calculation of the Higgs self-energy $\Sigma(p^2)$ diverges, which seems to make the pole mass also divergent. To solve this apparently infinite mass of the Higgs boson we need to renormalise the parameters of the theory to cancel the divergences in the self-energy graphs.

3.2.1 One-loop Higgs self-energy

Let us now carry out explicitly the new contribution to the self-energy at one-loop level which includes the new heavy neutrinos, which we will denote as $\Sigma_2(p^2)$ ¹. As explained in Section 3.1, the flavour eigenstates ν_L and N_R are not mass eigenstates. The latter are obtained by diagonalizing the mass matrix, Eq. (3.11), and constructing the Majorana mass fields n_{light} and n_{heavy} , Eqs. (3.28, 3.29). For the ease of notation, we will rename $n_1 \equiv n_{\text{light}}$, with mass $m_1 \equiv m_{\text{light}}$, and $n_2 \equiv n_{\text{heavy}}$, with mass $m_2 \equiv m_{\text{heavy}}$.

We can rewrite the Yukawa interaction between the Higgs and the left- and right-handed neutrinos, Eq. (3.6), in terms of the mass eigenstates, n_1 and n_2 . Considering only one family of leptons, it is given by

$$\mathcal{L}_{\text{int}} = -\frac{y_N}{\sqrt{2}}h \left[\frac{m_D}{M_R} (\bar{n}_2 n_2 - \bar{n}_1 n_1) + \left(1 - \frac{m_D^2}{M_R^2} \right) \bar{n}_1 n_2 \right], \quad (3.37)$$

with $n_1 \simeq \nu_L + (\nu_L)^C$ and $n_2 \simeq N_R + (N_R)^C$ for $m_D \ll M_R$ (cf. Eqs. (3.28, 3.29)), with masses²

$$m_1 \simeq -m_D \frac{m_D}{M_R}, \quad (3.38)$$

$$m_2 \simeq M_R. \quad (3.39)$$

We observe that the vertices $h\bar{n}_1 n_1$ and $h\bar{n}_2 n_2$ are suppressed by a factor m_D/M_R . Therefore, in the limit $m_D \ll M_R$ the the main contribution to the Higgs mass correction at one loop order is the one with both n_1 and n_2 inside the loop, Fig. 3.3. The term proportional to m_D^2/M_R^2 in the $h\bar{n}_1 n_2$ vertex is also neglected.

In order to compute the contribution to the Higgs self-energy, it is necessary to consider the Feynman rules for Majorana fermions, which differ from the usual Dirac fermions Feynman rules. For example, Majorana fermion lines do not carry an arrow which indicates the fermion number flow, and an arbitrary orientation (fermion flow) must be chosen. Likewise, self-energy loops with two identical Majorana fermions receive the usual combinatorial factor $\frac{1}{2}$ for identical particles, since Majorana fields are self-conjugate, i.e. they are their own

¹The subscript in $\Sigma_2(p^2)$ comes from considering the self-energy $\Sigma(p^2)$ as a Taylor expansion in the couplings. In this sense, the subscript in $\Sigma_2(p^2)$ denotes order $|y_D|^2$, which is the lowest loop-order we can consider for the fermionic loop.

²Note that here M_R , even if written in capital letters, is not a matrix, but just the mass parameter of the right-handed neutrino

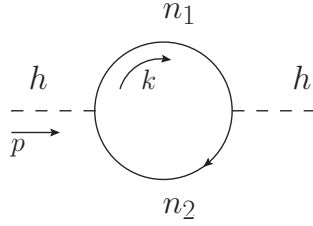


Figure 3.3: Relevant Feynman diagram of the loop-contribution to the Higgs self-energy from the neutrino-loop in terms of the mass eigenstates n_1 and n_2 , with $m_1 \simeq -m_D^2/M_R$ and $m_2 \simeq M_R$; p is the external momentum and k is the loop-momentum.

antiparticle. For a complete set of Majorana Feynman rules, see e.g. [36, 37]. Following the Majorana Feynman rules, the contribution to the Higgs self-energy from the Majorana mass eigenstates n_1 and n_2 is given by

$$\begin{aligned}
 -i\Sigma_2(p^2)|_{1\text{-loop}} &= \text{---} \text{---} \text{---} \text{---} \\
 &= (-1) \frac{i^2 |y_N|^2}{2} \int \frac{d^4 k}{(2\pi)^4} \frac{\text{Tr} [i(\not{k} + m_1) \cdot i((\not{k} - \not{p}) + m_2)]}{(k^2 - m_1^2) ((k - p)^2 - m_2^2)}, \quad (3.40)
 \end{aligned}$$

where the factor (-1) comes from the fermionic loop.

This integral is clearly divergent in the UV, which can be easily observed by counting the power of the momentum in the nominator and the denominator. Roughly speaking, a diagram diverges unless there are more powers of momentum in the denominator than in the numerator. To see this schematically, let us define the superficial degree of divergence D as the difference

$$D = (\text{power of } k \text{ in numerator}) - (\text{power of } k \text{ in denominator}) \quad (3.41)$$

and introduce a momentum cut-off in the UV by replacing

$$\int^\infty dk \rightarrow \int^\Lambda dk. \quad (3.42)$$

Naively, we expect to have a divergence proportional to Λ^D when $D > 0$, a $\log \Lambda$ divergence when $D = 0$, and no divergence when $D < 0$. The momentum structure of Eq. (3.40) is

$$\int \frac{d^4 k}{k^2} \rightarrow D = 2 \quad \text{and} \quad \int \frac{d^4 k}{k^4} \rightarrow D = 0. \quad (3.43)$$

Therefore, we expect the first integral to diverge quadratically and the second to diverge logarithmically.

We should note that this naive power-counting method does not always reflect the actual behaviour in the UV of a diagram. Indeed, there are three possible situations that can lead to a wrong prediction [38]: diagrams with $D < 0$ might still diverge due to divergent sub-diagrams contained in it; possible symmetries of the theory can cause cancellations among infinite terms, reducing or even eliminating the divergence of a diagram; and finally, trivial diagrams without propagators or loops have $D = 0$ but no divergences.

Let us now perform the calculation of the integral in Eq. (3.40) explicitly. First we compute the trace in the nominator

$$\text{Tr} [(k + m_1) \cdot ((k - p) + m_2)] = 4k \cdot (k - p) + 4m_1 m_2. \quad (3.44)$$

Therefore, the loop integral is given by

$$\begin{aligned} -i\Sigma_2(p^2) &= -\frac{|y_N|^2}{2} \int \frac{d^4 k}{(2\pi)^4} \frac{4[k \cdot (k - p) + m_1 m_2]}{(k^2 - m_1^2)((k^2 - p^2) - m_2^2)} \\ &= -\frac{|y_N|^2}{2} \int_0^1 dx \int \frac{d^4 k}{(2\pi)^4} \frac{4[k \cdot (k - p) + m_1 m_2]}{((k - xp)^2 - \Delta)^2} \\ &= -\frac{|y_N|^2}{2} \int_0^1 dx \int \frac{d^4 \tilde{k}}{(2\pi)^4} \frac{4[\tilde{k}^2 + m_1 m_2 - x(1-x)p^2]}{(\tilde{k}^2 - \Delta)^2} \\ &= 4i \frac{|y_N|^2}{2} \int_0^1 dx \int \frac{d^4 k_E}{(2\pi)^4} \left(\frac{k_E^2}{(k_E^2 + \Delta)^2} + \frac{x(1-x)p^2 - m_1 m_2}{(k_E^2 + \Delta)^2} \right), \end{aligned} \quad (3.45)$$

where we have introduced an auxiliary Feynman parameter x in the second line, a change of variable $\tilde{k} := k - xp$ in the third line and a Wick rotation to Euclidean space in the fourth line, with the definitions:

$$k^0 := ik_E^0, \quad \vec{k} := \vec{k}_E. \quad (3.46)$$

We have also defined

$$\Delta := xp^2(x - 1) + x(m_2^2 - m_1^2) + m_1^2. \quad (3.47)$$

After Wick-rotating the integral to Euclidean space, we can perform the integral in spherical coordinates. For clarity, we split the integral in momentum into two pieces,

$$\begin{aligned} I_1(p^2) &= \int \frac{d^4 k_E}{(2\pi)^4} \frac{k_E^2}{(k_E^2 + \Delta)^2} \\ &= \frac{1}{8\pi^2} \int_0^\infty \frac{|k_E|^5}{(|k_E|^2 + \Delta)^2} \quad (\text{Spherical coord.}) \\ &= \left[\frac{|k_E|^2}{2} - \Delta \log(\Delta + |k_E|^2) - \frac{1}{2} \frac{\Delta^2}{(\Delta + |k_E|^2)} \right]_0^\infty, \end{aligned} \quad (3.48)$$

$$\begin{aligned} I_2(p^2) &= \int \frac{d^4 k_E}{(2\pi)^4} \frac{1}{(k_E^2 + \Delta)^2} \\ &= \frac{1}{8\pi^2} \int_0^\infty \frac{|k_E|^3}{(|k_E|^2 + \Delta)^2} \quad (\text{Spherical coord.}) \\ &= \left[\log(\Delta + |k_E|^2) + \frac{1}{2} \frac{\Delta}{(\Delta + |k_E|^2)} \right]_0^\infty, \end{aligned} \quad (3.49)$$

where we have used the general d -dimensional formula

$$\int \frac{d^d k_E}{(2\pi)^d} = \int \frac{d\Omega_d}{(2\pi)^d} \int |k_E|^{d-1} d|k_E| \quad (3.50)$$

with

$$\int d\Omega_d = \frac{2\pi^{d/2}}{\Gamma(d/2)} \quad (3.51)$$

to perform the integrals in spherical coordinates. $\Gamma(x)$ is the Gamma-function. Since we are working in $d = 4$ dimensions, here we only need to use $\Gamma(2) = 1$. Further properties of $\Gamma(x)$ will be given in the next subsection.

Here we see explicitly that the first integral diverges quadratically, while the second one diverges logarithmically, as we take $|k_E|$ to infinity, leading to an apparently non-sensible result for the Higgs self-energy once quantum effects are taken into account. To cure the theory from these divergences we have to regularise and renormalise it. We will discuss the regularisation and renormalisation procedure in the following.

3.2.2 Regularisation

There are different regularisation methods. Here we will only discuss two of them: the hard cut-off regularisation and the dimensional regularisation. For further reading on these and other regularisation methods, such as Pauli Vilar's and the derivative methods, see e.g. Schwartz [9] and Peskin & Schröder [38].

Hard cut-off regularisation

In the cut-off regularisation, an ultraviolet momentum cut-off Λ is imposed on the upper limit of the momentum integral, which is taken to infinity at the end of the calculation, imposing the limit $\Lambda \rightarrow \infty$.

Using a cut-off regulator, the integrals in Eqs. (3.48, 3.49) give

$$I_1(p^2) = \frac{1}{2}\Lambda^2 - \Delta \log\left(\frac{\Lambda^2}{\Delta} + 1\right) - \frac{1}{2}\frac{\Delta^2}{\Delta + \Lambda^2} + \frac{1}{2}\Delta \quad (3.52)$$

$$I_2(p^2) = \frac{1}{2}\log\left(\frac{\Lambda^2}{\Delta} + 1\right) + \frac{1}{2}\frac{\Delta}{\Delta + \Lambda^2} - \frac{1}{2} \quad (3.53)$$

Thus, when $\Lambda \rightarrow \infty$, the first integral gives a quadratic and a logarithmic divergence while the second one gives a logarithmic divergence. Terms proportional to $1/\Lambda^2$ will drop as Λ approaches infinity. Writing all the terms together, the loop integral in Eq. (3.40) gives

$$-i\Sigma_2(p^2) = i|y_N|^2 \int_0^1 dx \left[\Lambda^2 - 2\Delta \log\left(\frac{\Lambda^2}{\Delta} + 1\right) + (x(1-x)p^2 - m_1 m_2) \log\left(\frac{\Lambda^2}{\Delta} + 1\right) \right] \quad (3.54)$$

with $\Delta = xp^2(x-1) + x(m_2^2 - m_1^2) + m_1^2$. Although the use of a cut-off is straightforward, it is cumbersome to use within perturbation theory, especially because of the loss of Lorentz invariance. In fact, for practical calculations in perturbation theory it is most convenient to use another regulator method, called dimensional regularisation, which also preserves space-time and gauge symmetries.

Dimensional regularisation

In dimensional regularisation, space-time is generalized to d dimensions. After performing certain integral tricks, the logarithmic divergences of the integral will appear as poles in four dimensions. The pole can be reabsorbed in the counterterms, so that the final result is finite.

To perform the calculation in dimensional regularisation one can use the following d -dimensional integrals in Minkowski space [38]:

$$\int \frac{d^d k}{(2\pi)^d} \frac{1}{(k^2 - \Delta)^n} = \frac{(-1)^n i \Gamma(n - \frac{d}{2})}{(4\pi)^{d/2} \Gamma(n)} \left(\frac{1}{\Delta}\right)^{n - \frac{d}{2}}, \quad (3.55)$$

$$\int \frac{d^d k}{(2\pi)^d} \frac{k^2}{(k^2 - \Delta)^n} = \frac{(-1)^{n-1} i d \Gamma(n - \frac{d}{2} - 1)}{(4\pi)^{d/2} 2 \Gamma(n)} \left(\frac{1}{\Delta}\right)^{n - \frac{d}{2} - 1}, \quad (3.56)$$

to compute the one-loop integral in Eq. (3.40). Here $\Gamma(x)$ is the Gamma-function. A useful property of $\Gamma(x)$ is:

$$\Gamma(n) = (n - 1)! \quad (3.57)$$

for all positive integer n . We will also need its expansion near its poles, which is given by

$$\Gamma(x) = \frac{1}{x} - \gamma + \mathcal{O}(x) \quad (3.58)$$

near $x = 0$, and

$$\Gamma(x) = \frac{(-1)^n}{n!} \left(\frac{1}{x+n} - \gamma + 1 + \dots + \frac{1}{n} + \mathcal{O}(x+n) \right) \quad (3.59)$$

near $x = -n$. Here γ is the Euler-Mascheroni constant, $\gamma \approx 0.5772$.

The integrals in Minkowski space that we need to compute are

$$\tilde{I}_1(p^2) = \int \frac{d^4 k}{(2\pi)^4} \frac{k^2}{(k^2 - \Delta)^2} \quad (3.60)$$

$$\tilde{I}_2(p^2) = \int \frac{d^4 k}{(2\pi)^4} \frac{1}{(k^2 - \Delta)^2}. \quad (3.61)$$

We first generalize the space-time dimensions of the integrals to d dimensions and then apply the formulas in Eqs. (3.55, 3.56):

$$\begin{aligned} \tilde{I}_1(p^2) &= \int \frac{d^d k}{(2\pi)^d} \frac{k^2}{(k^2 - \Delta)^2} \\ &= \frac{-i}{(4\pi)^{d/2} 2} \frac{d \Gamma(1 - d/2)}{\Gamma(2)} \left(\frac{1}{\Delta}\right)^{1 - d/2} \\ &= \frac{-i}{(4\pi)^{2 - \epsilon/2}} \left(2 - \frac{\epsilon}{2}\right) \Gamma\left(\frac{\epsilon}{2} - 1\right) \left(\frac{1}{\Delta}\right)^{\epsilon/2 - 1} \\ &= -i \frac{2\Delta}{(4\pi)^2} \left(\frac{2}{\epsilon} - \gamma + \log(4\pi) + \frac{1}{2} - \log(\Delta) + \mathcal{O}(\epsilon)\right), \end{aligned} \quad (3.62)$$

$$\begin{aligned}
\tilde{I}_2(p^2) &= \int \frac{d^d k}{(2\pi)^d} \frac{1}{(k^2 - \Delta)^2} \\
&= \frac{i}{(4\pi)^{d/2}} \frac{\Gamma(2 - d/2)}{\Gamma(2)} \left(\frac{1}{\Delta}\right)^{2-d/2} \\
&= \frac{i\Gamma(\epsilon/2)}{(4\pi)^{2-\epsilon/2}} \left(\frac{1}{\Delta}\right)^{\epsilon/2} \\
&= \frac{i}{(4\pi)^2} \left(\frac{2}{\epsilon} - \gamma + \log(4\pi) - \log(\Delta) + \mathcal{O}(\epsilon)\right), \tag{3.63}
\end{aligned}$$

with $\epsilon := 4 - d$ defined as a small deviation of the space-time dimension from $d = 4$. Here we have used:

$$\Gamma\left(\frac{\epsilon}{2} - 1\right) = \frac{1}{\epsilon/2 - 1} \Gamma\left(\frac{\epsilon}{2}\right) \tag{3.64}$$

and $\Gamma(2) = 1$, from Eq. (3.57); the Taylor expansion around $x = 0$

$$\frac{1}{x-1} = (1+x+\dots) \tag{3.65}$$

to expand $\frac{1}{\epsilon/2-1}$; and the trick

$$x^{\epsilon/2} = e^{\log x^{\epsilon/2}} = e^{\epsilon/2 \log x} = 1 + \frac{\epsilon}{2} \log x + \mathcal{O}(\epsilon^2) \tag{3.66}$$

for $\epsilon \rightarrow 0$, to expand the terms with $\epsilon/2$ in the exponent.

In order to keep the Yukawa coupling y_N dimensionless in d -dimensional space-time, we have to add an appropriate power of auxiliary energy scale μ_R to y_N ,

$$y_N \rightarrow \mu_R^{\epsilon/2} y_N. \tag{3.67}$$

Using again the trick in Eq. (3.66), the new arbitrary energy scale μ_R , called regularisation scale, compensates the dimensional quantity Δ in the logarithm of Eqs. (3.62, 3.63).

The loop integral in Eq. (3.40) in dimensional regularisation gives

$$-i\Sigma_2(p^2) = i \frac{|y_N|^2}{8\pi^2} \int_0^1 dx \left[\Delta - (m_1 m_2 - x(1-x)p^2 - 2\Delta) \left(\frac{2}{\epsilon} - \gamma - \log\left(\frac{\Delta}{4\pi\mu_R^2}\right)\right) \right], \tag{3.68}$$

where terms proportional to ϵ have been neglected, since $\epsilon \rightarrow 0$ for $d = 4$. As can be seen from this expression, in dimensional regularisation the logarithmic divergence appears as a $1/\epsilon$ pole. The quadratic divergence manifest itself as a $1/\epsilon$ pole in $d = 2$ [9].

3.2.3 Renormalisation

Since we want the Green's function $G(p^2)$ defined in Eq. (3.32) to be finite, we must remove the infinities from the self-energy through renormalisation. This is done by defining a renormalised field and a renormalised mass, which are finite, and absorbing the divergences in a finite set of appropriately chosen counterterms.

In first place, we define our renormalised Higgs field as

$$h_R = \frac{1}{\sqrt{Z_h}} h_0, \quad (3.69)$$

where the subscript R stands for renormalised and 0 for bare field. The quantity Z_h is some (formally infinite) number that renormalises h_0 order by order in perturbation theory. For the tree level theory, $Z_h = 1$. To account for radiative corrections we write

$$Z_h = 1 + \delta_h \quad (3.70)$$

where δ_h is the Higgs field counterterm, which has a formal Taylor expansion in the couplings. We can also write

$$m_R^2 = \frac{1}{Z_m} m_0^2 \quad (3.71)$$

and expand $Z_m = 1 + \delta_m$, with δ_m being the mass counterterm³. Then

$$m_0^2 = m_R^2 + m_R^2 \delta_m. \quad (3.72)$$

Until now, all the calculations that we have performed have been with the bare fields and bare mass parameter. However, it is the Green's function of the renormalised fields that should be finite. We define

$$\langle h_0(x) h_0(y) \rangle = \int \frac{d^4 p}{(2\pi i)^4} e^{-ip(x-y)} iG^{\text{bare}}(p^2) \quad (3.73)$$

as the bare Green's function, and

$$\langle h_R(x) h_R(y) \rangle = \int \frac{d^4 p}{(2\pi i)^4} e^{-ip(x-y)} iG^R(p^2), \quad (3.74)$$

as the renormalised Green's function, and expect $G^R(p^2)$ to be finite. Using the definition of the renormalised fields,

$$G^R(p^2) = \frac{1}{Z_h} G^{\text{bare}}(p^2). \quad (3.75)$$

From Eq. (3.35), we have

$$iG^{\text{bare}}(p^2) = \frac{i}{m^2 - m_0^2 - \Sigma_2(p^2) + \dots}, \quad (3.76)$$

³We follow the convention used in Schwartz [9] for the definitions of the counterterms. Another common convention is to define $\delta_m = Z_h m_0^2 - m_R^3$, which is used, for example, in Peskin & Schroeder [38].

where the dots denote higher order loop corrections. From the bare Green's function we can then compute the renormalised Green's function,

$$\begin{aligned}
iG^R(p^2) &= \frac{1}{1 + \delta_h} iG^{\text{bare}} \\
&= \left(\frac{1}{1 + \delta_h} \right) \frac{i}{p^2 - m_0^2 - \Sigma_2(p^2) + \dots} \\
&= \frac{i}{p^2 - m_0^2 + \delta_h p^2 - \delta_h m_0^2 - \Sigma_2(p^2) + \dots} \\
&= \frac{i}{p^2 - m_R^2 + \delta_h p^2 - (\delta_h + \delta_m)m_R - \Sigma_h(p^2) + \dots}, \tag{3.77}
\end{aligned}$$

where we have used Eq. (3.72), $m_0^2 = m_R^2 + m_R^2 \delta_m$, in the last row. Note that the term $\delta_2 \Sigma_2(p^2)$ and those proportional to $\delta_h \delta_m$ which appear after multiplying the two denominators in the second line are of higher loop order, and are therefore reabsorbed in the dots. This part will be neglected when performing calculations up to one-loop order. Eq. (3.77) can be more conveniently written as

$$iG^R(p^2) = \frac{i}{p^2 - m_R^2 - \Sigma_R(p^2)} \tag{3.78}$$

with $\Sigma_R(p^2) = \Sigma_2(p^2) + \delta_h p^2 - (\delta_h + \delta_m)m_R + \dots$ being the renormalised self-energy. Choosing properly the counterterms such that they cancel exactly the infinities of the self-energy order by order we will obtain finite values for m_R and Σ_R , and therefore obtaining a finite result for the renormalised Green's function, as desired.

Let us now write the bare free Lagrangian, Eq. (3.30), in terms of the new renormalised fields:

$$\begin{aligned}
\mathcal{L}_h &= \frac{1}{2} Z_h \partial_\mu h_R \partial^\mu h_R - \frac{1}{2} Z_h Z_m m_R 2h_R^2 \\
&= \partial_\mu h_R \partial^\mu h_R - \frac{1}{2} m_{h,R}^2 h_R^2 + \frac{1}{2} \delta_h \partial_\mu h_R \partial^\mu h_R - \frac{1}{2} (\delta_h + \delta_m) m_R^2 h_R^2. \tag{3.79}
\end{aligned}$$

This is the Lagrangian for renormalised perturbation theory. We observe that it is split into two parts: one identical to the bare Lagrangian but written in terms of the renormalised fields and the renormalised parameters, and one containing the counterterms that will absorb the infinities coming from the loop calculations. The counterterm part can be interpreted as interactions and can be used in Feynman diagrams. Thus, the new set of Feynman rules in terms of the renormalised parameters and the counterterms is given by

$$\begin{array}{c} p \\ \text{---} \end{array} = \frac{i}{p^2 - m_R^2} \tag{3.80}$$

$$\text{---} \otimes \text{---} = i (\delta_h (p^2 - m_R^2) + \delta_m m_R^2) \tag{3.81}$$

The propagator is identical to the bare-propagator, but substituting the bare mass by the renormalised one. The counterterm gives an extra vertex, denoted with a cross, which must be included in our loop calculations. With these new Feynman rules it is possible to perform perturbation theory using only renormalised and counterterm parameters, and obtain finite results. This is called renormalised perturbation theory.

Including now the counterterm part in the calculation, we can compute the renormalised self-energy at one-loop as

$$\begin{aligned}
 -i\Sigma_R(p^2)|_{1\text{-loop}} &= \text{---} \bigcirc \text{---} + \text{---} \otimes \text{---} \\
 &= -i\Sigma_2(p^2) + i(\delta_h(p^2 - m_R^2) + \delta_m m_R^2), \quad (3.82)
 \end{aligned}$$

where $\Sigma_2(p^2)$ is given by Eq. (3.54) (cut-off regularisation)/ Eq. (3.68) (dimensional regularisation). With a proper definition of the counterterms to cancel the divergences in $\Sigma_2(p^2)$, $\Sigma_R(p^2)$ has a finite value.

We have imposed that the counterterms must absorb the infinities appearing in the self-energy graphs. However, when defining the counterterms we are free to choose their finite part and $G_R(p^2)$ will still be finite for any of the definitions. To get rid of this ambiguity and give a precise interpretation of the renormalised parameters it is necessary to fix the finite parts of the counterterms using a set of renormalisation conditions. These conditions are arbitrary and define our renormalisation or subtraction scheme. The most widely used schemes are:

On-shell scheme.

In the on-shell scheme, the counterterms are chosen such that the renormalised mass parameter m_R corresponds to the physical (pole) mass, m_{pole}^2 . This is done imposing the conditions:

$$p^2 - m_R^2 - \Sigma(p^2)|_{p^2=m_{\text{pole}}^2=m_R^2} = 0, \quad (3.83)$$

$$\text{Res} \left(\frac{i}{p^2 - m_R^2 - \Sigma(p^2)} \Big|_{p^2=m_{\text{pole}}^2=m_R^2} \right) = 1, \quad (3.84)$$

which imply

$$\Sigma_R(p^2 = m_{\text{pole}}^2 = m_R^2) = 0, \quad (3.85)$$

$$\frac{d}{dp^2} \Sigma_R(p^2) \Big|_{p^2=m_{\text{pole}}^2=m_R^2} = 0. \quad (3.86)$$

Minimal Subtraction (MS) scheme.

In this scheme, the counterterms are chosen to have no finite parts, but just to cancel exactly the infinities in divergent quantities. When performing the regularisation in dimensional regularisation, this corresponds to removing all the $(1/\epsilon)$ poles, for $\epsilon = 4 - d$.

Modified Minimal Subtraction ($\overline{\text{MS}}$ or MS-bar) scheme.

Normally, in dimensional regularisation the $(1/\epsilon)$ poles are accompanied by terms involving γ and $\log(4\pi)$. The prescription in the $\overline{\text{MS}}$ scheme is to subtract these terms as well, together with the $(1/\epsilon)$ poles.

To illustrate the subtraction procedures and see which are the most relevant differences between them, we will compute the counterterms in the on-shell scheme and in the $\overline{\text{MS}}$

scheme, applying them to the result for the Higgs self-energy in dimensional regularisation, Eq. (3.68).

Let us start with the on-shell scheme. Applying the first on-shell renormalisation condition, Eq. (3.85), we obtain

$$\delta_m m_R^2 = \Sigma_2(p^2 = m_{\text{pole}}^2 = m_R^2) \quad (3.87)$$

Then, applying the second on-shell renormalisation condition, Eq. (3.86), we get

$$\begin{aligned} \delta_2 &= \frac{d}{dp^2} \Sigma_2(p^2) \Big|_{p^2=m_{\text{pole}}^2=m_R^2} \\ &= \frac{-2|y_n|^2}{(4\pi)^2} \int_0^1 dx x(x-1) \left(1 + \frac{2}{\epsilon} - \gamma + \ln\left(\frac{4\pi\mu^2}{\Delta}\right) - \frac{x(x-1)}{\Delta} \right) \Big|_{p^2=m_{\text{pole}}^2=m_R^2}, \end{aligned} \quad (3.88)$$

with $\Delta = x(x-1)p^2 + x(m_2^2 - m_1^2) + m_1^2$.

The counterterms in the $\overline{\text{MS}}$ scheme are obtained by simply requiring them to cancel the $(1/\epsilon)$ pole term and the $\ln(4\pi)$ and γ factors. They are given by

$$\delta_2 = \frac{|y_N|^2}{3(4\pi)^2} \left(\frac{2}{\epsilon} - \gamma + \ln(4\pi) \right) \quad (3.89)$$

and

$$\delta_m = \frac{2|y_N|^2}{(4\pi)^2} \left(\frac{m_2^2 + m_1^2 - m_1 m_2}{m_R^2} - \frac{1}{6} \right) \left(\frac{2}{\epsilon} - \gamma + \ln(4\pi) \right). \quad (3.90)$$

Although in the on-shell scheme there is a clear interpretation of the renormalised mass, which simply corresponds to the physical (pole) mass, the computation of the counterterms is much more involved than in the $\overline{\text{MS}}$ scheme, as can be already seen by comparing the results obtained for both schemes. It is actually often easier to perform loop calculations in $\overline{\text{MS}}$ and then convert the masses back to the pole mass at the end rather than to do the computations in terms of the pole mass from the beginning [9]⁴.

3.2.4 Higgs mass radiative correction

In this section we recap the results obtained through the regularisation and renormalisation procedure for the calculation of the radiative corrections to the Higgs mass. As we have seen, the one-loop self-energy graph $\Sigma_2(p^2)$ involving the new right-handed neutrino which contributes to the Higgs propagator is divergent. However, it is possible to remove this divergence by renormalising the Higgs bare field into a renormalised field, $h_R = Z_h^{1/2} h_0$, and redefining the bare mass in terms of a renormalised mass, $m_R^2 = Z_m^{-1} m_0$. The renormalisation factors can be expanded around the classical values: $Z_h = 1 + \delta_h$, $Z_m = 1 + \delta_m$, where δ_h and δ_m are known as counterterms, which can be chosen such that they cancel the infinite

⁴In fact, the $\overline{\text{MS}}$ scheme is the one used in most of modern quantum field theory calculation, not only because it is simpler, but also because it is free of ambiguities related to non-perturbative effects in QCD, associated with particles such as quarks which never appear as asymptotic states, and for which the pole mass is not a useful mass definition [9].

contributions of the Higgs self-energy graph leading to a renormalised finite propagator. The cancellation fixes the infinite parts of the counterterms but the finite parts are arbitrary. The different conventions for fixing the finite parts are known as subtraction schemes.

From Eq. (3.85) we see that in the on-shell scheme the renormalised mass, which is set to be the physical (pole) mass in this scheme, does not receive radiative corrections by definition. However, in the $\overline{\text{MS}}$ -scheme, the renormalised mass parameter m_R does get radiative corrections. Indeed, inserting the result for the self-energy loop graph (in dimensional regularisation), Eq. (3.68), and the counterterms, Eqs. (3.89, 3.90), into the renormalised self-energy, Eq. (3.82), we obtain

$$\begin{aligned} -i\Sigma_R(p^2)|_{1\text{-loop}} &= \text{---} \text{---} \text{---} \text{---} \text{---} \text{---} + \text{---} \otimes \text{---} \text{---} \\ &= -i\Sigma_2(p^2) + i(\delta_h(p^2 - m_R^2) + \delta_m m_R^2) \\ &= \frac{2i|y_N|^2}{(4\pi)^2} \int_0^1 dx \left\{ \Delta + (x(1-x)p^2 - 2x(m_2^2 - m_1^2) - 2m_1^2 + m_1 m_2) \ln \left(\frac{\mu^2}{\Delta} \right) \right\}. \end{aligned} \quad (3.91)$$

We can simplify the expression by using the see-saw relation $m_2 \gg m_1$,

$$-i\Sigma_R(p^2)|_{1\text{-loop}} \simeq \frac{2i|y_N|^2}{(4\pi)^2} \int_0^1 dx \left\{ \Delta - \ln \left(\frac{\mu^2}{\Delta} \right) (x(1-x)p^2 - 2xm_2^2) \right\}, \quad (3.92)$$

with $\Delta \simeq x(x-1)p^2 + xm_2^2$.

From the definition of the pole mass as being the pole in the propagator, and using our sign convention, the contribution of the renormalised self-energy at $p^2 = m_{\text{pole}}^2$ corresponds to a positive shift of the renormalised mass parameter squared m_R^2 ,

$$m_{\text{pole}}^2 = m_R^2 + \Sigma_R(m_{\text{pole}}^2). \quad (3.93)$$

In this sense, we can refer to the renormalised self-energy contribution as the radiative correction to the renormalised mass parameter, which we will denote as $\delta m_h^2 \equiv \Sigma_R(m_{\text{pole}}^2)$. Note that the above expression defines the pole mass and is independent of the subtraction scheme.

Since the heavy right-handed neutrino is expected to be much larger than the physical Higgs mass, $M_h = m_{\text{pole}} = 125$ GeV, we can approximate $\Sigma_R(p^2 = m_{\text{pole}}^2)$ by $\Sigma_R(p^2 = 0)$, which simplifies Eq. (3.92). Using this approximation and integrating over the Feynman parameter x we obtain

$$-i\Sigma_R(p^2 = 0) = \frac{2i|y_N|^2}{(4\pi)^2} m_2^2 \left(1 + \ln \left(\frac{\mu_R^2}{m_2^2} \right) \right). \quad (3.94)$$

This can be rewritten in terms of the mass of the light SM neutrino m_ν and the new heavy right-handed neutrino using the see-saw relations, Eqs. (3.38, 3.39),

$$m_\nu \equiv m_1 \simeq -m_D \frac{m_D}{M_R} \quad (3.95)$$

$$m_2 \simeq M_R \quad (3.96)$$

where we have identified the light mass eigenvalue m_1 with the mass of the light active neutrino m_ν ; and the relation between the Yukawa coupling and the Dirac mass

$$m_D = \frac{v}{\sqrt{2}} y_N. \quad (3.97)$$

Substituting this relations in equation (3.94) we obtain

$$-i\Sigma_R(p^2 = 0) = \frac{-i}{4\pi^2} \frac{m_\nu M_R^3}{v^2} \left(1 + \ln \left(\frac{\mu_R^2}{M_R^2} \right) \right). \quad (3.98)$$

Therefore, using the definition $\delta m_h^2 \equiv \Sigma_R(m_{\text{pole}}^2) \simeq \Sigma_R(p^2 = 0)$ we finally obtain from Eq. (3.94) and Eq. (3.98) that the radiative correction to the renormalised mass parameter m_R in the $\overline{\text{MS}}$ scheme computed in dimensional regularisation is given by

$$\begin{aligned} \delta m_h^2 &= -\frac{|y_N|^2}{8\pi^2} m_2^2 \left(1 + \ln \left(\frac{\mu_R^2}{m_2^2} \right) \right) \\ &= \frac{1}{4\pi^2} \frac{m_\nu M_R^3}{v^2} \left(1 + \ln \left(\frac{\mu_R^2}{M_R^2} \right) \right). \end{aligned} \quad (3.99)$$

This equation points to the hierarchy problem that is inherent to theories with fundamental scalars. Indeed, we observe that the Higgs mass correction is proportional to the new heavy neutrino mass M_R and, therefore, the larger the heavy neutrino mass is, the larger the correction to the Higgs mass will become. In other words, low energy physics is sensitive to UV physics, which does not decouple from the theory. This anti-intuitive behaviour might imply a high degree of fine-tuning to accommodate the experimental data on the physical Higgs mass if the see-saw scale is much larger than the electroweak scale.

Choosing the renormalisation scale to be the new large energy scale, $\mu_R^2 = M_R^2$, we finally obtain

$$\begin{aligned} \delta m_h^2(\mu_R^2 = M_R^2) &= -\frac{1}{8\pi^2} |y_N|^2 m_2^2 \\ &= \frac{1}{4\pi^2} \frac{m_\nu M_R^3}{v^2}, \end{aligned} \quad (3.100)$$

in agreement with the literature [39, 40]⁵ up to a factor 1/2.

Renormalisation scale

Before we continue the discussion about the influence of the heavy neutrino mass on the Higgs mass correction, we want to comment on the renormalisation scale, μ_R . Recall that this is an auxiliary scale without any physical meaning, which was introduced as a technical tool in the dimensional regularisation to keep the Yukawa coupling dimensionless in d space-time dimensions and compensate the mass dimensions inside the logarithmic terms (see Eq. (3.67) and the explanation below). Therefore, physical quantities must not depend on it.

⁵Note that in [39] the correction is computed for the μ^2 parameter of the Higgs potential while here we have computed the correction to the Higgs mass parameter m_h^2 after SSB. They are related by $m_h^2 = 2\mu^2$.

From the definition of the mass pole, Eq. (3.93), and using our notation $\delta m_h^2 \equiv \Sigma_R(m_{\text{pole}}^2)$, we can write

$$m_{\text{pole}}^2 = m_R^2(\mu_R^2) + \delta m_h^2(\mu_R^2), \quad (3.101)$$

where we have made explicit the dependence of the renormalised mass and the corresponding radiative corrections on the renormalisation scale μ_R . We know that the pole mass is a fixed number which can be measured by experiments and should not depend on the renormalisation scale. Therefore, the μ_R -dependence of $\delta m_h^2(\mu_R)$ must be compensated by the change of $m_R^2(\mu_R)$ with the energy scale.

From minimizing the Higgs potential we obtained in Section 2.1.3 the relation between the Higgs bare mass parameter m_h^2 and the bare quartic coupling λ (Eq. (2.52)). Similarly to the renormalisation of the bare mass and the bare field, the quartic coupling λ must be also renormalised. The relation between the mass and the quartic coupling holds after renormalising them, so we can write

$$m_R^2(\mu_R^2) = 2\lambda_R(\mu_R^2)v^2, \quad (3.102)$$

where λ_R is the renormalised quartic coupling. The dependence of λ_R on the renormalisation scale is encoded in its beta function, which above the energy $\mu_R = M_R$ should include an extra term to cancel the dependence of δm_h^2 on μ_R^2 . Substituting Eq. (3.102) into Eq. (3.101) we obtain

$$m_{\text{pole}}^2 = 2\lambda_R(\mu_R^2)v^2 + \delta m_h^2(\mu_R^2). \quad (3.103)$$

Thus, a change in the radiative correction $\delta m_h^2(\mu_R^2)$ produced by a shift in the renormalisation scale $\mu_R^2 \rightarrow \tilde{\mu}_R^2$ will be compensated by the corresponding change of the running coupling $\lambda_R(\mu_R^2) \rightarrow \lambda_R(\tilde{\mu}_R^2)$, so that the pole mass remains μ_R -independent.

Loop diagrams lead to terms with logarithms of the type $\ln\left(\frac{q^2}{\mu_R^2}\right)$, where q is a combination of the external momenta of the diagrams and the masses of the particles involved. Thus, in perturbation theory the radiative corrections are written as an expansion of $\left(\ln\left(\frac{q^2}{\mu_R^2}\right)\right)^n$. From this we see that if the chosen μ_R^2 differs a lot from q^2 large contributions appear and the perturbation theory breaks down, since higher order terms become relevant. This is known as the problem of large logarithms and it is solved by the renormalisation group, which ensures that observables are independent of the renormalisation conditions, in particular, of the scales at which we choose to define our renormalised quantities [9]⁶. In order to avoid these large logarithm problem and work with fixed-order perturbation theory, we chose the renormalisation scale to $\mu_R = M_R$, so that the logarithm in Eq. (3.99) cancels.

⁶For further reading on the large logarithm problem and the renormalisation scale we refer to Chapter 23 of Schwartz [9].

3.3 RESULTS AND DISCUSSION

In the previous section we have computed the radiative correction to the Higgs mass that a right-handed heavy neutrino would introduce in the framework of the type I see-saw model for the simplified case of only one lepton family. In this section we want to use this result to establish a limit on the mass of this new heavy neutrino, assuming, from a naturalness point of view, that the correction to the Higgs mass should not be larger than the Higgs mass itself, $M_h \simeq 125$ GeV.

The Higgs mass correction depends both on the sterile heavy neutrino and the active light neutrino mass. The absolute value of the active neutrino masses is unknown, and only upper bounds have been set, as summarized in Section 2.2.2. From beta spectroscopy experiments, it is known that $m_{\nu_e}^{(\text{eff})} \equiv (\sum_i |U_{ei}|^2 m_{\nu_i}^2)^{1/2} < 2.3$ eV (see Eq. (2.65)). In the basis where the charged lepton mass matrix is diagonal, the absolute value of an element of the neutrino mass-matrix cannot exceed the largest neutrino mass, which can be proved by means of the Cauchy-Schwarz's inequality [41]. Thus,

$$m_{\nu_{\text{max}}} < 2.3 \text{ eV}. \quad (3.104)$$

Following this limit, we have considered two benchmark values for the light neutrino masses: $m_\nu = 2$ eV and $m_\nu = 1 \times 10^{-3}$ eV. Figure 3.4 shows the dependence of the Higgs mass correction (normalized to the Higgs mass squared M_h^2) on the heavy neutrino mass M_R , Eq. (3.100), for $m_\nu = 2$ eV (green) and $m_\nu = 1 \times 10^{-3}$ eV (orange). The dashed horizontal lines correspond to the conditions: $\delta m_h^2 \sim M_h^2$ (blue), $\delta m_h^2 \sim 0.1 M_h^2$ (pink) and $\delta M_h^2 \sim 0.01 M_h^2$ (yellow). Assuming the weakest naturalness condition $\delta m_h^2/M_h^2 \sim 1$, i.e. the radiative corrections to the Higgs mass parameter squared to be at most of the order of the physical Higgs mass squared, we obtain the following limits on the triplet mass:

$$m_\nu = 2 \text{ eV} \quad \Rightarrow \quad M_R \leq 2.7 \times 10^6 \text{ GeV}, \quad (3.105)$$

$$m_\nu = 1 \times 10^{-3} \text{ eV} \quad \Rightarrow \quad M_R \leq 3.3 \times 10^7 \text{ GeV}. \quad (3.106)$$

Thus, in order not to get too large contributions to the Higgs mass from the new heavy right-handed neutrino, M_R should be no larger than $\mathcal{O}((10^6 - 10^7) \text{ GeV})$ for $m_\nu \sim \mathcal{O}((10^{-3} - 1) \text{ eV})$.

We should note that the calculations have been done in the simplified case of only one family of neutrinos. Therefore, the limits on M_R should be only taken as estimates, since the existence of three families, which imply mixing angles and phases, could modify to a certain extent the relation between the masses of the light and heavy neutrinos. Although the study of the three family case is out of the scope of this work, we will give the existing results from the literature and briefly comment on them at the end of this section.

Table 3.1 summarizes the limits on the different mass scales and Yukawa coupling for our benchmark light neutrino masses $m_\nu = 2$ eV and $m_\nu = 1 \times 10^{-3}$ eV. The right-handed neutrino mass range is taken between the electroweak scale and the upper limit given by the naturalness condition. As can be seen in Fig. 3.4, from naturalness we demand the right-handed neutrino not to be extremely heavy, so that the quantum corrections to the Higgs mass do not grow too large. However, too small values of the right-handed neutrino

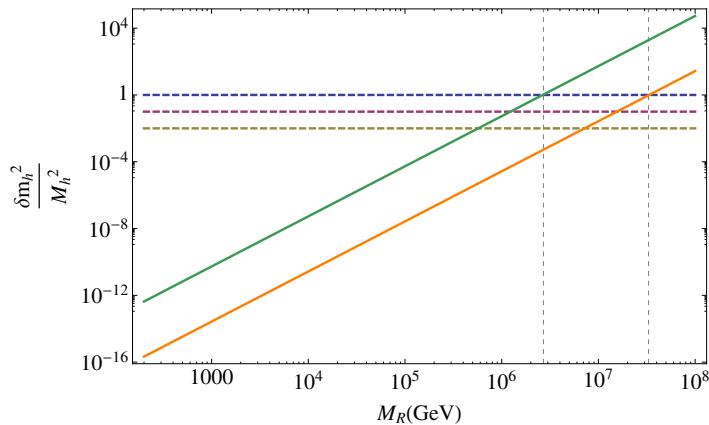


Figure 3.4: Dependence of the Higgs mass correction normalized to the Higgs mass on the mass of the new heavy right-handed neutrino M_R within the framework of the type I see-saw model for $m_\nu = 2$ eV (green) and $m_\nu = 1 \times 10^{-3}$ eV (orange). The dashed lines correspond to the conditions: $\delta m_h^2 \sim M_h^2$ (blue), $\delta m_h^2 \sim 0.1 M_h^2$ (pink) and $\delta m_h^2 \sim 0.01 M_h^2$ (yellow), with $M_h = 125$ GeV.

m_ν (eV)	M_R (GeV)	m_D (MeV)	y_D
2	$\mathcal{O}(10^2 - 10^6)$	$\mathcal{O}(10^{-3} - 10)$	$\mathcal{O}(10^{-8} - 10^{-4})$
1×10^{-3}	$\mathcal{O}(10^2 - 10^7)$	$\mathcal{O}(10^{-2} - 1)$	$\mathcal{O}(10^{-7} - 10^{-5})$

Table 3.1: Order of magnitude of the mass scales and neutrino Yukawa couplings present in the type I see-saw model for the two benchmark light neutrino masses (m_ν) under consideration. The lowest value for the right-handed neutrino mass (M_R) is taken to be at the electroweak scale while the maximum value corresponds to the upper bound from the naturalness condition $\delta m_h^2/M_h^2 \sim 1$.

mass would imply the loss of the see-saw as a suppression mechanism through the relation $m_\nu \simeq -m_D^2/M_R$ and the need of fine-tuning the Dirac neutrino mass parameter m_D in order to realize small values of m_ν . For illustration, we can compare the results to the electron, which has the smallest Yukawa coupling in the SM, with $m_e \simeq 0.5$ MeV and $y_e \sim 10^{-6}$. Taking the largest values for the right-handed neutrino mass allowed by our naturalness condition, $M_R \sim \mathcal{O}(10^6 - 10^7)$ GeV, we obtain Dirac masses and Yukawa couplings for the neutrinos of similar order of magnitude than for the electron. However, the smaller the right-handed neutrino mass, the smaller the Dirac mass needed to satisfy the smallness of the observed neutrino masses (cf. (3.95)) and thus, the smaller the Yukawa coupling (cf. (3.97)). Therefore, considering too small values for the right-handed neutrinos would make us run into a new problem: to explain why neutrinos are so weakly coupled to the Higgs.

Note that this reasoning holds only for the one-family approximation. As pointed out in Section 3.1, in the general case of three (or more) heavy neutrino families, it is possible to have a low scale see-saw with $M_R \sim \mathcal{O}(1$ TeV) and a Dirac mass matrix M_D at the electroweak scale and still generate small neutrino masses if enough structure cancellations are present in the M_D and M_R matrices. We refer to Refs. [32, 35] and the references therein for further reading on this topic.

Three right-handed heavy neutrino scenario

The naturalness of the type I see-saw in the three-flavour scenario has been studied in Ref. [42]. In this article, the authors enlarge the SM particle content with three right-handed heavy neutrinos and calculate the radiative correction to the Higgs mass introduced by these new particles⁷. Imposing that these corrections should not exceed the electroweak scale results in three bounds, one for each right-handed neutrino mass. Requiring the corrections to be less than 1 TeV, they obtain [42]:

$$M_{N_1} \lesssim 4 \times 10^7 \text{ GeV}, \quad (3.107)$$

$$M_{N_2} \lesssim 7 \times 10^7 \text{ GeV}, \quad (3.108)$$

$$M_{N_3} \lesssim 3 \times 10^7 \text{ GeV} \left(\frac{0.05 \text{ eV}}{m_{\nu_{\min}}} \right)^{1/3}, \quad (3.109)$$

where $m_{\nu_{\min}}$ denotes the lightest neutrino mass. Note that their naturalness condition, i.e. accepting radiative corrections up to 1 TeV, is more relaxed than the one we have been using, $\delta m_h^2 \leq m_h^2 \sim 10^2 \text{ GeV}$. Applying our more stringent condition the quoted limits, Eqs. (3.107 - 3.109), are reduced by a factor of $10^{2/3} \sim 5$.

Taking this limits we can observe that in order not to have too large radiative corrections and thus satisfy our naturalness condition, the heavy neutrino masses should be roughly of the order of $(10^6 - 10^7) \text{ GeV}$, except on one of them, which can be indefinitely large for model with a massless neutrino. This result for the three-family scenario is the same than the simplified case of only one family, which we have studied in detail in this work.

It also worth to remark that these upper bounds obtained from naturalness considerations in the three-flavour type I see-saw are not compatible with baryogenesis via leptogenesis, which typically requires masses for the right-handed neutrinos larger than $\mathcal{O}((10^8 - 10^9) \text{ GeV})$, as pointed out in [42]. For further details on the different mechanisms for leptogenesis within the type I see-saw scenario and the implications from naturalness, we refer to [42] and references therein.

⁷The radiative correction given in [42] is actually for the electroweak μ^2 parameter of the Higgs potential, which is related to the Higgs mass by $m_h^2 = 2\mu^2$ (cf. Eq. (2.52)) after SSB. The UV-sensitivity due to the quadratic dependence on the large scale is the same for the two parameters, independently of whether the computation is done before or after SSB. Thus, the conclusions obtained from either approach are equivalent.

4 TYPE II SEE-SAW MODEL

In the type II see-saw model, the minimal SM particle content is enlarged by the addition of a $SU(2)_L$ -triplet Δ of complex scalar fields, which transforms as $(\mathbf{1}, \mathbf{3}, 1)$ under the SM $SU(3)_C \times SU(2)_L \times U(1)_Y$ gauge group:

$$\Delta = \frac{\sigma^i}{\sqrt{2}} \Delta_i = \begin{pmatrix} \delta^+/\sqrt{2} & \delta^{++} \\ \delta^0 & -\delta^+/\sqrt{2} \end{pmatrix}, \quad (4.1)$$

with $\Delta_1 = (\delta^{++} + \delta^0)/\sqrt{2}$, $\Delta_2 = i(\delta^{++} - \delta^0)/\sqrt{2}$, $\Delta_3 = \delta^+$. The minimal Lagrangian for this model is given by

$$\mathcal{L} = \mathcal{L}_{\text{kinetic}} + \mathcal{L}_Y - \mathcal{V}(\Phi, \Delta), \quad (4.2)$$

where the kinetic and Yukawa interaction terms are,

$$\mathcal{L}_{\text{kinetic}} = \mathcal{L}_{\text{kinetic}}^{\text{SM}} + \text{Tr} \left[(D_\mu \Delta)^\dagger (D^\mu \Delta) \right] \quad (4.3)$$

and

$$\mathcal{L}_Y = \mathcal{L}_Y^{\text{SM}} - (Y_\Delta)_{ij} L_{Li}^T C i \sigma_2 \Delta L_{Lj} + \text{h.c.} \quad (4.4)$$

Here C is the Dirac charge conjugation matrix with respect to the Lorentz group and $D_\mu \Delta$ is the covariant derivative of the scalar triplet, given by

$$D_\mu \Delta = \partial_\mu \Delta + i \frac{g}{2} [\sigma^a W_\mu^a, \Delta] + \frac{g'}{2} B_\mu \Delta \quad (a = 1, 2, 3) \quad (4.5)$$

where g and g' are the weak and hypercharge interaction couplings, respectively.

The potential can be written as [43]¹

$$\begin{aligned} \mathcal{V}(\Phi, \Delta) = & -m_\Phi^2 \Phi^\dagger \Phi + \frac{\lambda}{2} (\Phi^\dagger \Phi)^2 + M_\Delta^2 \text{Tr}(\Delta^\dagger \Delta) + \frac{\lambda_1}{2} \left[\text{Tr}(\Delta^\dagger \Delta) \right]^2 \\ & + \frac{\lambda_2}{2} \left(\left[\text{Tr}(\Delta^\dagger \Delta) \right]^2 - \text{Tr} \left[(\Delta^\dagger \Delta)^2 \right] \right) + \lambda_4 (\Phi^\dagger \Phi) \text{Tr}(\Delta^\dagger \Delta) + \lambda_5 \Phi^\dagger [\Delta^\dagger, \Delta] \Phi \\ & + \left(\frac{\Lambda_6}{\sqrt{2}} \Phi^T i \sigma_2 \Delta^\dagger \Phi + \text{h.c.} \right), \end{aligned} \quad (4.6)$$

where Φ is the SM Higgs doublet,

$$\Phi = \begin{pmatrix} \phi^+ \\ \phi^0 \end{pmatrix} \quad (4.7)$$

¹Note that in order to be consistent with Ref. [43], on which this section will be based, we have changed the notation of the mass and quartic parameter of the scalar doublet with respect to Section 2 to $\mu^2 \rightarrow m_\Phi^2$ and $\lambda \rightarrow \lambda/2$.

with ϕ^+ and ϕ^0 being two scalar complex fields. The coupling Λ_6 is a dimensionfull parameter, with mass dimension one. The coupling constants λ_i ($i = 1, 2, 4, 5$) can be chosen to be real through a phase redefinition of the field Δ . The parameter m_Φ^2 is chosen to be positive to ensure the spontaneous electroweak symmetry breaking of $SU(2)_L \times U(1)_Y$ gauge group to $U(1)_Q$ through the Higgs mechanism, in which the neutral component of the SM Higgs doublet acquires a vacuum expectation value (vev), $\langle \phi^0 \rangle = v/\sqrt{2}$ (see Section 2.1.3).

The electroweak symmetry breaking (EWSB) conditions are obtained after minimizing the scalar potential with respect to Φ and Δ , and are given by

$$m_\Phi^2 = \frac{1}{2}\lambda v^2 - \Lambda_6 v_\Delta + \frac{1}{2}(\lambda_4 - \lambda_5)v_\Delta^2, \quad (4.8)$$

$$M_\Delta^2 = \frac{1}{2}\frac{\Lambda_6 v^2}{v_\Delta} - \frac{1}{2}(\lambda_4 - \lambda_5)v^2 - \frac{1}{2}\lambda_1 v_\Delta^2. \quad (4.9)$$

where v_Δ is the vev of the neutral component of the scalar triplet, normalized as $\langle \delta^0 \rangle = v_\Delta/\sqrt{2}$.

It can be shown that the non-zero v_Δ contributes to the gauge boson masses at tree level [43]:

$$M_W^2 = \frac{g^2}{2}(v^2 + 2v_\Delta^2), \quad M_Z^2 = \frac{g^2}{2\cos^2\theta_W}(v^2 + 4v_\Delta^2), \quad (4.10)$$

where g is the $SU(2)_L$ coupling constant and θ_W is the Weinberg angle. This makes the ρ -parameter deviate from unity at tree level,

$$\rho \equiv \frac{M_W^2}{M_Z^2 \cos^2\theta_W} = \frac{1 + \frac{2v_\Delta^2}{v^2}}{1 + \frac{4v_\Delta^2}{v^2}}. \quad (4.11)$$

The electroweak precision data constraints set the experimental bound $\rho = 1.0004_{-0.0004}^{+0.0003}$ [8], which requires

$$\frac{v_\Delta}{v} < 0.02, \quad v_\Delta \lesssim 5 \text{ GeV}. \quad (4.12)$$

Therefore, we will always be working in the limit $v_\Delta \ll v$.

4.1 NEUTRINO MASSES

In the type II see-saw model, a Majorana mass term for the neutrinos is generated through the Yukawa coupling term between the left-handed leptons and the triplet when the neutral component of Δ develops a vev v_Δ , $\langle \delta^0 \rangle = v_\Delta/\sqrt{2}$,

$$\mathcal{L}_Y \supset - (Y_\Delta)_{ij} L_i^T C i \sigma_2 \Delta L_j + \text{h.c.} \quad \longrightarrow \quad - \frac{v_\Delta}{\sqrt{2}} (Y_\Delta)_{ij} \nu_{Li}^T C \nu_{Lj} + \text{h.c.} \quad (4.13)$$

Then, the neutrino mass matrix is given by ²

$$(M_\nu)_{ij} = \sqrt{2}v_\Delta (Y_\Delta)_{ij}. \quad (4.14)$$

²Recall that a Majorana mass term has the form $\frac{1}{2}\psi_i^C M_{ij}\psi_j$, where the factor $\frac{1}{2}$ is present to take into account that ψ and ψ^C are not independent.

In the limit $v_\Delta \ll v$, we obtain from Eq. (4.9)

$$v_\Delta = \frac{\Lambda_6 v^2}{2M_\Delta^2 + v^2(\lambda_4 - \lambda_5)}. \quad (4.15)$$

Then, for masses of the triplet much larger than the electroweak scale, i.e. $M_\Delta \gg v$, Eq. (4.14) becomes

$$M_\nu \simeq \sqrt{2} \frac{\lambda_6 v^2}{2M_\Delta} Y_\Delta, \quad (4.16)$$

where we have defined the dimensionless parameter $\lambda_6 \equiv \Lambda_6/M_\Delta$. This equation resembles a typical see-saw formula with $M_\nu \propto M_\Delta^{-1}$. The structure of the Yukawa coupling matrix Y_Δ is related to the mass matrix and it is therefore constrained by low-energy oscillation data. From Eq. (4.14), we obtain

$$Y_\Delta = \frac{M_\nu}{\sqrt{2}v_\Delta} = \frac{1}{\sqrt{2}v_\Delta} U_{\text{PMNS}}^* M_\nu^{\text{diag}} U_{\text{PMNS}}^\dagger, \quad (4.17)$$

where $M_\nu^{\text{diag}} = \text{diag}(m_1, m_2, m_3)$ is the diagonal neutrino mass eigenvalue matrix and U_{PMNS} is the Pontecorvo-Maki-Nakagawa-Sakata (PMNS) mixing matrix, given in Eq. (2.60).

In order to illustrate the size of the Yukawa couplings, we choose a normal hierarchy for the neutrino masses with $m_1 = 0$ and assume the Majorana phases to be zero. Using the best-fit values of Table 2.2, we obtain the following structure of the Yukawa coupling matrix:

$$Y_\Delta = \frac{10^{-2} \text{ eV}}{v_\Delta} \times \begin{pmatrix} 0.19 + 0.09i & 0.08 - 0.45i & -0.49 - 0.51i \\ 0.08 - 0.45i & 2.52 - 0.05i & 2.15 - 0.09i \\ -0.49 - 0.51i & 2.15 - 0.09i & 3.01 + 0.05i \end{pmatrix} \quad (4.18)$$

From Eq. (4.18), we observe that there are two extreme cases:

- (i) **Large Yukawa couplings:** $(Y_\Delta)_{ij} \sim \mathcal{O}(1)$, which corresponds to small values of the triplet vev, $v_\Delta \sim \mathcal{O}(10^{-2} \text{ eV})$. Assuming that the Yukawa couplings should not be larger than unity for perturbation theory, this relation fixes a lower bound for the scalar triplet vev, $v_\Delta \gtrsim \mathcal{O}(10^{-2} \text{ eV})$.
- (ii) **Small Yukawa couplings:** $(Y_\Delta)_{ij} \sim \mathcal{O}(10^{-12})$, which correspond to large values of the triplet vev, $v_\Delta \sim \mathcal{O}(\text{GeV})$. Recall that the triplet vev has an upper bound of $v_\Delta \lesssim 5 \text{ GeV}$, which comes from the electroweak precision measurement of the ρ -parameter (see Eq. (4.12)).

4.2 SCALAR MASSES AND MIXING

Expanding the scalar fields ϕ^0 and δ^0 around their vevs,

$$\phi^0 = \frac{1}{\sqrt{2}}(v + \phi + i\chi), \quad (4.19)$$

$$\delta^0 = \frac{1}{\sqrt{2}}(v_\Delta + \delta + i\eta), \quad (4.20)$$

we obtain 10 real-valued field components:

$$\Phi = \begin{pmatrix} \phi^+ \\ \frac{1}{\sqrt{2}}(v + \phi + i\chi) \end{pmatrix}, \quad \Delta = \begin{pmatrix} \frac{\delta^+}{\sqrt{2}} & \delta^{++} \\ \frac{1}{\sqrt{2}}(v_\Delta + \delta + i\eta) & -\frac{\delta^+}{\sqrt{2}} \end{pmatrix}, \quad (4.21)$$

which lead to a 10×10 squared mass matrix for the scalars. There are seven physical massive eigenstates: $H^{\pm\pm}$, H^\pm , h , H^0 , A^0 , and three massless Goldstone bosons: G^\pm , G^0 , which are "eaten up" to give mass to the SM gauge bosons W^\pm , Z . The physical mass eigenvalues for the scalar sector are [43]

$$m_{H^{\pm\pm}}^2 = M_\Delta^2 + \frac{1}{2}(\lambda_4 + \lambda_5)v^2 + \frac{1}{2}(\lambda_1 + \lambda_2)v_\Delta^2, \quad (4.22)$$

$$m_{H^\pm}^2 = \left(M_\Delta^2 + \frac{1}{2}\lambda_4v^2 + \frac{1}{2}\lambda_1v_\Delta^2 \right) \left(1 + \frac{2v_\Delta^2}{v^2} \right), \quad (4.23)$$

$$m_{A^0}^2 = \left(M_\Delta^2 + \frac{1}{2}(\lambda_4 - \lambda_5)v^2 + \frac{1}{2}\lambda_1v_\Delta^2 \right) \left(1 + \frac{4v_\Delta^2}{v^2} \right), \quad (4.24)$$

$$m_h^2 = \frac{1}{2} \left(A + C - \sqrt{(A - C)^2 + 4B^2} \right), \quad (4.25)$$

$$m_{H^0}^2 = \frac{1}{2} \left(A + C + \sqrt{(A - C)^2 + 4B^2} \right), \quad (4.26)$$

with $A = \lambda v^2$, $B = -\frac{2v_\Delta}{v} (M_\Delta^2 + \frac{1}{2}\lambda_1v_\Delta^2)$, $C = M_\Delta^2 + \frac{1}{2}(\lambda_4 - \lambda_5)v^2 + \frac{3}{2}\lambda_1v_\Delta^2$. The doublet and triplet scalar fields mix in the charged, CP -even and CP -odd scalar sectors [43]

$$\begin{pmatrix} G^\pm \\ H^\pm \end{pmatrix} = \begin{pmatrix} \cos \beta' & \sin \beta' \\ -\sin \beta' & \cos \beta' \end{pmatrix} \begin{pmatrix} \phi^\pm \\ \delta^\pm \end{pmatrix}, \quad (4.27)$$

$$\begin{pmatrix} h \\ H^0 \end{pmatrix} = \begin{pmatrix} \cos \alpha & \sin \alpha \\ -\sin \alpha & \cos \alpha \end{pmatrix} \begin{pmatrix} \phi \\ \delta \end{pmatrix}, \quad (4.28)$$

$$\begin{pmatrix} G^0 \\ A^0 \end{pmatrix} = \begin{pmatrix} \cos \beta & \sin \beta \\ -\sin \beta & \cos \beta \end{pmatrix} \begin{pmatrix} \chi \\ \eta \end{pmatrix}, \quad (4.29)$$

where the mixing angles are given by:

$$\tan \beta' = \frac{\sqrt{2}v_\Delta}{v}, \quad (4.30)$$

$$\tan \beta = \frac{2v_\Delta}{v} = \sqrt{2} \tan \beta', \quad (4.31)$$

$$\tan 2\alpha = \frac{2B}{A - C} = \frac{4v_\Delta}{v} \frac{M_\Delta^2 + \frac{1}{2}\lambda_1v_\Delta^2}{M_\Delta^2 + \frac{1}{2}(\lambda_4 - \lambda_5 - 2\lambda)v^2 + \frac{3}{2}\lambda_1v_\Delta^2}. \quad (4.32)$$

In the limit $v_\Delta \ll v$, the mixing between the doublet and the triplet is small, unless the CP -even scalar h and H^0 are close to being mass-degenerated. Indeed, if $v_\Delta \ll v$ all the mixing angles tend to zero, since $\tan \beta'$, $\tan \beta$ and $\tan 2\alpha$ are all proportional to v_Δ/v . The only possible exception is if $m_h^2 \simeq m_{H^0}^2$, which implies that $A - C \simeq 0$ (see Eqs. (4.25-4.26) and note that B is negligible for $v_\Delta \ll v$). In this situation $\tan 2\alpha \rightarrow \infty$, which corresponds to a mixing angle of $\alpha \simeq 45^\circ$, i.e. maximal mixing between the neutral components of the doublet and the triplet. In the following, we will not consider this case, but we will study only the small-mixing case.

For $v_\Delta \ll v$, the mass of the lightest CP -even scalar h , which mainly corresponds to the scalar doublet ϕ , is simply given by³

$$m_h^2 = \lambda v^2, \quad (4.33)$$

like in the SM. Its mass is therefore independent of M_Δ . On the other hand, the other scalars have a M_Δ -dependent mass:

$$m_{H^{\pm\pm}}^2 \simeq M_\Delta^2 + \frac{1}{2}(\lambda_4 + \lambda_5)v^2, \quad (4.34)$$

$$m_{H^\pm}^2 \simeq M_\Delta^2 + \frac{1}{2}\lambda_4 v^2, \quad (4.35)$$

$$m_{A^0, H^0}^2 \simeq M_\Delta^2 + \frac{1}{2}(\lambda_4 - \lambda_5)v^2. \quad (4.36)$$

Note that the splitting between the dominantly triplet scalar masses is proportional to $\lambda_5 v^2$. In the case $M_\Delta^2 \gg v^2$, they would be all mass degenerated, with mass M_Δ . However, for triplet masses close to the electroweak scale $M_\Delta^2 \sim v^2$, the mass splitting could be noticeable. For example, for a mass of the single charged triplet component $m_{H^\pm}^2 = 400$ GeV and a coupling $\lambda_5 = 0.5$, the splitting would be of ~ 20 GeV.

4.3 VACUUM STABILITY AND UNITARITY CONDITIONS

It is known that the Higgs quartic coupling in the SM is driven to negative values at high energies, before the Planck scale is reached [44]. With the introduction of a scalar triplet, the new quartic scalar interactions between Φ and Δ could soften the decrease of the Higgs quartic coupling as the energy increases. However, with the new triplet scalar the vacuum stability conditions become more involved and it is no longer enough to check that the Higgs quartic couplings stays positive to ensure the stability of the electroweak vacuum.

The necessary and sufficient conditions which ensure the potential of the type II see-saw (Eq. (4.6)) is bounded from below have been studied in Refs. [45, 46]. Taking into account all field directions, they can be written as follows,

$$\lambda \geq 0, \quad (4.37a)$$

$$\lambda_1 \geq 0, \quad (4.37b)$$

$$2\lambda_1 + \lambda_2 \geq 0, \quad (4.37c)$$

$$\lambda_4 + \lambda_5 + \sqrt{\lambda\lambda_1} \geq 0, \quad (4.37d)$$

$$\lambda_4 - \lambda_5 + \sqrt{\lambda\lambda_1} \geq 0 \quad (4.37e)$$

$$\text{and} \quad (4.37f)$$

$$2|\lambda_5|\sqrt{\lambda_1} + \lambda_2\sqrt{\lambda} \geq 0 \quad \text{or} \quad \lambda_4 + \sqrt{(\lambda\lambda_2 + 2\lambda_5^2)(\lambda_1/\lambda_2 + 1/2)} > 0. \quad (4.37g)$$

³Recall the change of notation with respect to Section 2, $\lambda \rightarrow \lambda/2$. Thus, in this section's notation there is no factor of 2 in the relation between the mass and the quartic coupling, Eq. (3.102), in contrast with Eq. (2.52).

These vacuum stability conditions have been recently given in [45], where the authors corrected two of the conditions used previously in the literature, namely

$$\lambda_4 + \lambda_5 + \sqrt{\lambda \left(\lambda_1 + \frac{\lambda_2}{2} \right)} \geq 0, \quad (4.38a)$$

$$\lambda_4 - \lambda_5 + \sqrt{\lambda \left(\lambda_1 + \frac{\lambda_2}{2} \right)} \geq 0. \quad (4.38b)$$

As the authors discuss, these conditions are too strict: although potentials that satisfy them are bounded from below, not all potentials bounded from below obey them, i.e. they are sufficient but not necessary conditions. These two conditions must be substituted by the disjunction Eq. (4.37g), in which one of the two conditions must be satisfied in order to have a bounded from below potential.

In addition, constraints on the scalar potential parameters can be obtained by demanding tree-level unitarity to be preserved in a variety of scattering processes: scalar-scalar scattering, gauge-boson-gauge-boson scattering, and scalar-gauge-boson scattering. These have been studied in the type II see-saw model in, e.g. [46] (see also references therein). Demanding the tree level unitarity to be preserved for different elastic scattering processes the following constraints are obtained [43]:

$$\lambda \leq \frac{8}{3}\pi, \quad (4.39a)$$

$$\lambda_1 - \lambda_2 \leq 8\pi, \quad (4.39b)$$

$$4\lambda_1 + \lambda_2 \leq 8\pi, \quad (4.39c)$$

$$2\lambda_1 + 3\lambda_2 \leq 16\pi, \quad (4.39d)$$

$$|\lambda_5| \leq \frac{1}{2} \min \left[\sqrt{(\lambda \pm 8\pi)(\lambda_1 - \lambda_2 \pm 8\pi)} \right], \quad (4.39e)$$

$$|\lambda_4| \leq \frac{1}{\sqrt{2}} \sqrt{\left(\lambda - \frac{8}{3}\pi \right) (4\lambda_1 + \lambda_2 - 8\pi)}. \quad (4.39f)$$

In the following sections, we will use the vacuum stability and unitarity of scattering processes constraints, Eqs. (4.37a-4.37g) and Eqs. (4.39a-4.39f), to restrict the parameter space in the type II see-saw model by imposing them to be fulfilled up to the Planck scale.

4.4 HIGGS MASS RADIATIVE CORRECTIONS

The potential of the type II see-saw model couples the new heavy scalar triplet with the SM Higgs doublet. This coupling gives rise to loop-corrections involving the heavy scalar triplet, which will modify the bare mass of the Higgs particle through radiative corrections. The terms contributing to these corrections are:

$$\mathcal{L}_\Delta \supset -\lambda_4(\Phi^\dagger\Phi)\text{Tr}(\Delta^\dagger\Delta) - \lambda_5\Phi^\dagger[\Delta^\dagger, \Delta]\Phi - \left(\frac{\Lambda_6}{\sqrt{2}}\Phi^T i\sigma_2\Delta^\dagger\Phi + \text{h.c.} \right). \quad (4.40)$$

Similarly to the calculation of the radiative corrections in the type I see-saw model, we will work with d -dimensional regularisation and we will use the $\overline{\text{MS}}$ -scheme to remove the infinities that appear in the momentum integrals through the counterterms. The renormalisation procedure is analogous to the one explained in Section 3.2 for the type I case. For clarity, we will not draw the counterterm vertices when computing the self-energy of the Higgs mass, but we should keep in mind that they are actually present and are responsible to remove the $1/\epsilon$ -poles appearing in the loop-integrals. Similarly, we will not write explicitly the R -subindices standing for "renormalised" fields, masses and couplings, but consider the theory as already renormalised.

We define again $\delta m_h^2 \equiv \Sigma_R^2(m_{\text{pole}}^2)$ as the positive shift of the renormalised Higgs mass parameter in the Higgs full propagator (see Eq. (3.78)), which corresponds to the renormalised Higgs self-energy evaluated at the pole mass. Neglecting the Higgs physical (pole) mass $m_{\text{pole}} \equiv M_h \simeq 125$ GeV compared to the triplet mass M_Δ , we can write

$$\delta m_h^2 \equiv \Sigma_R^2(p^2 = m_{\text{pole}}^2) \simeq \Sigma_R^2(p^2 = 0), \quad (4.41)$$

where p^2 is the external momenta. In the following, we drop also the R -subindex of the renormalised self-energy function, $\Sigma_R^2(p^2) \rightarrow \Sigma^2(p^2)$, but consider it as being properly renormalised and, therefore, finite.

In this section we will use the Feynman Gauge, in which the Goldstone bosons are present as particles in our Feynman diagrams. In the limit $v_\Delta \ll v$, in which the mixing between the doublet and the triplet scalar is small, the Goldstone bosons G^0 and G^\pm correspond approximately to χ and ϕ^\pm as in the SM, and the triplet flavour eigenstates δ^0 , δ^\pm to the mass eigenstates A^0 , H^\pm (see Eqs.(4.27 - 4.29)). Working in this limit, we consider here the flavour triplet components δ^0 , δ^\pm as being the mass eigenstates. In addition, they are assumed to be mass-degenerated, with mass M_Δ .

The propagator for the Goldstone bosons is given by (see e.g. Section 1 of [47])

$$\Delta_{VV}(q^2) = \frac{i}{q^2 - \xi m_V^2 + i\epsilon}, \quad (4.42)$$

where $V = Z, W^\pm$ correspond to the gauge bosons and $\xi = 1$ for the Feynman gauge.

Let us study the three different terms in Eq. (4.40) independently by expanding them explicitly in terms of the fields contained in the Higgs doublet.

λ_4 -term

The first interaction term, proportional to λ_4 , gives

$$\begin{aligned} \mathcal{L}_\Delta &\supset -\lambda_4(\Phi^\dagger\Phi)\text{Tr}(\Delta^\dagger\Delta) \\ &= -\lambda_4 \left((\phi^+)^\dagger \phi^+ + (\phi^0)^\dagger \phi^0 \right) (\Delta^i)^\dagger \Delta^i \\ &\supset -\lambda_4 \left\{ \frac{1}{2} h h (\delta^i)^\dagger \delta^i + v h (\delta^i)^\dagger \delta^i \right\}, \end{aligned} \quad (4.43)$$

with $i = 0, +, ++$, i.e. summation over the three fields of the scalar triplet.

They give the following Feynman rules

$$\begin{aligned}
 \begin{array}{c} h \\ \diagdown \\ \diagup \\ h \end{array} & \begin{array}{c} \delta^i \\ \diagup \\ \diagdown \\ \delta^i \end{array} & = i2 \times \left(-\frac{1}{2}\lambda_4 \right) = -i\lambda_4 \\
 \\
 \begin{array}{c} h \\ \diagdown \\ \diagup \\ - \end{array} & \begin{array}{c} \delta^i \\ \diagup \\ \diagdown \\ \delta^i \end{array} & = -iv\lambda_4
 \end{aligned}$$

with $i = 0, \pm, \pm\pm$. The factor of two in the four point interaction vertex is due to the presence of two identical real h fields. There is no factor corresponding to the two δ^i fields because they are complex fields.

There are two one-loop diagrams contributing to the Higgs mass correction coming from these interaction vertices, which give the following amplitudes

$$\begin{aligned}
 -i\Sigma^2(p^2 = 0) \supset & \begin{array}{c} \delta^i \\ \curvearrowright \\ h \end{array} & = 3 \times (-i\lambda_4) \int \frac{d^4k}{(2\pi)^4} \frac{i}{k^2 - M_\Delta^2} \\
 & & = \frac{i}{16\pi^2} 3\lambda_4 M_\Delta^2 \left(1 + \ln \left(\frac{\mu_R^2}{M_\Delta^2} \right) \right), \quad (4.44)
 \end{aligned}$$

where the factor of three comes from the summation of the three possible scalars in the loop, $\delta^0, \delta^+, \delta^{++}$.

The second diagram gives

$$\begin{aligned}
 -i\Sigma^2(p^2 = 0) \supset & \begin{array}{c} \delta^i \\ \curvearrowright \\ h \end{array} & = 3 \times (-i\lambda_4 v)^2 \int \frac{d^4k}{(2\pi)^4} \frac{i^2}{(k^2 - M_\Delta^2)^2} \\
 & & = -\frac{i}{16\pi^2} 3\lambda_4^2 v^2 \ln \left(\frac{\mu_R^2}{M_\Delta^2} \right). \quad (4.45)
 \end{aligned}$$

For triplet masses larger than the electroweak scale, this contribution, which is proportional to $v^2 \sim \mathcal{O}(10^4 \text{ GeV}^2)$, is negligible compared to the contributions that are proportional to M_Δ^2 , assuming $M_\Delta \gg v$.

λ_5 -term

Let us now study the second interaction term, which is proportional to λ_5 . The relevant terms

from the type II see-saw Lagrangian are

$$\begin{aligned}
\mathcal{L}_\Delta &\supset -\lambda_5 \Phi^\dagger [\Delta^\dagger, \Delta] \Phi \\
&\supset -\lambda_5 (\phi^0)^\dagger \left[(\delta^{++})^\dagger \delta^{++} - \delta^0 (\delta^0)^\dagger \right] \phi^0 \\
&\supset -\lambda_5 \left\{ \left(\frac{1}{2} h h + v h \right) \left((\delta^{++})^\dagger \delta^{++} - (\delta^0)^\dagger \delta^0 \right) \right\}. \tag{4.46}
\end{aligned}$$

This gives the following Feynman rules

$$\begin{array}{cc}
\begin{array}{c} h \text{---} \diagup \quad \delta^{++} \\ \quad \times \\ h \text{---} \diagdown \quad \delta^{--} \end{array} &= i2 \times \left(-\frac{1}{2} \lambda_5 \right) = -i\lambda_5 & \begin{array}{c} h \text{---} \diagup \quad \delta^{++} \\ \quad < \\ h \text{---} \diagdown \quad \delta^{--} \end{array} &= -iv\lambda_5 \\
\begin{array}{c} h \text{---} \diagup \quad \delta^0 \\ \quad \times \\ h \text{---} \diagdown \quad \delta^0 \end{array} &= i2 \times \frac{1}{2} \lambda_5 = i\lambda_5 & \begin{array}{c} h \text{---} \diagup \quad \delta^0 \\ \quad < \\ h \text{---} \diagdown \quad \delta^0 \end{array} &= iv\lambda_5
\end{array}$$

As in the λ_4 Feynman rules, the factor of two in the four point interaction vertex is due to the presence of two identical real h fields.

The one-loop diagrams are also similar to the ones coming from the λ_4 -term. In this case we only have two possible scalars inside the loop: δ^{++} and δ^0 , since the contributions from δ^+ cancel in the commutator $[\Delta^\dagger, \Delta]$. These give:

$$\begin{aligned}
-i\Sigma^2(p^2=0) &\supset \begin{array}{c} \delta^i \\ \curvearrowright \\ h \text{---} \text{---} \text{---} \text{---} h \end{array} = (-i\lambda_5 + i\lambda_5) \int \frac{d^4k}{(2\pi)^4} \frac{i}{k^2 - M_\Delta^2} \\
&= 0 \tag{4.47}
\end{aligned}$$

and

$$\begin{aligned}
-i\Sigma^2(p^2=0) &\supset \begin{array}{c} \delta^i \\ \curvearrowright \\ h \text{---} \text{---} \text{---} \text{---} h \\ \delta^i \end{array} = 2 \times (i\lambda_5 v)^2 \int \frac{d^4k}{(2\pi)^4} \frac{i^2}{(k^2 - M_\Delta^2)^2} \\
&= -\frac{i}{16\pi^2} 2\lambda_5^2 v^2 \ln \left(\frac{\mu_R^2}{M_\Delta^2} \right), \tag{4.48}
\end{aligned}$$

with $i = \pm\pm, 0$ for the scalars inside the loop.

In the first loop diagram, the two contributions from the different scalars cancel due to the opposite signs in the Feynman rules. In the second diagram, the contributions do not cancel: since there are two vertices in this type of diagram, the relative sign disappears when squaring the vertex factor. However, similarly to the λ_4 -diagram, Eq. (4.45), its contribution is proportional to v^2 , which is negligible compared to the other contributions proportional to

M_Δ if we assume the mass of the triplet to be larger than the electroweak scale. Therefore, none of the diagrams coming from the λ_5 -term are relevant for the Higgs mass loop correction under this assumption.

Λ_6 -term

Finally, the third interaction term, which is proportional to Λ_6 , gives

$$\begin{aligned}\mathcal{L}_\Delta &\supset - \left(\frac{\Lambda_6}{\sqrt{2}} \Phi^T i\sigma_2 \Delta^\dagger \Phi + \text{h.c.} \right) \\ &= \frac{\Lambda_6}{\sqrt{2}} \left(\sqrt{2} \phi^0 \delta^- \phi^+ + \phi^0 (\delta^0)^\dagger \phi^0 - \phi^+ \delta^{--} \phi^+ \right) + \text{h.c.} \\ &\supset \frac{\Lambda_6}{\sqrt{2}} \left(\frac{1}{2} h \delta^0 h + h \delta^- \phi^+ + i \chi \delta^0 h \right) + \text{h.c.}\end{aligned}\quad (4.49)$$

The corresponding Feynman rules for the interaction vertices are:

There are three one-loop diagrams which contribute equally to the Higgs-mass correction. Its contribution to the self-energy is given by

$$\begin{aligned}-i\Sigma^2(p^2 = 0) &\supset \text{diagram} = -3 \times \frac{|\Lambda_6|^2}{2} \int \frac{d^4 k}{(2\pi)^4} \frac{i}{(k^2 - m_i^2)} \frac{i}{(k^2 - M_\Delta^2)} \\ &\simeq \frac{i}{16\pi^2} 3|\Lambda_6|^2 \left(1 + \ln \left(\frac{\mu_R^2}{M_\Delta^2} \right) \right),\end{aligned}\quad (4.50)$$

where m_i^2 corresponds to m_h^2 for the loop which contains the Higgs particle, and to m_V^2 if the internal line corresponds to the Goldston bosons χ or ϕ^\pm , with $V = Z, W^\pm$ being the SM gauge bosons. We have neglected these masses, which are at the electroweak scale, compared to the triplet mass M_Δ .

Writing together the main contributions to the Higgs-mass correction and using the definition $\delta m_h^2 \equiv \Sigma_R^2(m_{\text{pole}}^2) \simeq \Sigma_R^2(p^2 = 0)$ from Eq. (4.41), we finally obtain

$$\delta m_h^2 = -\frac{3}{16\pi^2} \left(\lambda_4 + \frac{|\lambda_6|^2}{2} \right) M_\Delta^2 \left(1 + \ln \left(\frac{\mu_R^2}{M_\Delta^2} \right) \right), \quad (4.51)$$

where the dimensionless coupling λ_6 is defined as $\lambda_6 \equiv \Lambda_6/M_\Delta$ and we have neglected terms proportional to v^2 .

4.5 THE RENORMALISATION GROUP EQUATIONS

To ensure that the vacuum stability and the unitary conditions presented in Section 4.3 are fulfilled up to the Planck scale, it is necessary to study their renormalisation group equations (RGEs). Depending on whether the renormalisation scale μ is below or above the new energy scale, determined by M_Δ , the RG running will be different, as we will show in this section. We will employ two-loop RGEs for the SM couplings and one-loop RGEs for the new couplings associated with the type II see-saw scenario. We follow the procedure specified in [43].

4.5.1 For $\mu < M_\Delta$

Below the see-saw scale M_Δ , the scalar triplet can be integrated out. This gives the following effective potential:

$$V_{\text{eff}}(\Phi) = -m_\Phi^2(\Phi^\dagger\Phi) + \frac{1}{2}(\lambda - \lambda_6^2)(\Phi^\dagger\Phi)^2. \quad (4.52)$$

Hence, the Higgs quartic coupling is shifted down to the SM coupling by a factor of λ_6^2 at $\mu = M_\Delta$ through the matching condition

$$\lambda_{\text{SM}} = \lambda - \lambda_6^2, \quad (4.53)$$

where $\lambda_{\text{SM}}(M_t) \simeq 0.13$ [44] and λ_6 can be written as

$$\lambda_6 \equiv \frac{\Lambda_6}{M_\Delta} = \frac{2v_\Delta M_\Delta}{v^2} \left(1 + \frac{v^2}{2M_\Delta^2}(\lambda_4 - \lambda_5) \right), \quad (4.54)$$

where Eq. (4.9) was used.

The two-loop RG equation for the Higgs quartic coupling is given by [43]

$$\frac{d\lambda}{d\ln\mu} = \frac{\beta_\lambda^{(1)}}{16\pi^2} + \frac{\beta_\lambda^{(2)}}{(16\pi^2)^2}, \quad (4.55)$$

where the one- and two-loop β -functions are given by

$$\beta_\lambda^{(1)} = 12\lambda^2 - \left(\frac{9}{5}g_1^2 + 9g_2^2 \right) \lambda + \frac{9}{4} \left(\frac{3}{25}g_1^4 + \frac{2}{5}g_1^2g_2^2 + g_2^4 \right) + 12y_t^2\lambda - 12y_t^4, \quad (4.56)$$

$$\begin{aligned} \beta_\lambda^{(2)} = & -78\lambda^3 + 18 \left(\frac{3}{5}g_1^2 + 3g_2^2 \right) \lambda^2 - \left(\frac{73}{8}g_2^4 - \frac{117}{20}g_1^2g_2^2 - \frac{1887}{200}g_1^4 \right) \lambda - 3\lambda y_t^4 \\ & + \frac{305}{8}g_2^6 - \frac{289}{40}g_1^2g_2^4 - \frac{1677}{200}g_1^4g_2^2 - \frac{3411}{1000}g_1^6 - 64g_3^2y_t^4 - \frac{16}{5}g_1^2y_t^4 - \frac{9}{2}g_2^4y_t^2 \\ & + 10\lambda \left(\frac{17}{20}g_1^2 + \frac{9}{4}g_2^2 + 8g_3^2 \right) y_t^2 - \frac{3}{5}g_1^2 \left(\frac{57}{10}g_1^2 - 21g_2^2 \right) y_t^2 - 72\lambda^2 y_t^2 + 60y_t^6. \end{aligned} \quad (4.57)$$

Here g_1 , g_2 and g_3 are the GUT couplings corresponding to the $U(1)_Y$, $SU(2)_L$ and $SU(3)_C$ interactions, which are related to the previous notation by $g_1 = \sqrt{5/3}g'$, $g_2 = g$ and $g_3 = g_S$. To determine the boundary condition for $\lambda(\mu)$ at a given renormalisation scale μ we use the

one-loop matching condition [48] for the SM Higgs boson pole mass M_h and its running mass $m_h(\mu) = \sqrt{\lambda(\mu)}v$:

$$\lambda(\mu) = \frac{M_h^2}{v^2} [1 + \Delta_h(\mu)]. \quad (4.58)$$

The expression for $\Delta_h(\mu)$ is explicitly given in Appendix A.1.

Apart from the RG equation for the quartic coupling, we also need to consider the RGEs and boundary conditions for the Yukawa couplings and the SM gauge couplings. The explicit expressions are given in Appendix A.1. For the SM fermions, we only keep the dominant top-quark Yukawa coupling terms. The coupled RGEs for λ , y_t and g_i ($i = 1, 2, 3$) have to be solved simultaneously, with the initial boundary conditions imposed at a common renormalisation scale. We first evolve the gauge coupling RGEs from $\mu = M_Z$ to $\mu = M_t$ without the top-Yukawa contribution, using as boundary conditions their $\overline{\text{MS}}$ values at the Z -pole [8]: $(\alpha_1, \alpha_2, \alpha_3)(M_Z) = (0.01618, 0.03354, 0.1184)$, where $\alpha_i \equiv g_i^2/4\pi$. Then we set the boundary conditions for the top-Yukawa coupling and the Higgs quartic coupling at a common scale $\mu = M_t$, and evolve them up to $\mu = M_\Delta$ along with the gauge couplings.

Using this procedure we find that the SM Higgs quartic coupling becomes negative at a renormalisation scale $\mu = 2 \times 10^{10}$ GeV for $M_h = 125$ GeV and the chosen parameter values as listed in Appendix A.1. This can be seen in Figure 4.1 (dashed blue line).

4.5.2 For $\mu > M_\Delta$

For energies larger than the triplet mass, $\mu \geq M_\Delta$, the β -function for the quartic coupling acquires two new contributions coming from the λ_4 and λ_5 terms in the scalar potential, Eq. (4.6):

$$\beta_\lambda^{(1)} \rightarrow \beta_\lambda^{(1)} + 6\lambda_4^2 + 4\lambda_5^2. \quad (4.59)$$

The positive sign of these new entries is a crucial feature in order to slow down the running of the quartic coupling or even change the overall sign of its β -function, thereby improving the electroweak vacuum stability in the type II see-saw model. The running of the electroweak couplings is also modified, whereas the running of the top-Yukawa coupling remains unchanged [43]. The change on the β -functions for g_i and the one-loop RGEs of the new scalar couplings of the type II see-saw model are given in Appendix A.1.

There are two types of solution that can stabilize the electroweak vacuum:

- (i) Large positive contribution to the β -function of λ , which can be realized by large values of $|\lambda_4|$ and/or $|\lambda_5|$ (see Eq. (4.59)).
- (ii) A positive discontinuous shift between λ_{SM} and λ at $\mu = M_\Delta$, which is possible through large values of $|\lambda_6|$ (see Eq. (4.53)).

Figure 4.1a illustrates case (i) and Figure 4.1b case (ii) considering the new-energy scale to be at $M_\Delta = 800$ GeV. In Figure 4.1a we have taken $\lambda_4 = 0.2$ and $\lambda_5 = 0.1$ and neglected λ_6 . It is clear how the decreasing trend of β -function of λ within the SM (dashed blue line)

is overcome thanks to the contribution of λ_4 and λ_5 to the β -function once the new scale is reached (solid red line). In Figure 4.1b we have used $\lambda_6 = 0.13$ and $\lambda_4 = 0.01$ and $\lambda_5 = 0.01$. Here the stability of the potential is achieved through the positive shift of λ (solid red line) with respect to λ_{SM} (dashed blue line) at the new-energy scale, which prevents the running of λ from becoming negative below the Planck scale. For illustration, the other couplings have been fixed to $\lambda_1 = \lambda_2 = 0.1$ in both cases, and the triplet vev $v_\Delta = 3.5$ eV in Figure 4.1a and $v_\Delta = 5$ GeV in Figure 4.1b.

Note that λ_6 is determined by Eq. (4.54). Thus, a sizeable value for λ_6 can only be achieved by a large value of the triplet vev if the triplet mass is considered to be in the low-energy range. In particular, for $M_\Delta = 800$ GeV, $\lambda_6 = 0.13$ for a triplet vev of $v_\Delta = 5$ GeV, which corresponds to the upper limit set by precision data (see Eq. (4.12)). Figure 4.1b shows this scenario. On the other hand, considering small values of the triplet mass and vev, such as $M_\Delta = 800$ GeV and $v_\Delta = 3.5$ eV, results in a value of $\lambda_6 \sim 10^{-10}$, which allows us to neglect its effect (Figure 4.1a).

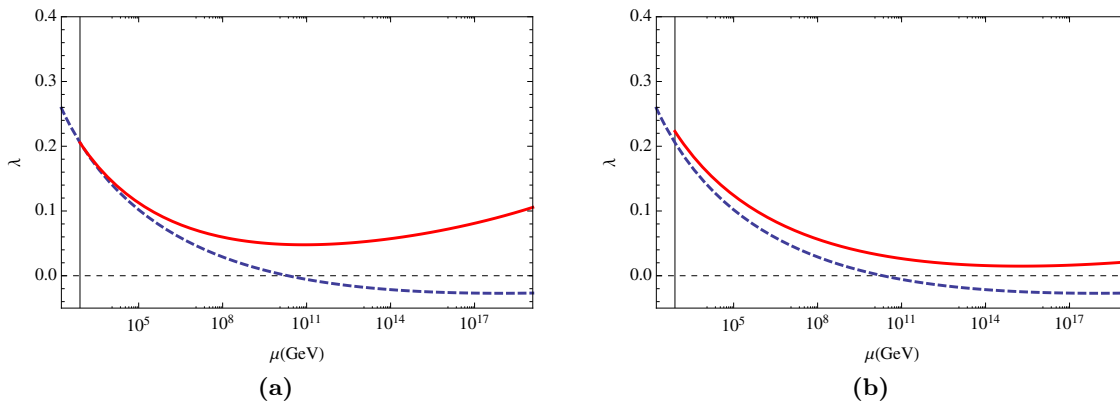


Figure 4.1: The RG running of λ up to the Planck scale in the SM (dashed blue line) and in the type II see-saw model (solid red line) with $M_\Delta = 800$ GeV. The SM quartic coupling becomes negative at $\mu = 2 \times 10^{10}$ GeV. The couplings of the type II scalar potential are chosen to be: (a) $\lambda_4 = 0.2$, $\lambda_5 = 0.1$ and negligible λ_6 , with $v_\Delta = 3.5$ eV; (b) $\lambda_4 = \lambda_5 = 0.01$ and $\lambda_6 = 0.13$, with $v_\Delta = 5$ GeV. The other couplings are fixed to $\lambda_1 = \lambda_2 = 0.1$ in both (a) and (b). The vertical line shows $\mu = M_\Delta$.

4.6 LEPTON FLAVOUR VIOLATION PROCESSES

The seven physical bosons introduced in the type II see-saw model contribute to many lepton flavour violation (LFV) processes. We will see in this section that the low scale see-saw case, with $100 \text{ GeV} < M_\Delta < 1 \text{ TeV}$, is severely constrained by experiments searching for LFV, which have set stringent bounds on the branching ratio of these processes.

As indicated in Section 4.1, the flavour structure of the couplings of the new scalar particles to the charged leptons is related to the light neutrino mass matrix through Eq. (4.14). Hence, the Yukawa coupling matrix Y_Δ cannot be chosen arbitrarily but is determined by the requirement of reproducing the data on neutrino oscillation parameters.

In this section we introduce the theoretical framework for the LFV decays $\mu \rightarrow e\gamma$, $\mu \rightarrow 3e$, $\tau \rightarrow e\gamma$, $\tau \rightarrow \bar{l}_i l_j l_k$ and the μ - e conversion in the nuclei. Using the best experimental limits on branching ratios from the non-observation of LFV processes, we determine the corresponding upper bounds on the Yukawa couplings. One can use these bounds to obtain a lower bound on the vev of the triplet v_Δ , in terms of the Higgs triplet mass M_Δ . However, as shown in different studies, e.g. [49, 50, 51], this limit can depend considerably on the Dirac and Majorana phases of the neutrino mixing matrix, the ordering and hierarchy of the active neutrino mass spectrum and the value of the reactor mixing angle θ_{13} .

The single and double charged Higgs scalars H^+ and H^{++} have, in general, different masses, m_{H^+} and $m_{H^{++}}$, with a splitting of the squared masses of $\frac{1}{2}\lambda_5 v^2$ (see Eqs. (4.34, 4.35)). Since the sign of λ_5 is not known a priori, both $m_{H^+} > m_{H^{++}}$ and $m_{H^+} < m_{H^{++}}$ are possible situations. For values of the triplet mass scale much larger than the electroweak scale this splitting is negligible, whereas for values close to the electroweak scale the splitting could be of few GeV and therefore noticeable. However, even in the case of a low-scale see-saw, the impact of the splitting in the LFV branching ratios is almost not perceptible, and therefore not relevant in our study. Thus, the mass difference will be neglected in the following and we will consider $m_{H^+} \cong m_{H^{++}} \equiv M_\Delta$.

The $\mu \rightarrow e\gamma$ decay

The branching ratio for $\mu \rightarrow e\gamma$ is given by [51, 52, 49]

$$\text{BR}(\mu \rightarrow e\gamma) = \frac{27\alpha_{\text{em}}}{64\pi G_F^2 M_\Delta^4} |(Y_\Delta^\dagger Y_\Delta)_{e\mu}|^2 \text{BR}(\mu \rightarrow e\bar{\nu}\nu), \quad (4.60)$$

where $\alpha_{\text{em}} \equiv q_e^2/4\pi = 1/137$ is the fine structure constant, $G_F = 1.17 \times 10^{-5} \text{ GeV}^{-2}$ is the Fermi constant and $\text{BR}(\mu \rightarrow e\bar{\nu}\nu) \simeq 100\%$ [8].

The current limit on $\text{BR}(\mu \rightarrow e\gamma)$ has been set by the MEG experiment at Paul Scherrer Institute (PSI), in Switzerland, to be 4.2×10^{-13} (90% C.L.) [53]. The upgraded experiment MEG II aims to achieve a sensitivity on the branching ratio of 4×10^{-14} after three years of data taking. It is expected to start taking data in 2017 [53].

The $\mu \rightarrow 3e$ decay

The branching ratio for $\mu \rightarrow 3e$ is given by [51, 52, 49]

$$\text{BR}(\mu \rightarrow 3e) = \frac{|(Y_\Delta)_{\mu e}|^2 |(Y_\Delta)_{ee}|^2}{4G_F^2 M_\Delta^4} \text{BR}(\mu \rightarrow e\bar{\nu}\nu). \quad (4.61)$$

The present limit is $\text{BR}(\mu \rightarrow 3e) < 1.0 \times 10^{-12}$ (90% C.L.) [54], published by SINDRUM Collaboration in 1988. The current Mu3e experiment at PSI aims for an ultimate sensitivity of $\text{BR}(\mu \rightarrow 3e) \sim 10^{-16}$ (90% C.L. in the absence of a signal) [55], four orders of magnitude better than previous searches. The sensitivity goal of 10^{-15} for the *Phase I* of the experiment represents already a significant improvement (3 orders of magnitude) with respect to the existing limit. First data collection is expected for 2017 [56].

The $\tau \rightarrow e\gamma$ and $\tau \rightarrow \mu\gamma$ decays

The branching ratio for $\tau \rightarrow e\gamma$ is given by [52]

$$\text{BR}(\tau \rightarrow e\gamma) = \frac{27\alpha_{\text{em}}}{64\pi G_F^2 M_\Delta^4} |(Y_\Delta^\dagger Y_\Delta)_{e\tau}|^2 \text{BR}(\tau \rightarrow e\bar{\nu}\nu), \quad (4.62)$$

where $\text{BR}(\tau \rightarrow e\bar{\nu}\nu) = 17.83 \pm 0.04\%$ [8]. The formula for $\text{BR}(\tau \rightarrow \mu\gamma)$ is analogous but with dependence on $|(Y_\Delta^\dagger Y_\Delta)_{\mu\tau}|^2$. The current upper limits for both decays are $\mathcal{O}(10^{-8})$ [8]. The specific values are given in Table 4.1.

The $\tau \rightarrow \bar{l}ll$ decay

The branching ratio for $\tau \rightarrow \bar{l}_i l_j l_k$ is given by [51]

$$\text{BR}(\tau \rightarrow \bar{l}_i l_j l_k) = \frac{S |(Y_\Delta)_{\tau i}|^2 |(Y_\Delta)_{jk}|^2}{4G_F^2 M_\Delta^4} \text{BR}(\tau \rightarrow \mu\bar{\nu}\nu), \quad (4.63)$$

Here $S = 1$ (2) for $j = k$ ($j \neq k$), i.e. having two identical (different) leptons in the final states.

The current limits on the branching ration of a τ lepton decaying to three charged leptons is $\text{BR}(\tau \rightarrow \bar{l}_i l_j l_k) < \mathcal{O}(10^{-8})$ [8]. The specific values are given in Table 4.1.

The $\mu - e$ conversion in the nuclei

The theoretical framework of the $\mu - e$ conversion in a nucleus is much more involved than the previous LFV-processes, since it also involves nuclear physics. Therefore, we will only quote the bounds from the literature and refer to Ref. [49] and the references therein for a complete description of the process and further information on the details of how the bounds are set.

The constrain on the corresponding Yukawa coupling matrix element is [49]

$$|(Y_\Delta^\dagger Y_\Delta)_{e\mu}| < 6 \times 10^{-4} \left(\frac{M_\Delta}{100 \text{ GeV}} \right)^2, \quad (4.64)$$

which provides a weaker constrain with respect to the one obtained from the $\mu \rightarrow e\gamma$ decay. Hence, we do not need to consider this process any further.

However, as pointed out in [49], for a see-saw scale in the range of (100 – 1000) GeV, the planned experiments on $\mu - e$ conversion in Al (COMET [57], Mu2e [58]) will provide the most sensitive probe of the LFV Yukawa couplings of the type II see-saw model at the TeV scale. The COMET experiment at J-PARC (Japan) plans to achieve a signal sensitivity on the branching ratio of 3×10^{-15} in 2017 in its Phase-I, followed by the COMET Phase-II with the sensitivity of 10^{-17} in 2020 [57]. The Mu2e experiment at Fermilab (USA) aims for a sensitivity of 6×10^{-17} . The data taking is expected to start in 2021 [58].

4.6.1 Summary of LFV-Bounds

Table 4.1 summarizes the experimental limits on the branching ratios for the different LFV processes discussed in the previous sections and the corresponding constraints on the various combinations of the Yukawa coupling matrix elements of the leptons to the scalar triplet. These upper bounds on the Yukawa couplings can be used to set lower bounds on the vev of the scalar triplet v_Δ for a given triplet mass M_Δ using Eq. (4.14), as noted in [52, 49]. In general, the prediction depends on the type of hierarchy of the neutrino mass spectrum: normal hierarchy (NH) or inverted hierarchy (IH). For a given spectrum, it also depends on the Majorana and Dirac phases, as well as on the value of the lightest neutrino mass, $m_{\nu_{\min}}$.

For illustration purposes, we have computed the lower limit of the product $v_\Delta M_\Delta$ for NH and IH considering $m_{\nu_{\min}} = 0$ and $m_{\nu_{\min}} = 0.2$ eV, which satisfy the current upper limits set by double-beta decay experiments and cosmology (see Section 2.2.2). We have also used the best fit values of the neutrino oscillation parameters from Table 2.2 and considered the cases of zero and non-zero Majorana phases, with $(\alpha_1 = \pi/3, \alpha_2 = \pi/2)$ in the second case. The results are summarized in Table 4.2. Note that taking the lightest neutrino mass to zero gives the least restrictive lower limit on $v_\Delta M_\Delta$, since it corresponds to the smallest values for the Yukawa couplings.

From Table 4.2, it can be observed that the most stringent bounds come from the $\mu \rightarrow e\gamma$ and $\mu \rightarrow 3e$ decays. The $\text{BR}(\mu \rightarrow e\gamma)$ is independent of the Majorana phases, since it is proportional to $|(Y_\Delta^\dagger Y_\Delta)_{e\mu}|$, and the diagonal matrix containing the Majorana phases, $\text{diag}(1, e^{i\alpha_1}, e^{i\alpha_2})$, cancels in the product $(Y_\Delta^\dagger Y_\Delta)$. Furthermore, it is also independent of the absolute neutrino mass. The $\text{BR}(\mu \rightarrow 3e)$ depends on the individual entries of the Yukawa matrix $|(Y_\Delta)_{\mu e}|$ and $|(Y_\Delta)_{ee}|$, which can vanish for specific values of the Majorana phases [41, 59]. It is known that the $|(Y_\Delta)_{ee}|$ element can vanish for the NH if the values of the smallest neutrino mass are within the range 10^{-3} eV $< m_1 < 10^{-2}$ eV, but cannot vanish for the IH. On the other hand, $|(Y_\Delta)_{\mu e}|$ can vanish both in the NH and in the IH for any value of the (allowed) smallest neutrino mass (for more details, see Ref. [41]). This means that, for specific values of the Majorana phases, the vanishing (or smaller) individual entries of the Yukawa matrix can lead to a vanishing (or reduced) branching ratio of the $\mu \rightarrow 3e$ process, evading a possible experimental observation. In this situation, also the bounds on $v_\Delta M_\Delta$ from the $\mu \rightarrow 3e$ process would be lowered (in case of total cancellation for the branching ratio, there would actually be no bound at all from this process). In view of this dependence of the bounds on the value of the Majorana phases, we will consider in the rest of our study only the limits set by the $\mu \rightarrow e\gamma$ process, which are independent of them.

Process	Experimental limit on BR	Constraint on	Bound $\left(\times \left(\frac{M_\Delta}{100 \text{ GeV}}\right)^2\right)$
$\mu \rightarrow e\gamma$	$< 4.2 \times 10^{-13}$ [53]	$ (Y_\Delta^\dagger Y_\Delta)_{e\mu} $	$< 2.4 \times 10^{-6}$
$\mu \rightarrow 3e$	$< 1.0 \times 10^{-12}$ [54]	$ (Y_\Delta)_{\mu e} (Y_\Delta)_{ee} $	$< 2.3 \times 10^{-7}$
$\tau \rightarrow e\gamma$	$< 3.3 \times 10^{-8}$ [8]	$ (Y_\Delta^\dagger Y_\Delta)_{e\tau} $	$< 1.6 \times 10^{-3}$
$\tau \rightarrow \mu\gamma$	$< 4.4 \times 10^{-8}$ [8]	$ (Y_\Delta^\dagger Y_\Delta)_{\mu\tau} $	$< 1.9 \times 10^{-3}$
$\tau \rightarrow e^+e^-e^-$	$< 2.7 \times 10^{-8}$ [8]	$ (Y_\Delta)_{\tau e} (Y_\Delta)_{ee} $	$< 9.2 \times 10^{-5}$
$\tau \rightarrow \mu^+\mu^-e^-$	$< 2.7 \times 10^{-8}$ [8]	$ (Y_\Delta)_{\tau\mu} (Y_\Delta)_{\mu e} $	$< 6.5 \times 10^{-5}$
$\tau \rightarrow e^+\mu^-\mu^-$	$< 1.7 \times 10^{-8}$ [8]	$ (Y_\Delta)_{\tau e} (Y_\Delta)_{\mu\mu} $	$< 7.3 \times 10^{-5}$
$\tau \rightarrow e^+e^-\mu^-$	$< 1.8 \times 10^{-8}$ [8]	$ (Y_\Delta)_{\tau e} (Y_\Delta)_{\mu e} $	$< 5.3 \times 10^{-5}$
$\tau \rightarrow \mu^+e^-e^-$	$< 1.5 \times 10^{-8}$ [8]	$ (Y_\Delta)_{\tau\mu} (Y_\Delta)_{ee} $	$< 6.9 \times 10^{-5}$
$\tau \rightarrow \mu^+\mu^-\mu^-$	$< 2.1 \times 10^{-8}$ [8]	$ (Y_\Delta)_{\tau\mu} (Y_\Delta)_{\mu\mu} $	$< 8.1 \times 10^{-5}$

Table 4.1: Experimental limits on the branching ratios of different LFV processes and the corresponding bounds on different combinations of Y_Δ in the type II see-saw model.

Process	$\frac{v_\Delta}{\text{eV}} \cdot \frac{M_\Delta}{100 \text{ GeV}}$			
	NH		IH	
	$m_1 = 0 \text{ eV}$	$m_1 = 0.2 \text{ eV}$	$m_3 = 0 \text{ eV}$	$m_3 = 0.2 \text{ eV}$
$\mu \rightarrow e\gamma$	> 6.9 (6.9)	> 6.9 (6.9)	> 7.4 (7.4)	> 7.4 (7.4)
$\mu \rightarrow 3e$	> 4.5 (3.5)	> 119.6 (167.6)	> 23.6 (41.5)	> 127.0 (157.5)
$\tau \rightarrow e\gamma$	> 0.30 (0.30)	> 0.30 (0.30)	> 0.30 (0.30)	> 0.30 (0.30)
$\tau \rightarrow \mu\gamma$	> 0.60 (0.57)	> 0.57 (0.57)	> 0.57 (0.57)	> 0.57 (0.57)
$\tau \rightarrow e^+e^-e^-$	> 0.28 (0.37)	> 6.42 (8.82)	> 1.14 (2.14)	> 6.0 (9.60)
$\tau \rightarrow \mu^+\mu^-e^-$	> 0.90 (0.57)	> 0.69 (9.73)	> 1.00 (1.72)	> 1.36 (8.70)
$\tau \rightarrow e^+\mu^-\mu^-$	> 1.11 (1.14)	> 7.33 (10.1)	> 0.84 (1.54)	> 6.70 (11.5)
$\tau \rightarrow e^+e^-\mu^-$	> 0.55 (0.37)	> 3.58 (10.8)	> 0.50 (2.68)	> 3.42 (10.8)
$\tau \rightarrow \mu^+e^-e^-$	> 0.60 (0.72)	> 1.58 (10.2)	> 2.96 (1.77)	> 3.05 (9.96)
$\tau \rightarrow \mu^+\mu^-\mu^-$	> 1.82 (1.85)	> 1.47 (9.55)	> 1.79 (1.04)	> 2.80 (9.80)

Table 4.2: Lower limit on the product $v_\Delta M_\Delta$ obtained from the experimental bounds on the branching ratio of different LFV processes (Table 4.1), for NH and IH, calculated using the best fit values of the neutrino oscillation data (Table 2.2), with Majorana phases $\alpha_1 = 0$, $\alpha_2 = 0$ ($\alpha_1 = \pi/3$, $\alpha_2 = \pi/2$) and assuming the lightest neutrino mass to be 0 eV and 0.2 eV.

4.7 OTHER CONSTRAINTS

In addition to the constraints imposed by the LFV experiments, there are other experimental constraints on the parameters of the type II see-saw model, which come from direct searches of the new scalar particles and from electroweak precision measurements. We review them briefly in this section.

4.7.1 Direct searches

The strongest limits on the see-saw scale come from the ongoing searches for double charged Higgs bosons at the LHC [60]. The possible production mechanisms are [43, 61, 62]

$$\begin{aligned} q\bar{q} &\rightarrow \gamma^*, Z^*, W^{\pm*}W^{\pm*} \rightarrow H^{++}H^{--} \\ q'\bar{q} &\rightarrow W^{\pm*} \rightarrow H^{\pm\pm}H^\mp, H^{\pm\pm}W^\mp. \end{aligned}$$

After being produced, they can decay to:

- (i) two same-sign charged leptons ($l^\pm l^\pm$),
- (ii) a pair of charged gauge bosons ($W^\pm W^\pm$),
- (iii) $W^\pm H^\pm$,

if kinematically allowed. The cascade channel (iii) is only possible in the case of non-degenerated mass values, $|m_{H^{++}} - m_{H^\pm}| \neq 0$.

Assuming mass-degeneracy for the triplet components, $m_{H^\pm} \cong m_{H^{++}} \equiv M_\Delta$, there are two regions that can be distinguished: for $v_\Delta < 10^{-4}$ GeV (large Yukawa couplings) the $l^\pm l^\pm$ is the dominant decay channel, while for $v_\Delta > 10^{-4}$ GeV (small Yukawa couplings) the decay to two charged bosons becomes dominant [63]. Direct searches for new-physics in events with same sign dileptons are being performed at the LHC. The absence of an excess of these events above the expected level of SM background allows to set a lower limit on the mass of the double charged boson [60]:

$$m_{H^{\pm\pm}} \gtrsim 465 - 550 \text{ GeV (95\%CL)}, \quad (4.65)$$

depending on the flavour of the final state leptons. Note that the mass limits vary with the branching ratio of the $H^{\pm\pm}$ decay into lepton pairs. The ones here presented are obtained assuming a 100% branching ratio in one of the channels. For lower branching ratios, the limits are lowered as well. In addition, this bound is valid only for small enough $v_\Delta < 10^{-4}$ GeV, for which the $l^\pm l^\pm$ -channel dominates, and small mass splitting of the different components of the triplet. For a sizeable mass splitting, the channel (iii) becomes important and one basically loses the same-sign dilepton channel [62]. In this case, the double charged Higgs boson follows the cascade decay channel:

$$H^{++} \rightarrow H^+W^{(*)} \rightarrow H^0/A^0W^{(*)}W^{(*)} \rightarrow \nu\nu W^{(*)}W^{(*)}$$

and the triplet could be completely missed [61].

In our study, we will consider $v \sim \mathcal{O}(\text{eV})$, for which the Yukawa couplings are still sizeable, and assume that the triplet component mass splitting is negligible. Therefore, the limit on the see-saw scale, Eq. (4.65), would be applicable. However, because the assumed branching ratio of 100% seems rather artificial, we will consider a lower limit $m_\Delta > 400 \text{ GeV}$, which corresponds to a 30% – 40% branching ratio in every channel.

4.7.2 Electroweak precision tests

Apart from the direct search limits, another constraint can be deduced from the electroweak precision data (EWPD). The main constraint comes from the oblique parameter T which is governed by the mass differences between the double and single charged Higgs bosons, $|\Delta M| \equiv |m_{H^+} - m_{H^{++}}|$. EWPD constrains this splitting to

$$|\Delta M| \lesssim 40 \text{ GeV}, \quad (4.66)$$

almost independently of the double charged Higgs mass [61].

From Eqs. (4.34 - 4.36) we see that the mass splitting among the triplet components is induced by the λ_5 -coupling:

$$m_{H^{++}}^2 - m_{H^+}^2 = \frac{1}{2}\lambda_5 v^2. \quad (4.67)$$

Therefore, λ_5 is constrained by the EWPD limit on the mass-splitting. A priori, λ_5 can be positive or negative, which corresponds the cases $m_{H^{++}} > m_{H^+}$ and $m_{H^{++}} < m_{H^+}$, respectively. Combining Eqs. (4.66, 4.67) we obtain

$$-\frac{2}{v^2} (2|\Delta M|m_{H^{++}} + |\Delta M|^2) \lesssim \lambda_5 \lesssim \frac{2}{v^2} (2|\Delta M|m_{H^{++}} - |\Delta M|^2). \quad (4.68)$$

From here it is observed that the smaller the mass of the double charged boson, the stronger the constraint. Taking the lowest limit from direct searches, Eq. (4.65), the constraint becomes

$$-1.1 \lesssim \lambda_5 \lesssim 1. \quad (4.69)$$

This constrain turns out to be less restrictive than the vacuum stability, perturbativity and unitarity constraints, and therefore has no impact on our analysis.

4.8 RESULTS AND DISCUSSION

4.8.1 Allowed Parameter Space

In this section, we analyse numerically the parameter space in the scalar sector of the type II see-saw model which satisfies the vacuum stability and unitarity conditions discussed in Section 4.3 and perturbativity of the couplings up to the Planck scale⁴. We also impose the different constraints coming from LFV experiments and direct searches, explained in the previous sections, which fix the allowed values of the triplet mass M_Δ and triplet vev v_Δ , and check that the restriction on λ_5 from electroweak precision data is fulfilled. In addition, we also study which part of the allowed parameter space fulfils also the naturalness condition, which we take as $|\delta m_h^2| \lesssim M_h^2$, i.e. that the radiative correction to the Higgs mass squared is, at most, of the order of the physical Higgs mass squared, $M_h^2 \simeq (125 \text{ GeV})^2$.

In particular, we focus on the low scale see-saw, so we only consider the case in which the scale of new physics M_Δ is in the TeV range, $M_\Delta \sim (400 \text{ GeV} - 3 \text{ TeV})$, which could be testable at the LHC and future colliders. The lowest possible see-saw scale is restricted by the experimental bounds (see Sections 4.3 and 4.7), and depends on the chosen vev of the triplet and the unknown neutrino mass and mixing parameters. For simplicity, we assume that the mass splitting of the triplet components is negligible, so that $m_{H^{++}} \simeq m_{H^+} \equiv M_\Delta$. We also restrict the study to small values for the triplet vev $v_\Delta \sim \mathcal{O}(\text{eV})$, in order to have sizeable Yukawa couplings. Indeed, using Eq. (4.18) we can write

$$Y_\Delta = \frac{10^{-2} \text{ eV}}{v_\Delta} \times \mathcal{O}(1)_{3 \times 3} \quad (4.70)$$

for NH, $m_{\nu_{\min}} = 0$ and all Majorana phases equal to zero. Thus, $v_\Delta \sim \mathcal{O}(\text{eV})$ implies $Y_\Delta \sim \mathcal{O}(10^{-2})$ in this scenario.

To obtain the allowed parameter space, we randomly generate sets of $(\lambda_1, \lambda_2, \lambda_4, \lambda_5)$ for a fixed triplet mass and vev, which fulfil the perturbativity, vacuum stability and unitarity conditions. We take these as initial values at $\mu = M_\Delta$ and solve simultaneously their RGEs up to the Planck scale. The value of the Higgs quartic coupling λ at $\mu = M_\Delta$ is obtained by running its SM RGE up to $\mu = M_\Delta$. At this energy its RG equation is modified to account for the new contributions coming from the interaction with the scalar triplet, as explained in Section 4.5. During the running of the couplings it is checked that the perturbativity, vacuum stability and unitarity conditions are always satisfied, so that only those sets of parameters that satisfy them up to the Planck scale are kept.

The parameter λ_6 is not randomly generated, but is calculated using Eq. (4.54) for every set of (λ_4, λ_5) once (M_Δ, v_Δ) are fixed. For typical values of $(\lambda_4, \lambda_5) \sim \mathcal{O}(0.1)$,

⁴For perturbativity to be satisfied up to the Planck scale, we impose that all quartic couplings must be smaller than 4π in the whole energy range.

λ_6 is given by

$$\lambda_6 = \frac{2v_\Delta M_\Delta}{v^2} \times \mathcal{O}(1). \quad (4.71)$$

Within our low scale see-saw ($M_\Delta \lesssim \mathcal{O}(\text{TeV})$) and small v_Δ ($v_\Delta \sim \mathcal{O}(\text{eV})$) scenario,

$$\lambda_6 \sim \mathcal{O}(10^{-11} - 10^{-9}). \quad (4.72)$$

Therefore, in this scenario, λ_6 is very small in comparison with the other couplings. In particular, its effect on the SM Higgs quartic coupling, $\lambda_{\text{SM}} = \lambda - \lambda_6^2$, is negligible and thus, it cannot contribute significantly to stabilize the running of λ such that it remains positive up to the Planck scale. Its contribution to the Higgs mass correction, Eq. (4.51), is also negligible compared to the contribution proportional to λ_4 .

Fig. 4.2 and Fig. 4.3 show the allowed parameter space for the type II see-saw model, which satisfies the perturbativity, vacuum stability and unitarity conditions up to the Planck scale (blue) and also those which, in addition, also satisfy the naturalness condition $|\delta m_h^2| \lesssim M_h^2$ at $\mu = M_\Delta$ (pink). As benchmark values for the triplet vev we have considered $v_\Delta = 3.5$ eV (Fig. 4.2) and $v_\Delta = 0.5$ eV (Fig. 4.2). The experimental bound from direct searches sets $M_\Delta \gtrsim 400$ GeV, while LFV experiments⁵ impose $M_\Delta > 200$ GeV for $v_\Delta = 3.5$ eV and $M_\Delta > 1.4$ TeV for $v_\Delta = 0.5$ eV (see Table 4.2). According to this, we have considered the range $400 \text{ GeV} < M_\Delta < 1 \text{ TeV}$ for $v_\Delta = 3.5$ eV and $1.4 \text{ TeV} < M_\Delta < 3 \text{ TeV}$ for $v_\Delta = 0.5$ eV. For illustration, we have chosen normal hierarchy (NH) of the neutrino masses and we have assumed the minimal neutrino mass and the Majorana phases to be zero. The values shown correspond to the initial values of the parameters, i.e. the values at $\mu = M_\Delta$. The allowed parameter space for different configurations, such as $m_{\nu_{\text{min}}} \neq 0$ and/or inverted hierarchy (IH) for the neutrino masses, can be found in Appendix A.2.

For the low scale see-saw with $M_\Delta \lesssim 3 \text{ TeV}$ and small vev, $v_\Delta \sim \mathcal{O}(\text{eV})$, the parameter scan shows that the parameter space is roughly restricted to the values

$$\begin{aligned} 0 < \lambda_1 < 0.5 \\ -4\pi < \lambda_2 < 4\pi \\ -0.1 < \lambda_4 < 0.5 \\ -0.4 < \lambda_5 < 0.4 \end{aligned} \quad (4.73)$$

independently of the hierarchy of the neutrino masses, the values of $m_{\nu_{\text{min}}}$ and the Majorana phases. Nevertheless, due to the vacuum stability and unitarity conditions, not all values in these ranges are allowed, but present various correlations, as we will discuss in the following.

Fig. 4.2a shows the allowed parameter space in the (λ_1, λ_2) plane. The restriction on the lower value of λ_1 is $\lambda_1 > 0$, while for λ_2 it is $\lambda_2 \geq -2\lambda_1$, which correspond to the second and third vacuum stability conditions, Eqs. (4.37b, 4.37c). The upper bounds

⁵Recall that we will only consider the bounds from $\mu \rightarrow e\gamma$, since they are independent of the Majorana phases and the absolute neutrino mass scale. See Section 4.6.1 for a more detailed discussion.

of λ_1 and λ_2 come from the perturbativity condition, i.e. imposing that the couplings should be smaller than 4π up to the Planck scale.

Fig. 4.2b shows the allowed parameter space in the (λ_4, λ_5) plane. Since the values of λ_6 are too small to influence the running of λ , the only possibility to prevent λ from becoming negative at high energies is to have large enough values of $|\lambda_4|$ and/or $|\lambda_5|$. Therefore, the region around $(\lambda_4, \lambda_5) = (0, 0)$ is forbidden, since the RG equation for λ in the vicinity of this region is almost identical to its SM RG equation (see Eq. (4.59)), and hence, we would hit the SM vacuum instability $\lambda < 0$ below the Planck scale, violating the first stability condition, Eq. (4.37a). The fourth and fifth vacuum stability conditions, Eqs. (4.37d, 4.37d), set a lower and an upper bound on λ_5 : $\lambda_5 \geq -\lambda_4 - \sqrt{\lambda\lambda_1}$ and $\lambda_5 \leq \lambda_4 + \sqrt{\lambda\lambda_1}$, which exclude the region of large $|\lambda_5|$ for small λ_4 . Large values of both λ_4 and λ_5 are excluded by imposing perturbativity up to the Planck scale.

Fig. 4.2c shows the scatter plot in the $(|\lambda_4|, \lambda_6)$ plane. As explained before, in the low scale see-saw and for small triplet vev, λ_6 takes very small values and its effect both in the RG equation of λ and in the Higgs mass correction are negligible compared to the other parameters. Indeed, from this plot we observe that λ_6 is of the order $\mathcal{O}(10^{-11} - 10^{-10})$, while λ_4 is mainly of the order $\mathcal{O}(0.1)$.

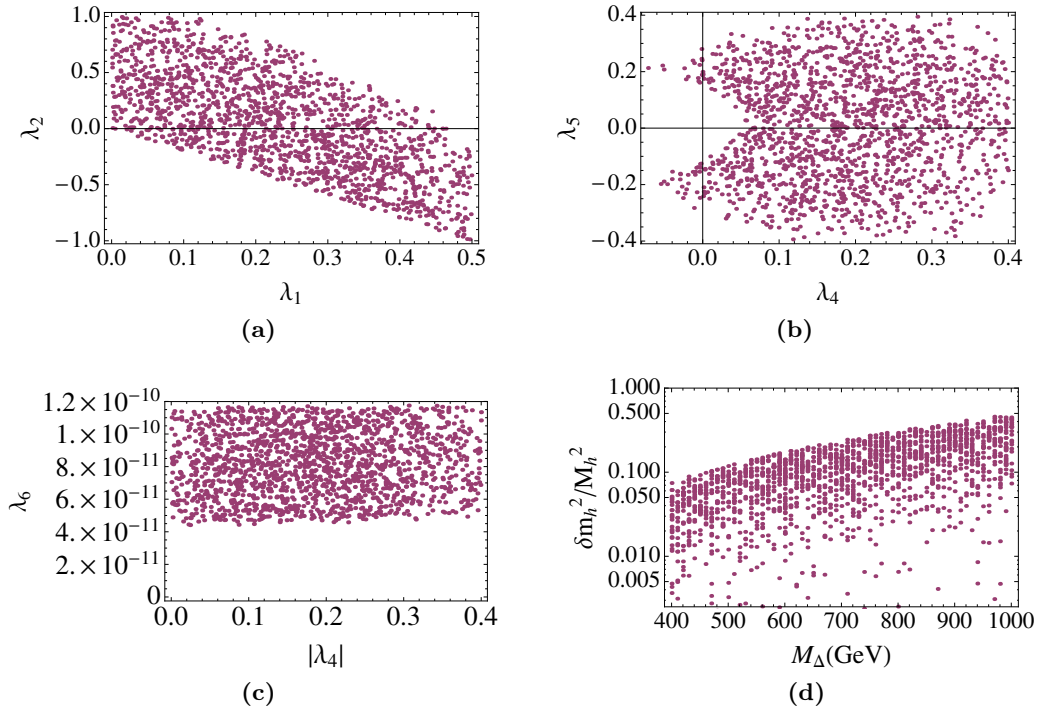


Figure 4.2: Allowed parameter space in the (a) (λ_1, λ_2) plane, (b) (λ_4, λ_5) plane, (c) $(|\lambda_4|, \lambda_6)$ plane and (d) $(M_\Delta, |\delta m_h^2|/M_h^2)$ plane, for $v_\Delta = 3.5$ eV and $200 \text{ GeV} < M_\Delta < 1 \text{ TeV}$ in the type II see-saw model. It has been calculated considering NH and setting $m_{\nu_{\min}} = 0$ and the Majorana phases equal to zero. All points satisfy the vacuum stability, unitarity and perturbativity conditions up to Planck scale and the naturalness condition $|\delta m_h^2| \leq M_h^2$ at $\mu = M_\Delta$. The values shown correspond to the parameters at $\mu = M_\Delta$.

Finally, Fig. 4.2d shows the correction to the Higgs mass, Eq. (4.51), for different values of M_Δ , obtained for the different values of the allowed parameter space. The correction has been normalized to the Higgs mass squared so that the naturalness condition reads $|\delta m_h^2|/M_h^2 \lesssim 1$. As we can see, for $v_\Delta = 3.5$ eV and $200 \text{ GeV} < M_\Delta < 1 \text{ TeV}$ all the parameter space which is allowed by the perturbativity, vacuum stability and unitarity conditions up to the Planck scale satisfies always the naturalness condition, i.e. the correction to the Higgs mass squared that the new scalar triplet induces is always smaller than the physical Higgs mass squared, with $M_h = 125 \text{ GeV}$.

Fig. 4.3 shows the same allowed parameter space planes as Fig. 4.2 but for $v_\Delta = 0.5$ eV. Lowering the triplet vev requires the triplet masses to be larger in order to fulfil the LFV bounds. In particular, for $v_\Delta = 0.5$ eV the triplet mass is required to be larger than 1.4 TeV. Here we have studied the range $1.4 \text{ TeV} < M_\Delta < 3 \text{ TeV}$. The (λ_1, λ_2) and (λ_4, λ_5) parameter space are the same compared to the ones for $v_\Delta = 3.5$ eV. Similarly to the previous case, the values of λ_6 obtained from Eq. (4.54) are of the order $\mathcal{O}(10^{-11})$ and its effect is negligible in our study. The main difference appears in the values of the correction to the Higgs mass, Fig. 4.3d. Neglecting λ_6 from Eq. (4.51) we get

$$\delta m_h^2 \simeq \frac{3}{16\pi^2} \lambda_4 M_\Delta^2 \quad (4.74)$$

at $\mu = M_\Delta$. Since now we are considering larger values of M_Δ , it would be possible that for some values of the parameter space the correction to the Higgs mass squared became larger than the physical Higgs mass squared, breaking the naturalness condition $|\delta m_h^2| \leq M_h^2$. This is in fact the case, as can be seen in Fig. 4.3b and Fig. 4.3d: for large values of M_Δ and λ_4 the naturalness condition is not fulfilled (blue points). Nevertheless, there still exist a large parameter space for the whole range of M_Δ in which the naturalness condition is still satisfied (pink points). However, the larger the mass of the triplet and the value of λ_4 , the smaller the allowed parameter space. Thus, from a naturalness point of view, small values of M_Δ and λ_4 are favoured.

In Appendix A.2 we show the results for some different configurations of the neutrino mass and mixing parameters. The dependence of the allowed parameter space on the neutrino mass and mixing parameters is only present in the RG equations of the couplings. The allowed parameter space which satisfies the perturbativity, vacuum stability and unitarity conditions up to the Planck scale are roughly the same, independently of the hierarchy and the value of $m_{\nu_{\min}}$, showing that this dependence is not significant in our analysis. Therefore, the same results that we have stated previously also apply for the different configurations of the neutrino mass and mixing parameters, as long as small triplet masses ($M_\Delta \lesssim \mathcal{O}(\text{TeV})$) and small triplet vevs ($v_\Delta \sim \mathcal{O}(\text{eV})$) are considered.

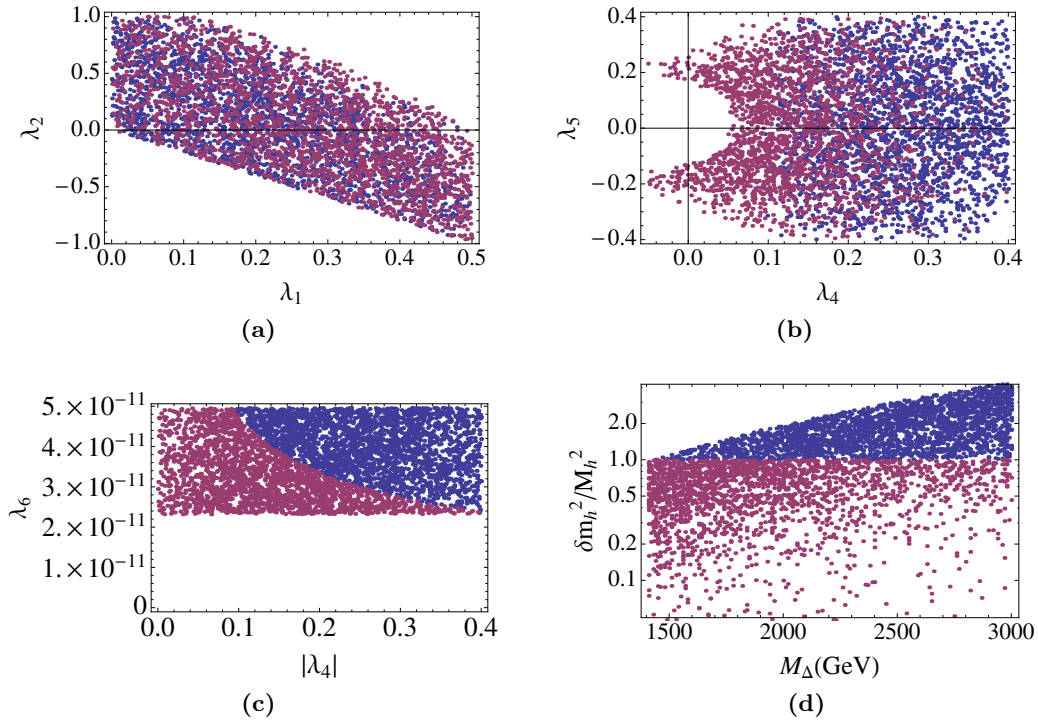


Figure 4.3: Allowed parameter space in the (a) (λ_1, λ_2) plane, (b) (λ_4, λ_5) plane, (c) $(|\lambda_4|, \lambda_6)$ plane and (d) $(M_\Delta, |\delta m_h^2|/M_h^2)$ plane, for $v_\Delta = 0.5$ eV and 1.4 TeV $< M_\Delta < 3$ TeV in the see-saw type II model. It has been calculated considering IH and setting $m_{\nu_{\min}} = 0$ and the Majorana phases equal to zero. All points satisfy the vacuum stability, unitarity and perturbativity conditions up to Planck scale. The pink points also satisfy the naturalness condition $|\delta m_h^2| \leq M_h^2$ at $\mu = M_\Delta$, while the blue ones do not. The values shown correspond to the parameters at $\mu = M_\Delta$.

4.8.2 Future prospects

In the previous section we have seen that there exist a relatively large parameter space in which the vacuum stability, unitarity and perturbativity conditions are satisfied for masses below ~ 3 TeV. The naturalness condition is also satisfied by a large subset of this allowed parameter space. For masses above ~ 3 TeV, the allowed values from naturalness become more and more restricted, being almost non-existent for triplet masses above ~ 4 TeV. This suggests that, if the type II see-saw model is realized in nature, masses below 3 TeV would be favoured if one expects the radiative corrections to the Higgs mass not to be too large. In this section we study if the existence of a low-scale triplet could be probed by LFV experiments. In particular, we discuss here the prospects for the future LFV experiments MEG II [53] and Mu3e [56], which will search for $\mu \rightarrow e\gamma$ and $\mu \rightarrow 3e$ decays, respectively, and will set in case of non-observation the most stringent limits on the triplet mass.

Figure 4.4 shows the dependence of the $\text{BR}(\mu \rightarrow e\gamma)$ predicted by the type II see-saw model, Eq. (4.60), on the triplet mass M_Δ for $v_\Delta = 3.5$ eV (Fig. 4.4a) and $v_\Delta = 0.5$ eV (Fig. 4.4b) (blue line). The horizontal lines denote the sensitivities of the MEG

experiment (pink) and the expected sensitivity of the upgraded experiment MEG II (dashed yellow). As can be seen from the figures, for $v_\Delta = 3.5$ eV ($v_\Delta = 0.5$ eV) the current limit set by the MEG experiment is $M_\Delta \geq 200$ GeV ($M_\Delta \geq 1.4$ TeV), while MEG II will be able to probe up to ~ 350 GeV (~ 2.5 TeV). As explained in Section 4.6.1, the branching ratio of this process is independent of the Majorana phases and the absolute neutrino mass.

Figure 4.5 shows the dependence of the $\text{BR}(\mu \rightarrow 3e)$ predicted by the type II see-saw model, Eq. (4.61), on the triplet mass M_Δ . In this case the branching ratio depends on the neutrino mass and mixing parameters. For illustration, we show the results for $v_\Delta = 3.5$ eV for NH (Fig. 4.5a) and IH (Fig. 4.5b) and for $v_\Delta = 0.5$ eV for NH (Fig. 4.5c) and IH (Fig. 4.5d). The smallest neutrino mass is taken to be $m_{\nu_{\min}} = 0$ eV (blue) and $m_{\nu_{\min}} = 0.02$ eV (orange) and the Majorana matrices to be zero (solid line) and $(\alpha_1 = \pi/3, \alpha_2 = \pi/2)$ (dashed line). The horizontal lines denote the current limit set by the Sindrum experiment (pink) and the sensitivities which are expected to be reached at the Mu3e experiment in its Phase I (dashed yellow) and Phase II (dashed green). As can be seen from the figures, the masses up to which the future experiments will be able to probe depend strongly on the neutrino mass and mixing parameters, ranging from few hundred GeV to several TeV. Recall that masses much larger than 3 TeV would introduce large corrections, violating naturalness. It is worth to remark again that the elements of the Yukawa mixing matrix which are relevant for the branching ratio of this process, $|Y_{ee}|$ and $|Y_{e\mu}|$, can vanish for specific values of the mixing parameters making the branching ratio decrease and even cancel, which leads to the possibility for this LFV process to hide from experiments, as was explained in Section 4.6.1.

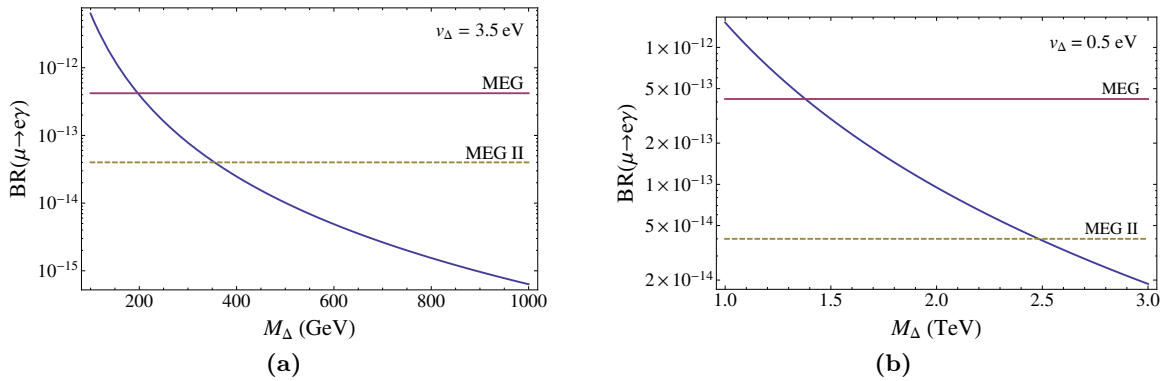


Figure 4.4: Predicted $\text{BR}(\mu \rightarrow e\gamma)$ in the type II see-saw model (blue line) for (a) $v_\Delta = 3.5$ eV and (b) $v_\Delta = 0.5$ eV. The horizontal lines denote the current sensitivity of the MEG experiment (pink) and the expected sensitivity of the upgraded MEG II experiment.

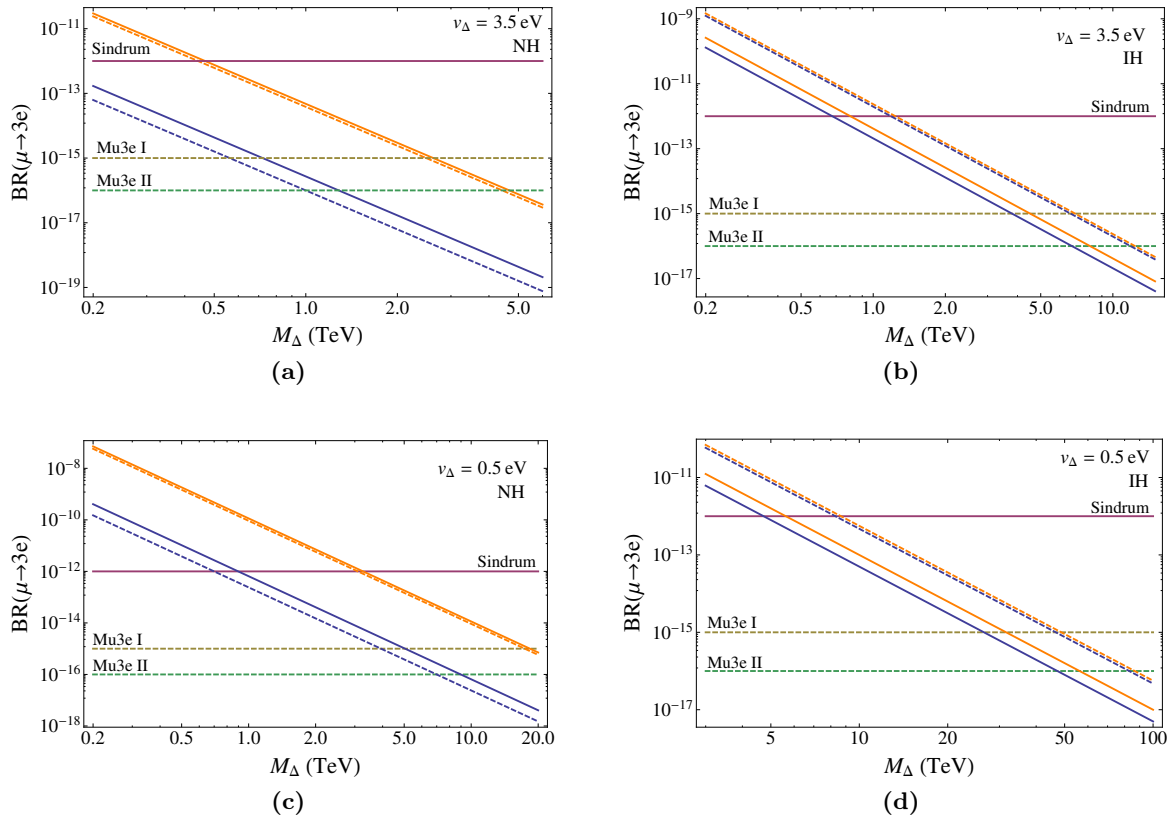


Figure 4.5: Predicted $\text{BR}(\mu \rightarrow 3e)$ in the type II see-saw model for $v_\Delta = 3.5$ eV with (a) NH and (b) IH; and for $v_\Delta = 0.5$ eV with (c) NH and (d) IH. The smallest neutrino mass is taken to be $m_{\nu,\min} = 0$ eV (blue) and $m_{\nu,\min} = 0.02$ eV (orange) and the Majorana phases to be zero (solid line) and $(\alpha_1 = \pi/3, \alpha_2 = \pi/2)$ (dashed line). The horizontal lines denote the current limit set by Sindrum (pink) and the expected sensitivities of the future experiment Mu3e in its Phase I (yellow) and Phase II (green).

5 CONCLUSIONS

The observation of neutrino oscillations and the implication that neutrinos are massive requires physics beyond the Standard Model (SM). Different models have been proposed to explain both the mechanism to generate neutrino masses and the reason why these masses are so small. The so-called see-saw models are probably the most popular ones. In this thesis, we have focused on the type I and type II see-saw models, which account for small neutrino masses through the tree level exchange of a heavy fermion singlet and a heavy scalar triplet, respectively. The extension of the SM by new heavy particles could lead to a hierarchy problem if the new quantum corrections to the Higgs mass is too large. By imposing as the naturalness criterion that the radiative corrections to the Higgs mass parameter squared should be, at most, of the order of the physical Higgs mass squared, we have set limits on the parameters and the new energy scale introduced in the each of the studied see-saw models.

First, we have studied the type I see-saw model. The one-loop radiative correction to the Higgs mass parameter squared induced by the new heavy right-handed neutrino has been obtained in the simplified case of one family of leptons. This correction has been written in terms of measurable quantities: the mass of the light and heavy neutrino and the vacuum expectation value (vev) of the Higgs field. The analysis has been performed for two benchmark values of the light neutrino mass: $m_\nu = 2$ eV, which corresponds to the experimental upper limit; and a smaller value of $m_\nu = 1 \times 10^{-3}$ eV. Imposing the naturalness criterion, it is found that the allowed mass of the heavy neutrino can take values up to 2.7×10^6 GeV for $m_\nu = 2$ eV, and 3.3×10^7 GeV for $m_\nu = 1 \times 10^{-3}$ eV. Therefore, if $m_\nu \sim \mathcal{O}((10^{-3} - 1)$ eV), only for right-handed neutrino masses larger than $\mathcal{O}((10^6 - 10^7)$ GeV) a hierarchy problem arises within the type I see-saw model. The limits found in our study are comparable to the ones obtained in the literature for the generalization to the three-family case. Note that these bounds are incompatible with the lower limits imposed by leptogenesis, which typically requires masses above $\mathcal{O}(10^8)$ GeV). Therefore, in most of the scenarios, it is not possible to account for baryogenesis via leptogenesis and preserve naturalness simultaneously within the type I see-saw model.

Second, we have considered the type II see-saw model. The one-loop radiative corrections to the Higgs mass parameter squared involving the new scalar triplet field components have been explicitly calculated. In the calculations and in the rest of the study it has been assumed that the scalar doublet and scalar triplet are not mixed, and that the splitting between the triplet components is negligible. These are valid assumptions within our analysis. We have restricted the study to the low-scale scenario, with triplet masses up to the TeV scale, which could be testable at the LHC or future

colliders and LFV experiments. We have considered values of the triplet vev of the order of the eV, which lead to sizeable Yukawa couplings between the triplet and the leptons. We have first restricted the parameter space by imposing the current experimental constraints and vacuum stability and unitarity of different scattering processes up to the Planck scale. In our studies, the allowed parameter region do not show any dependence on the neutrino mass and mixing parameters, neither on the hierarchy of the neutrino masses. Of the allowed parameter space, all the parameter sets satisfy the naturalness condition below 1 TeV and a large subset satisfies it for masses between 1 TeV and 3 TeV. For higher masses, the naturalness is violated by most of the parameter sets. From this analysis we can conclude that the introduction of a scalar triplet with a mass below 3 TeV could account for neutrino masses within the type II see-saw model without introducing a hierarchy problem, while larger masses would be disfavoured by naturalness. Within the studied scenario, the existence of a scalar triplet with a mass around the TeV scale and a vev of the order of the eV could be probed not only by direct detection at high-energy particle colliders but also at experiments searching for LFV decays. In the case of the $\mu \rightarrow e\gamma$ decay, which is independent of the absolute neutrino mass scale and the Majorana phases, the upgraded experiment MEG II would be able to probe triplet masses up to 350 GeV for $v_\Delta = 3.5$ eV and up to 2.5 TeV for $v_\Delta = 0.5$ eV. In the case of the $\mu \rightarrow 3e$ decay, the limits depend strongly on the the hierarchy of the neutrino masses and the neutrino mass and mixing parameters. Minimal neutrino masses $m_{\nu_{\min}}$ different than zero increase the branching ratio of the process, while different values of Majorana phases can enhance or reduce it and even lead to a total cancellation. For triplet vevs of the order of the eV, the Mu3e experiment could be able to probe triplet masses ranging from few hundred GeV to several TeV, if this cancellation does not occur.

A APPENDIX

A.1 RGEs AND MATCHING CONDITIONS IN THE SEE-SAW TYPE II MODEL

The running Higgs mass in the $\overline{\text{MS}}$ scheme is related to its pole mass by the matching condition given by Eq. (4.58), where [48]

$$\Delta_h(\mu) = \frac{G_F M_Z^2}{\sqrt{2} 8\pi^2} \left[\xi f_1(\xi, \mu) + f_0(\xi, \nu) + \frac{1}{\xi} f_{-1}(\xi, \mu) \right], \quad (\text{A.1})$$

with $\xi \equiv M_h^2/M_Z^2$. The loop-functions $f(\xi)$ are given by:

$$\begin{aligned} f_1(\xi, \mu) &= 6 \ln \left(\frac{\mu^2}{M_h^2} \right) + \frac{3}{2} \ln \xi - \frac{1}{2} \mathcal{Z} \left(\frac{c_W^2}{\xi} \right) - \ln c_W^2 + \frac{9}{2} \left(\frac{25}{9} - \frac{\pi}{\sqrt{3}} \right), \\ f_0(\xi) &= 6 \ln \left(\frac{\mu^2}{M_Z^2} \right) \left[1 + 2c_W^2 - 2 \frac{M_t^2}{M_Z^2} \right] + \frac{3c_W^2 \xi}{\xi - c_W^2} \ln \frac{\xi}{c_W^2} \ln \frac{\xi}{c_W^2} + 2\mathcal{Z} \left(\frac{1}{\xi} \right) + 4c_W^2 \mathcal{Z} \left(\frac{c_W^2}{\xi} \right) \\ &\quad + \left(\frac{3c_W^2}{s_W^2} + 12c_W^2 \right) \ln c_W^2 - \frac{15}{2} (1 + 2c_W^2) - 3 \frac{M_t^2}{M_Z^2} \left[2\mathcal{Z} \left(\frac{M_t^2}{M_Z^2 \xi} \right) + 4 \ln \frac{M_t^2}{M_Z^2} - 5 \right], \\ f_{-1}(\xi) &= 6 \ln \left(\frac{\mu}{M_Z^2} \right) \left[1 + 2c_W^4 - 4 \frac{M_t^4}{M_Z^4} \right] - 6\mathcal{Z} \left(\frac{1}{\xi} \right) - 12c_W^4 \mathcal{Z} \left(\frac{c_W^2}{\xi} \right) - 12c_W^4 \ln c_W^2 \\ &\quad + 8(1 + 2c_W^2) + 24 \frac{M_t^4}{M_Z^4} \left[\ln \frac{M_t^2}{M_Z^2} - 2 + \mathcal{Z} \left(\frac{M_t^2}{M_Z^2 \xi} \right) \right], \end{aligned} \quad (\text{A.2})$$

with $s_W^2 \equiv \sin^2 \theta_W, c_W^2 \equiv \cos^2 \theta_W$ being θ_W the weak mixing angle and

$$\mathcal{Z}(z) = \begin{cases} 2\mathcal{A} \tan^{-1}(1/\mathcal{A}) & (z > 1/4) \\ \mathcal{A} \ln[(1 + \mathcal{A})/(1 - \mathcal{A})] & (z < 1/4) \end{cases} \quad (\text{A.3})$$

with $\mathcal{A} = \sqrt{|1 - 4x|}$.

The two-loop RG equation for the top-quark Yukawa coupling is:

$$\frac{dy_t}{d \ln \mu} = \left(\frac{\beta_t^{(1)}}{16\pi^2} + \frac{\beta_t^{(2)}}{(16\pi^2)^2} \right) \quad (\text{A.4})$$

where [64]:

$$\beta_t^{(1)} = \frac{9}{2}y_t^2 - \left(\frac{17}{20}g_1^2 + \frac{9}{4}g_2^2 + 8g_3^2 \right), \quad (\text{A.5})$$

$$\begin{aligned} \beta_t^{(2)} = & -12y_t^4 + \left(\frac{393}{80}g_1^2 + \frac{225}{16}g_2^2 + 36g_3^2 \right) y_t^2 + \frac{1187}{600}g_1^4 - \frac{9}{20}g_1^2g_2^2 + \frac{19}{15}g_1^2g_3^2 \\ & - \frac{23}{4}g_2^4 + 9g_2^2g_3^2 - 108g_3^4 + \frac{3}{2}\lambda^2 - 6\lambda y_t^2. \end{aligned} \quad (\text{A.6})$$

The boundary condition for $y_t(\mu)$ can be determined from the matching condition between the running top quark mass $m_t(\mu) = y_t(\mu)v/\sqrt{2}$ and its pole mass M_t [43], analogous to Eq. (4.58):

$$y_t(\mu) = \frac{\sqrt{2}M_t}{v}[1 + \Delta_t(\mu)], \quad (\text{A.7})$$

where $\Delta_t(\mu)$ gets contributions from QCD as well as electroweak corrections. The explicit expression up to $\mathcal{O}(\alpha_3^2)$ for the QCD part and $\mathcal{O}(\alpha)$ for the electroweak part is given by [43]:

$$\begin{aligned} \Delta_t(\mu) = & \left[\ln \left(\frac{M_t^2}{\mu^2} \right) - \frac{4}{3} \right] \left(\frac{\alpha_3(\mu)}{\pi} \right) + (1.0414N_L - 14.3323) \left(\frac{\alpha_3(\mu)}{\pi} \right)^2 \\ & + \frac{1}{3} \left[\ln \left(\frac{M_t^2}{\mu^2} \right) + \frac{11}{2} - r + 2r(2r - 3) \ln(4r) - 8r^2 \left(\frac{1}{r} - 1 \right)^{3/2} \cos^{-1}(\sqrt{r}) \right] \\ & + a_t + b_t \ln \left(\frac{M_h}{300\text{GeV}} \right) + c_t \ln \left(\frac{M_t}{175\text{GeV}} \right) \end{aligned} \quad (\text{A.8})$$

where N_L is the number of massless quark flavours, $r \equiv M_h^2/4M_t^2$. For $\mu = M_t$, the numerical coefficients $(a_t, b_t, c_t) = (-6.90, 1.73, -5.82) \times 10^{-3}$ [43]. The $\mathcal{O}(\alpha\alpha_3^2)$ and $\mathcal{O}(\alpha_3^2)$ terms whose contributions are less than 0.5% have been neglected.

The two-loop RG equations for the SM gauge couplings are given by [64, 65]:

$$\frac{dg_i}{d \ln \mu} = -\frac{g_i^3}{16\pi^2}b_i - \frac{g_i^3}{(16\pi^2)^2} \sum_{j=1}^3 b_{ij}g_j^2 - \frac{g_i^3y_t^2}{(16\pi^2)^2}a_i, \quad (\text{A.9})$$

where the β -function coefficients are given by:

$$b_i = -\frac{2}{3}N_F - \frac{1}{10}, \quad b_2 = \frac{22}{3} - \frac{2}{3}N_F - \frac{1}{6}, \quad b_3 = 11 - \frac{2}{3}N_F, \quad (\text{A.10})$$

$$b_{ij} = \begin{pmatrix} 0 & 0 & 0 \\ 0 & \frac{136}{3} & 0 \\ 0 & 0 & 102 \end{pmatrix} - \frac{N_F}{2} \begin{pmatrix} \frac{19}{15} & \frac{1}{5} & \frac{11}{30} \\ \frac{5}{3} & \frac{49}{3} & \frac{2}{3} \\ \frac{44}{15} & 4 & \frac{79}{3} \end{pmatrix} - \begin{pmatrix} \frac{9}{10} & \frac{3}{10} & 0 \\ \frac{50}{10} & \frac{19}{6} & 0 \\ 0 & 0 & 0 \end{pmatrix} \quad (\text{A.11})$$

and $a_i = (\frac{17}{10}, \frac{3}{2}, 2)$. In Eq. (A.10), N_F is the effective number of flavours below the renormalisation scale μ . Therefore, when evolving the coupled RGEs for λ , y_t and g_i , Eqs. (4.55), (A.4) and (A.9), we set $N_F = 5$ for $\mu < M_t$ and $N_F = 6$ for $\mu \geq M_t$.

The one-loop RG equations for the new scalar couplings in the type II see-saw model are given by [66, 67]:

$$16\pi^2 \frac{d\lambda_1}{d\ln\mu} = - \left(\frac{36}{5}g_1^2 + 24g_2^2 \right) \lambda_1 + \frac{108}{25}g_1^4 + 18g_2^4 + \frac{72}{5}g_1^2g_2^2 + 14\lambda_1^2 + 4\lambda_1\lambda_2 + 2\lambda_2^2 + 4\lambda_4^2 + 4\lambda_5^2 + 4\text{Tr}[\mathbf{S}_\Delta]\lambda_1 - 8\text{Tr}[\mathbf{S}_\Delta^2], \quad (\text{A.12})$$

$$16\pi^2 \frac{d\lambda_2}{d\ln\mu} = - \left(\frac{36}{5}g_1^2 + 24g_2^2 \right) \lambda_2 + 12g_2^4 - \frac{144}{5}g_1^2g_2^2 + 3\lambda_2^2 + 12\lambda_1\lambda_2 - 8\lambda_5^2 + 4\text{Tr}[\mathbf{S}_\Delta]\lambda_2 + 8\text{Tr}[\mathbf{S}_\Delta^2], \quad (\text{A.13})$$

$$16\pi^2 \frac{d\lambda_4}{d\ln\mu} = - \left(\frac{9}{2}g_1^2 + \frac{33}{2}g_2^2 \right) \lambda_4 + \frac{27}{25}g_1^4 + 6g_2^4 + (8\lambda_1 + 2\lambda_2 + 6\lambda + 4\lambda_4 + 6y_t^2 + 2\text{Tr}[\mathbf{S}_\Delta]) \lambda_4 + 8\lambda_5 \quad (\text{A.14})$$

$$16\pi^2 \frac{d\lambda_5}{d\ln\mu} = - \frac{9}{2}g_1^2\lambda_5 - \frac{33}{2}g_2^2\lambda_5 - \frac{18}{5}g_1^2g_2^2 + (2\lambda_1 - 2\lambda_2 + 2\lambda + 8\lambda_4 + 6y_t^2 + 2\text{Tr}[\mathbf{S}_\Delta]) \lambda_5 \quad (\text{A.15})$$

Here $\mathbf{S}_\Delta = Y_\Delta^\dagger Y_\Delta$ and its corresponding RG equation is given by:

$$16\pi^2 \frac{d\mathbf{S}_\Delta}{d\ln\mu} = 12\mathbf{S}_\Delta^2 - 3 \left(\frac{3}{5}g_1^2 + 3g_2^2 \right) \mathbf{S}_\Delta + 4\text{Tr}[\mathbf{S}_\Delta]\mathbf{S}_\Delta. \quad (\text{A.16})$$

In our analysis, we do not consider the RGE for λ_6 because, at one-loop level, it is decoupled from the other RGEs. Its expression is given in Ref [66].

Following the best fit values given by the Particle Data Group (PDG) for the gauge-boson masses and the Higgs boson mass [8]:

$$\begin{aligned} M_W &= 80.385 \pm 0.015 \text{ GeV} \\ M_Z &= 91.1876 \pm 0.0021 \text{ GeV} \\ M_h &= 125.09 \pm 0.21 \pm 0.11 \end{aligned}$$

we take $M_W = 80.4\text{GeV}$ and $M_Z = 91.2$ for the W and Z pole masses and $M_h = 125.1$ for the Higgs boson pole mass in our analysis, unless otherwise specified.

For the top quark pole mass, we use the resulting combined measurement performed by the CDF and D0 experiments at the Tevatron collider and the ATLAS and CMS experiments at the Large Hadron Collider (LHC): $M_t = 173.34 \pm 0.27(\text{stat}) \pm 0.71(\text{syst}) \text{ GeV}$ [68], which is consistent with the average of published measurements from Tevatron Runs evaluated by the PDG: $173.21 \pm 0.51 \pm 0.71 \text{ GeV}$ [8].

For the other SM parameters appearing in Eqs. (4.58) and (A.7), we use the PDG central values: $G_F = 1.166 \times 10^{-5} \text{ GeV}^{-2}$ for the Fermi coupling constant and $\alpha(M_t) = 1/127.9$ for the fine structure constant.

A.2 PARAMETER SCAN PLOTS

Here we show the allowed parameter space in the type II see-saw model for different values of $m_{\nu_{\min}}$: $m_{\nu_{\min}} = 0$ and $m_{\nu_{\min}} = 0.2$ eV, considering normal hierarchy (NH) and inverted hierarchy (IH) and zero Majorana phases. The different plots show: (a) the (λ_1, λ_2) plane, (b) the (λ_4, λ_5) plane, (c) the $(|\lambda_4|, \lambda_6)$ plane and (d) the $(M_\Delta, |\delta m_h^2|/M_h^2)$ plane. We have considered two benchmark scenarios: $v_\Delta = 3.5$ eV with $200 \text{ GeV} < M_\Delta < 1 \text{ TeV}$ and $v_\Delta = 0.5$ eV with $1.4 < \text{TeV} < M_\Delta < 3 \text{ TeV}$. All points satisfy the vacuum stability, unitarity and perturbativity conditions up to Planck scale. In addition, those which also satisfy the naturalness condition $|\delta m_h^2| \leq M_h^2$ at $\mu = M_\Delta$ are denoted in pink, while those that do not are denoted in blue. The values shown correspond to the parameters at $\mu = M_\Delta$. The specific values of $m_{\nu_{\min}}$ and v_Δ and hierarchy chosen in each case is indicated on the header of each set of plots, as well as in their caption.

These plots complement Fig. 4.2 and Fig 4.3. They all have roughly the same allowed parameter space, showing that the oscillation and mixing parameters, as well as the minimal neutrino mass, do not visibly affect the allowed regions in the context of a low scale see-saw scenario. To demonstrate this, we show in Fig. A.1 the superposition of the allowed parameter space for $v_\Delta = 3.5$ eV in the four studied cases: NH with $m_{\nu_{\min}} = 0$ (blue) and $m_{\nu_{\min}} = 0.2$ eV (pink) and IH with $m_{\nu_{\min}} = 0$ (yellow) and $m_{\nu_{\min}} = 0.2$ eV (green).

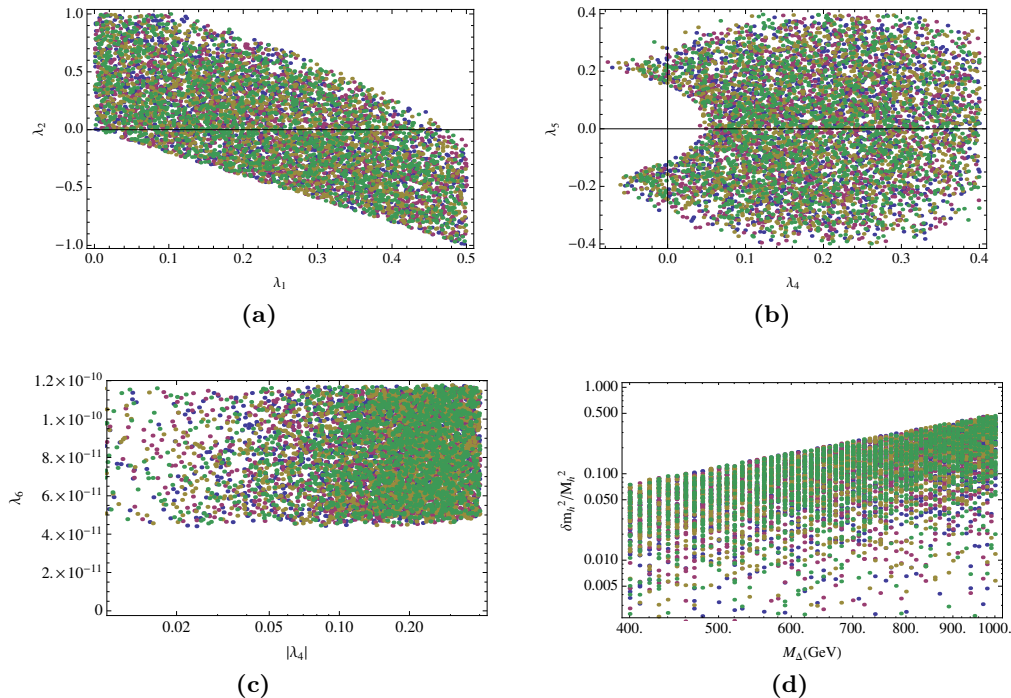
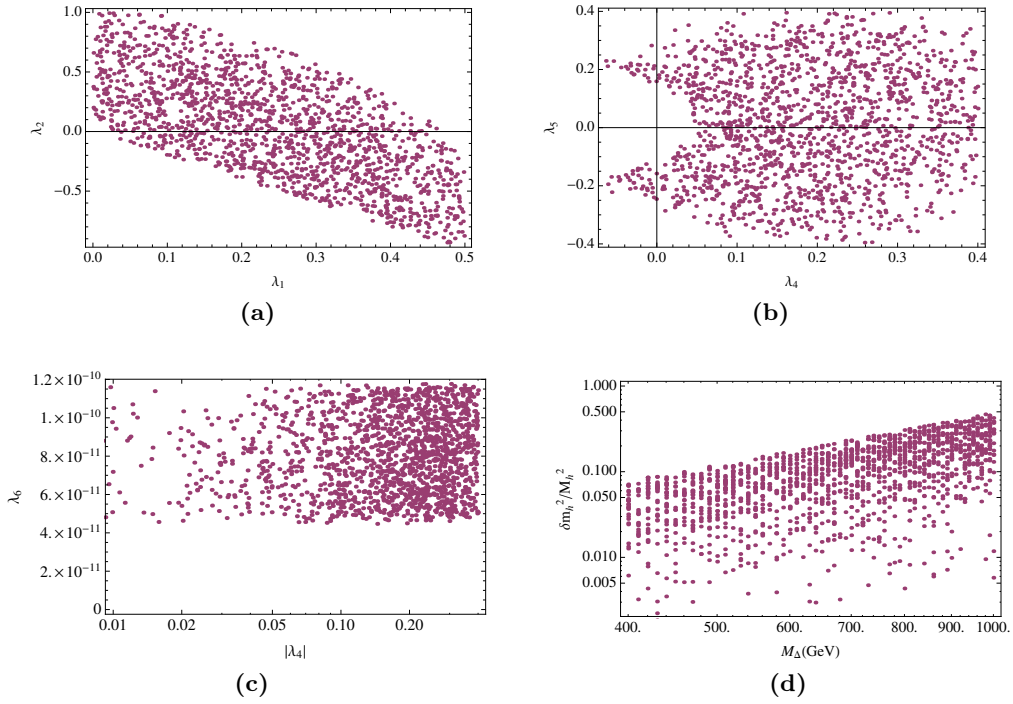
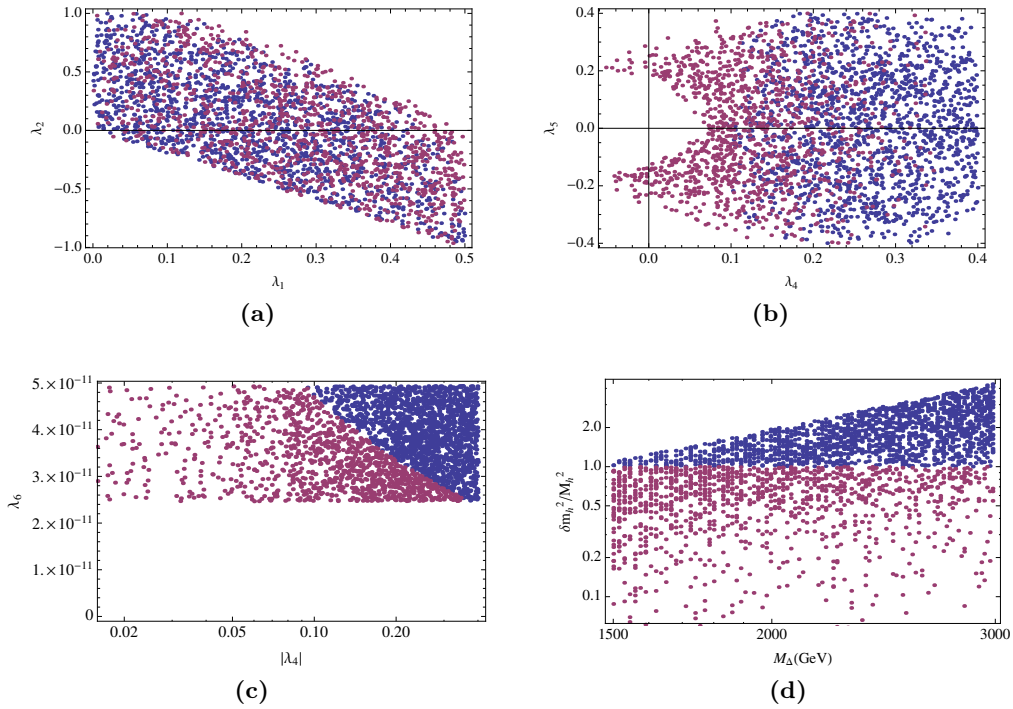


Figure A.1: Same as Fig. 4.2 ($v_\Delta = 3.5$ eV) for NH, $m_{\nu_{\min}} = 0$ eV (blue); NH, $m_{\nu_{\min}} = 0.2$ eV (pink); IH, $m_{\nu_{\min}} = 0$ eV (yellow); IH, $m_{\nu_{\min}} = 0.2$ eV (green); and zero Majorana phases (see also text above).

A.2.1 IH - $m_{\nu_{\min}} = 0$, zero Majorana phases.Figure A.2: Same as Fig. 4.2 ($v_{\Delta} = 3.5$ eV) but for IH, $m_{\nu_{\min}} = 0$ and zero Majorana phases.Figure A.3: Same as Fig. 4.3 ($v_{\Delta} = 0.5$ eV) but for IH, $m_{\nu_{\min}} = 0$ and zero Majorana phases.

A.2.2 NH - $m_{\nu_{\min}} = 0.2$ eV, zero Majorana phases.

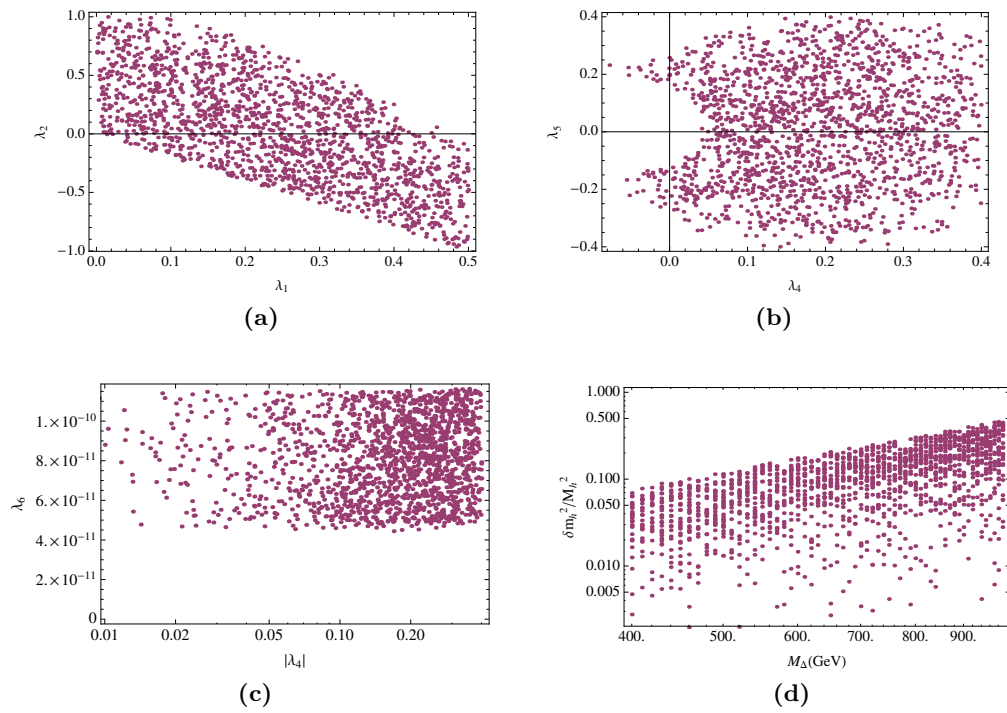


Figure A.4: Same as Fig. 4.2 ($v_\Delta = 3.5$ eV) but for NH, $m_{\nu_{\min}} = 0.2$ eV and zero Majorana phases.

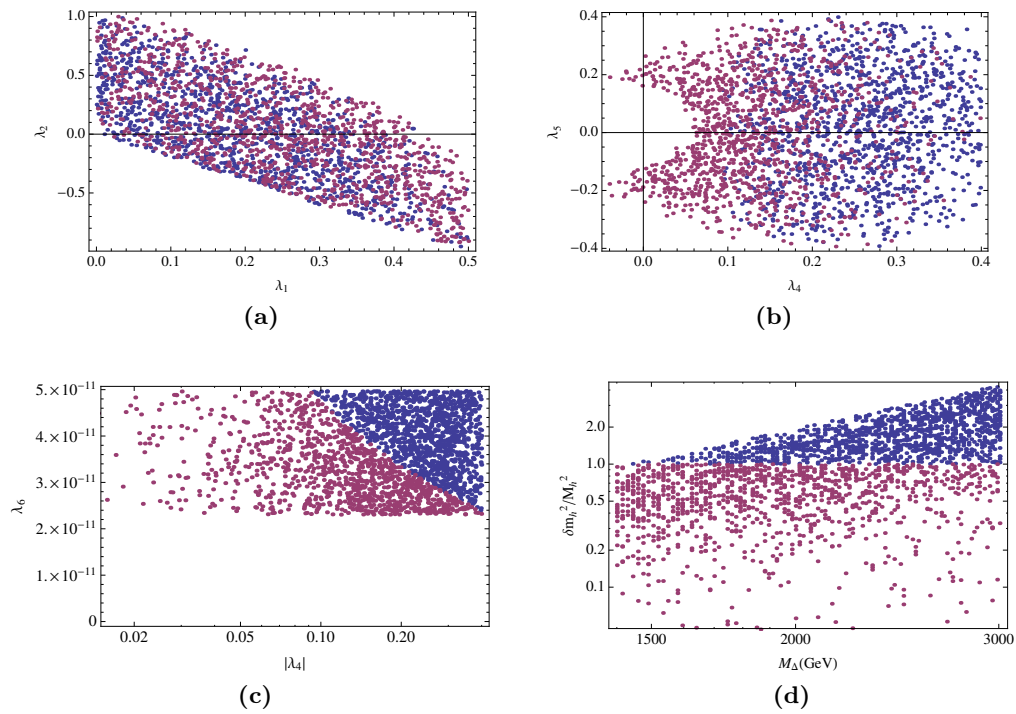


Figure A.5: Same as Fig. 4.3 ($v_\Delta = 0.5$ eV) but for NH, $m_{\nu_{\min}} = 0.2$ eV and zero Majorana phases.

A.2.3 IH - $m_{\nu_{\min}} = 0.2$ eV, zero Majorana phases.

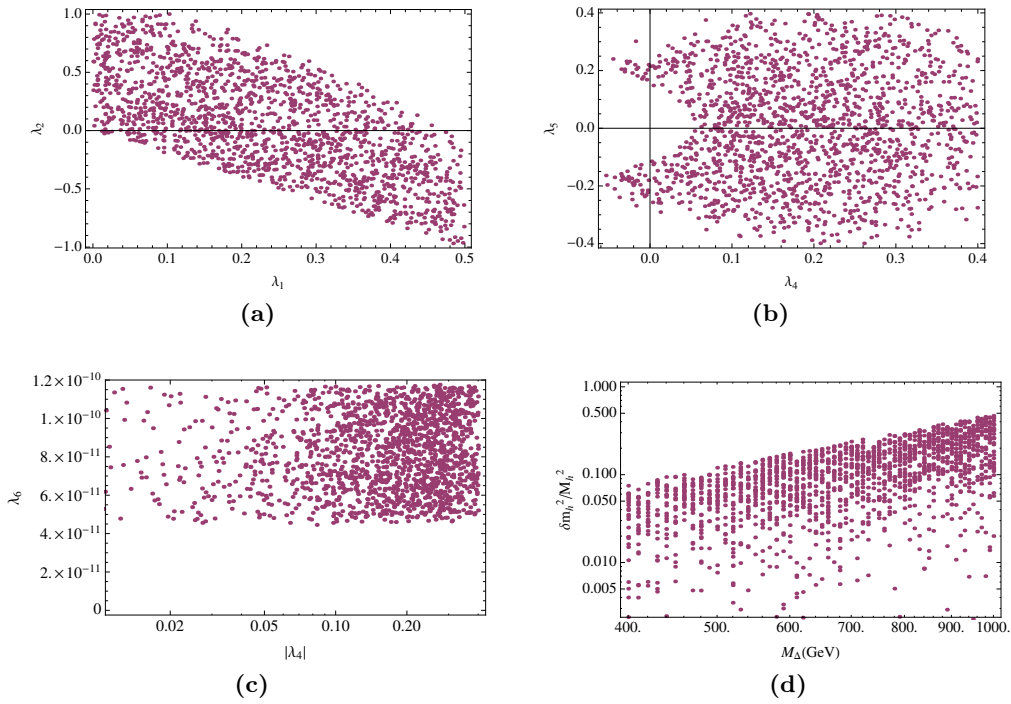


Figure A.6: Same as Fig. 4.2 ($v_{\Delta} = 3.5$ eV) but for IH, $m_{\nu_{\min}} = 0.2$ eV and zero Majorana phases.

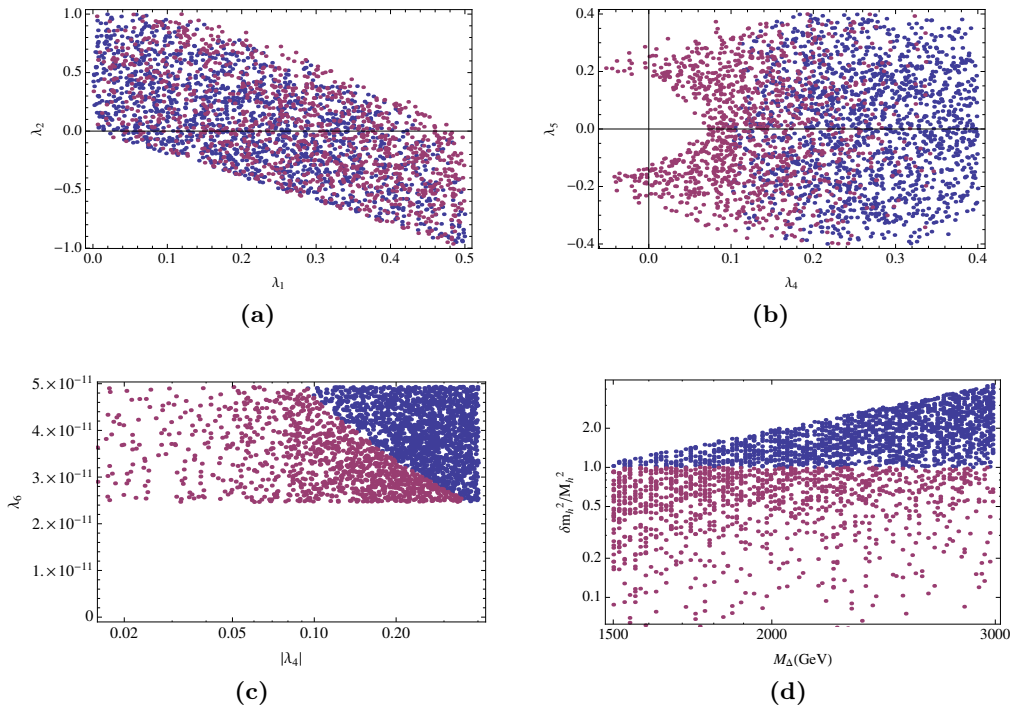


Figure A.7: Same as Fig. 4.3 ($v_{\Delta} = 0.5$ eV) but for IH, $m_{\nu_{\min}} = 0.2$ eV and zero Majorana phases.

B BIBLIOGRAPHY

- [1] G. 't Hooft. “Naturalness, chiral symmetry, and spontaneous chiral symmetry breaking”. In: *NATO Sci. Ser. B* 59 (1980), pp. 135–157.
- [2] R. Davis Jr., D. S. Harmer, and K. C. Hoffman. “Search for neutrinos from the sun”. In: *Phys. Rev. Lett.* 20 (1968), pp. 1205–1209.
- [3] Y. Fukuda et al., Super-Kamiokande Collaboration. “Evidence for oscillation of atmospheric neutrinos”. In: *Phys. Rev. Lett.* 81 (1998), pp. 1562–1567. arXiv: [hep-ex/9807003](#) [[hep-ex](#)].
- [4] K. Eguchi et al., KamLAND Collaboration. “First results from KamLAND: Evidence for reactor anti-neutrino disappearance”. In: *Phys. Rev. Lett.* 90 (2003), p. 021802. arXiv: [hep-ex/0212021](#) [[hep-ex](#)].
- [5] M. H. Ahn et al., K2K Collaboration. “Indications of neutrino oscillation in a 250 km long baseline experiment”. In: *Phys. Rev. Lett.* 90 (2003), p. 041801. arXiv: [hep-ex/0212007](#) [[hep-ex](#)].
- [6] A. Abada et al. “Low energy effects of neutrino masses”. In: *JHEP* 12 (2007), p. 061. arXiv: [0707.4058](#) [[hep-ph](#)].
- [7] S. Weinberg. “Baryon and Lepton Nonconserving Processes”. In: *Phys. Rev. Lett.* 43 (1979), pp. 1566–1570.
- [8] K. A. Olive et al., Particle Data Group. “Review of Particle Physics”. In: *Chin. Phys.* C38 (2014), p. 090001.
- [9] Matthew D. Schwartz. *Quantum Field Theory and the Standard Model*. Cambridge University Press, 2014.
- [10] G. Aad et al., ATLAS Collaboration. “Observation of a new particle in the search for the Standard Model Higgs boson with the ATLAS detector at the LHC”. In: *Phys. Lett.* B716 (2012), pp. 1–29. arXiv: [1207.7214](#) [[hep-ex](#)].
- [11] S. Chatrchyan et al., CMS Collaboration. “Observation of a new boson at a mass of 125 GeV with the CMS experiment at the LHC”. In: *Phys. Lett.* B716 (2012), pp. 30–61. arXiv: [1207.7235](#) [[hep-ex](#)].
- [12] J. Wess and B. Zumino. “Supergauge Transformations in Four-Dimensions”. In: *Nucl. Phys.* B70 (1974), pp. 39–50.
- [13] A. Salam and J. A. Strathdee. “Supergauge Transformations”. In: *Nucl. Phys.* B76 (1974), pp. 477–482.
- [14] W. A. Bardeen. “On naturalness in the standard model”. In: *Ontake Summer Institute on Particle Physics Ontake Mountain, Japan, August 27-September 2, 1995*. 1995.

- [15] N. Arkani-Hamed, S. Dimopoulos, and G. R. Dvali. “The Hierarchy problem and new dimensions at a millimeter”. In: *Phys. Lett.* B429 (1998), pp. 263–272. arXiv: [hep-ph/9803315](#) [[hep-ph](#)].
- [16] L. Randall and R. Sundrum. “A Large mass hierarchy from a small extra dimension”. In: *Phys. Rev. Lett.* 83 (1999), pp. 3370–3373. arXiv: [hep-ph/9905221](#) [[hep-ph](#)].
- [17] H. E. Logan. “TASI 2013 lectures on Higgs physics within and beyond the Standard Model”. In: (2014). arXiv: [1406.1786](#) [[hep-ph](#)].
- [18] S. L. Glashow, J. Iliopoulos, and L. Maiani. “Weak Interactions with Lepton-Hadron Symmetry”. In: *Phys. Rev.* D2 (1970), pp. 1285–1292.
- [19] A. Marrone et al. “Three-neutrino mixing: status and prospects”. In: *J. Phys. Conf. Ser.* 718.6 (2016), p. 062042.
- [20] Ch. Kraus et al. “Final results from phase II of the Mainz neutrino mass search in tritium beta decay”. In: *Eur. Phys. J.* C40 (2005), pp. 447–468. arXiv: [hep-ex/0412056](#) [[hep-ex](#)].
- [21] A. Osipowicz et al., KATRIN Collaboration. “KATRIN: A Next generation tritium beta decay experiment with sub-eV sensitivity for the electron neutrino mass. Letter of intent”. In: (2001). arXiv: [hep-ex/0109033](#) [[hep-ex](#)].
- [22] W. Rodejohann. “Neutrino-less Double Beta Decay and Particle Physics”. In: *Int. J. Mod. Phys.* E20 (2011), pp. 1833–1930. arXiv: [1106.1334](#) [[hep-ph](#)].
- [23] M. Agostini et al., GERDA Collaboration. “Results on Neutrinoless Double- β Decay of ^{76}Ge from Phase I of the GERDA Experiment”. In: *Phys. Rev. Lett.* 111.12 (2013), p. 122503. arXiv: [1307.4720](#) [[nucl-ex](#)].
- [24] A. Gando et al., KamLAND-Zen Collaboration. “Limit on Neutrinoless $\beta\beta$ Decay of ^{136}Xe from the First Phase of KamLAND-Zen and Comparison with the Positive Claim in ^{76}Ge ”. In: *Phys. Rev. Lett.* 110.6 (2013), p. 062502. arXiv: [1211.3863](#) [[hep-ex](#)].
- [25] J. B. Albert et al., EXO-200 Collaboration. “Search for Majorana neutrinos with the first two years of EXO-200 data”. In: *Nature* 510 (2014), pp. 229–234. arXiv: [1402.6956](#) [[nucl-ex](#)].
- [26] A. Gando et al., KamLAND-Zen Collaboration. “Search for Majorana Neutrinos near the Inverted Mass Hierarchy Region with KamLAND-Zen”. In: *Phys. Rev. Lett.* 117.8 (2016). [Addendum: *Phys. Rev. Lett.* 117, no. 10, 109903 (2016)], p. 082503. arXiv: [1605.02889](#) [[hep-ex](#)].
- [27] P. A. R. Ade et al., Planck Collaboration. “Planck 2013 results. XVI. Cosmological parameters”. In: *Astron. Astrophys.* 571 (2014), A16. arXiv: [1303.5076](#) [[astro-ph.CO](#)].
- [28] S. R. Coleman and E. J. Weinberg. “Radiative Corrections as the Origin of Spontaneous Symmetry Breaking”. In: *Phys. Rev.* D7 (1973), pp. 1888–1910.
- [29] S. Weinberg. “Living in the multiverse”. In: *In *Carr, Bernard (ed.): Universe or multiverse?** 29-42. 2005. arXiv: [hep-th/0511037](#) [[hep-th](#)].
- [30] V. Agrawal et al. “The Anthropic principle and the mass scale of the standard model”. In: *Phys. Rev.* D57 (1998), pp. 5480–5492. arXiv: [hep-ph/9707380](#) [[hep-ph](#)].
- [31] P. W. Graham, D. E. Kaplan, and S. Rajendran. “Cosmological Relaxation of the Electroweak Scale”. In: *Phys. Rev. Lett.* 115.22 (2015), p. 221801. arXiv: [1504.07551](#) [[hep-ph](#)].

-
- [32] W. Grimus and L. Lavoura. “The Seesaw mechanism at arbitrary order: Disentangling the small scale from the large scale”. In: *JHEP* 11 (2000), p. 042. arXiv: [hep-ph/0008179](#) [[hep-ph](#)].
- [33] Z. Xing. “Naturalness and Testability of TeV Seesaw Mechanisms”. In: *Prog. Theor. Phys. Suppl.* 180 (2009), pp. 112–127. arXiv: [0905.3903](#) [[hep-ph](#)].
- [34] A. Ibarra. “Constraints and tests of the TeV scale see-saw mechanism”. In: *J. Phys. Conf. Ser.* 408 (2013), p. 012018.
- [35] Z. Xing. “TeV Neutrino Physics at the Large Hadron Collider”. In: *Int. J. Mod. Phys. A* 24 (2009), pp. 3286–3296. arXiv: [0901.0209](#) [[hep-ph](#)].
- [36] A. Denner et al. “Compact Feynman rules for Majorana fermions”. In: *Phys. Lett.* B291 (1992), pp. 278–280.
- [37] A. Denner et al. “Feynman rules for fermion number violating interactions”. In: *Nucl. Phys.* B387 (1992), pp. 467–481.
- [38] Michael E. Peskin and Daniel V. Schroeder. *An Introduction to quantum field theory*. The Advanced Book Program, Westview Press, 1995.
- [39] F. Vissani. “Do experiments suggest a hierarchy problem?” In: *Phys. Rev.* D57 (1998), pp. 7027–7030. arXiv: [hep-ph/9709409](#) [[hep-ph](#)].
- [40] M. Farina, D. Pappadopulo, and A. Strumia. “A modified naturalness principle and its experimental tests”. In: *JHEP* 08 (2013), p. 022. arXiv: [1303.7244](#) [[hep-ph](#)].
- [41] W. Grimus and P. O. Ludl. “Correlations of the elements of the neutrino mass matrix”. In: *JHEP* 12 (2012), p. 117. arXiv: [1209.2601](#) [[hep-ph](#)].
- [42] J. D. Clarke, R. Foot, and R. R. Volkas. “Electroweak naturalness in the three-flavor type I seesaw model and implications for leptogenesis”. In: *Phys. Rev.* D91.7 (2015), p. 073009. arXiv: [1502.01352](#) [[hep-ph](#)].
- [43] P. S. Bhupal Dev et al. “125 GeV Higgs Boson and the Type-II Seesaw Model”. In: *JHEP* 03 (2013). [Erratum: *JHEP*05,049(2013)], p. 150. arXiv: [1301.3453](#) [[hep-ph](#)].
- [44] D. Buttazzo et al. “Investigating the near-criticality of the Higgs boson”. In: *JHEP* 12 (2013), p. 089. arXiv: [1307.3536](#) [[hep-ph](#)].
- [45] C. Bonilla, R. M. Fonseca, and J. W. F. Valle. “Consistency of the triplet seesaw model revisited”. In: *Phys. Rev.* D92.7 (2015), p. 075028. arXiv: [1508.02323](#) [[hep-ph](#)].
- [46] A. Arhrib et al. “The Higgs Potential in the Type II Seesaw Model”. In: *Phys. Rev.* D84 (2011), p. 095005. arXiv: [1105.1925](#) [[hep-ph](#)].
- [47] T. Plehn. “Lectures on LHC Physics”. In: *Lect. Notes Phys.* 844 (2012), pp. 1–193. arXiv: [0910.4182](#) [[hep-ph](#)].
- [48] A. Sirlin and R. Zucchini. “Dependence of the Quartic Coupling $H(m)$ on $M(H)$ and the Possible Onset of New Physics in the Higgs Sector of the Standard Model”. In: *Nucl. Phys.* B266 (1986), pp. 389–409.
- [49] D. N. Dinh et al. “The $\mu - e$ Conversion in Nuclei, $\mu \rightarrow e\gamma, \mu \rightarrow 3e$ Decays and TeV Scale See-Saw Scenarios of Neutrino Mass Generation”. In: *JHEP* 08 (2012). [Erratum: *JHEP*09,023(2013)], p. 125. arXiv: [1205.4671](#) [[hep-ph](#)].
- [50] T. Fukuyama, H. Sugiyama, and K. Tsumura. “Constraints from muon $g-2$ and LFV processes in the Higgs Triplet Model”. In: *JHEP* 03 (2010), p. 044. arXiv: [0909.4943](#) [[hep-ph](#)].

- [51] A. G. Akeroyd, M. Aoki, and H. Sugiyama. “Lepton Flavour Violating Decays $\tau \rightarrow \text{anti-l ll}$ and $\mu \rightarrow e \gamma$ in the Higgs Triplet Model”. In: *Phys. Rev.* D79 (2009), p. 113010. arXiv: [0904.3640 \[hep-ph\]](#).
- [52] J. Chakraborty, P. Ghosh, and W. Rodejohann. “Lower Limits on $\mu \rightarrow e \gamma$ from New Measurements on U_{e3} ”. In: *Phys. Rev.* D86 (2012), p. 075020. arXiv: [1204.1000 \[hep-ph\]](#).
- [53] T. Mori, MEG Collaboration. “Final Results of the MEG Experiment”. In: *30th Rencontres de Physique de La Vallée d’Aoste La Thuile, Aosta valley, Italy, March 6-12, 2016*. 2016. arXiv: [1606.08168 \[hep-ex\]](#).
- [54] U. Bellgardt et al., SINDRUM Collaboration. “Search for the Decay $\mu^+ \rightarrow e^+ e^+ e^-$ ”. In: *Nucl. Phys.* B299 (1988), pp. 1–6.
- [55] A. Blondel et al. “Research Proposal for an Experiment to Search for the Decay $\mu \rightarrow eee$ ”. In: (2013). arXiv: [1301.6113 \[physics.ins-det\]](#).
- [56] A. Perrevoort, Mu3e Collaboration. “Status of the Mu3e Experiment at PSF”. In: *EPJ Web Conf.* 118 (2016), p. 01028. arXiv: [1605.02906 \[physics.ins-det\]](#).
- [57] Y. Nakazawa et al., COMET Collaboration. “COMET Experiment searching for muon to electron conversion”. In: *PoS FPCP2015* (2015), p. 058.
- [58] L. Morescalchi. “The Mu2e Experiment at Fermilab”. In: *Proceedings, 24th International Workshop on Deep-Inelastic Scattering and Related Subjects (DIS 2016): Hamburg, Germany, April 11-25, 2016*. 2016. arXiv: [1609.02021 \[hep-ex\]](#).
- [59] A. Merle and W. Rodejohann. “The Elements of the neutrino mass matrix: Allowed ranges and implications of texture zeros”. In: *Phys. Rev.* D73 (2006), p. 073012. arXiv: [hep-ph/0603111 \[hep-ph\]](#).
- [60] G. Aad et al., ATLAS Collaboration. “Search for anomalous production of prompt same-sign lepton pairs and pair-produced doubly charged Higgs bosons with $\sqrt{s} = 8$ TeV pp collisions using the ATLAS detector”. In: *JHEP* 03 (2015), p. 041. arXiv: [1412.0237 \[hep-ex\]](#).
- [61] E. J. Chun, H. M. Lee, and P. Sharma. “Vacuum Stability, Perturbativity, EWPD and Higgs-to-diphoton rate in Type II Seesaw Models”. In: *JHEP* 11 (2012), p. 106. arXiv: [1209.1303 \[hep-ph\]](#).
- [62] A. Melfo et al. “Type II Seesaw at LHC: The Roadmap”. In: *Phys. Rev.* D85 (2012), p. 055018. arXiv: [1108.4416 \[hep-ph\]](#).
- [63] P. Fileviez Perez et al. “Neutrino Masses and the CERN LHC: Testing Type II Seesaw”. In: *Phys. Rev.* D78 (2008), p. 015018. arXiv: [0805.3536 \[hep-ph\]](#).
- [64] M. E. Machacek and M. T. Vaughn. “Two Loop Renormalization Group Equations in a General Quantum Field Theory. 3. Scalar Quartic Couplings”. In: *Nucl. Phys.* B249 (1985), pp. 70–92.
- [65] H. Arason et al. “Renormalization group study of the standard model and its extensions. 1. The Standard model”. In: *Phys. Rev.* D46 (1992), pp. 3945–3965.
- [66] M. A. Schmidt. “Renormalization group evolution in the type I+ II seesaw model”. In: *Phys. Rev.* D76 (2007). [Erratum: *Phys. Rev.* D85,099903(2012)], p. 073010. arXiv: [0705.3841 \[hep-ph\]](#).

- [67] W. Chao and H. Zhang. “One-loop renormalization group equations of the neutrino mass matrix in the triplet seesaw model”. In: *Phys. Rev. D* 75 (2007), p. 033003. arXiv: [hep-ph/0611323](#) [[hep-ph](#)].
- [68] “First combination of Tevatron and LHC measurements of the top-quark mass”. In: (2014). arXiv: [1403.4427](#) [[hep-ex](#)].

ACKNOWLEDGEMENTS

First of all, I would like to thank my supervisor Werner Rodejohann for giving me the opportunity to work on the exciting topic of neutrino physics at the Max Planck Institute for Nuclear Physics (MPIK) and guiding me during this whole year. I would also like to thank him for letting me participate in the 36th and 37th Heidelberg Graduate Days and in the Summer School "Taller de Altas energías – TAE2016" at Centro de Ciencias Pedro Pascual (Benasque), where I had the chance to learn a lot about the exciting world of particle physics.

I would like to thank Jörg Jäckel for being my second advisor. I hope he enjoyed reading this thesis.

I would like to express my gratitude to Fundación Mutua Madrileña, whose scholarship gave me the opportunity to continue my studies and covered my whole Master in Physics at the University of Heidelberg.

I would like to thank all the people from the MPIK, with whom I have had the opportunity to discuss not only about physics but also about a great variety of interesting stuff. I would like to specially thank Manfred Lindner as the director of our division, for providing such a nice atmosphere in the group; Bhupal Dev, for sharing his Mathematica code and helping me make it work; Pascal and Alex, for carefully reading and commenting the thesis and for being great tutors in the Standard Model courses, and Sebastian, for his comments and ideas; Kevin, to whom I owe the beautiful layout of this thesis; Kai, for holding such a memorable Polterabend before his wedding; Miguel, Dani, Philipp, Tom, Moritz, Johannes, Juri, Rasmus and all the rest of our theoretical division, with whom I have shared so many coffees, birthday cakes and tasty meals; and of course my officemate and friend Clara, with whom I have shared six great years full of laughs and adventures, and also physics.

I would like to thank Toni Pich, for his patient and thorough help with all my questions about renormalization and for always giving me his honest advice.

I would also like to thank my flatmates Michelle, Franzi, Silke and Chuong, for being so awesome and sweet and making me feel at home these two years. I specially thank Basti, for his valuable help read proofing the whole thesis and for sharing with me uncountable Sunday morning pancakes, among other thousand things.

Finally, I want to thank my parents, Anna and Jordi, for all their sincere support, wise guidance and infinite love, and my sister Marta, for loving me as a Sheldonina.

Ithaka

As you set out for Ithaka
hope the voyage is a long one,
full of adventure, full of discovery.
Laistrygonians and Cyclops,
angry Poseidon don't be afraid of them:
you'll never find things like that on your way
as long as you keep your thoughts raised high,
as long as a rare excitement
stirs your spirit and your body.
Laistrygonians and Cyclops,
wild Poseidon—you won't encounter them
unless you bring them along inside your soul,
unless your soul sets them up in front of you.

Hope the voyage is a long one.
May there be many a summer morning when,
with what pleasure, what joy,
you come into harbors seen for the first time;
may you stop at Phoenician trading stations
to buy fine things,
mother of pearl and coral, amber and ebony,
sensual perfume of every kind
as many sensual perfumes as you can;
and may you visit many Egyptian cities
to gather stores of knowledge from their scholars.

Keep Ithaka always in your mind.
Arriving there is what you are destined for.
But do not hurry the journey at all.
Better if it lasts for years,
so you are old by the time you reach the island,
wealthy with all you have gained on the way,
not expecting Ithaka to make you rich.

Ithaka gave you the marvelous journey.
Without her you would not have set out.
She has nothing left to give you now.

And if you find her poor, Ithaka won't have fooled you.
Wise as you will have become, so full of experience,
you will have understood by then what these Ithakas mean.

C.P. Cavafy (1863 – 1933)
Translated by E. Keeley and P. Sherrard

Erklärung:

Ich versichere, dass ich diese Arbeit selbstständig verfasst habe und keine anderen als die angegebenen Quellen und Hilfsmittel benutzt habe.

Heidelberg, den 1. November 2016

.....